Identifying the Molecular Mechanisms of Radiation-Induced Epithelial-Mesenchymal Plasticity in Human Oral Squamous Carcinoma Cells under Glucose Stress

A thesis submitted in fulfilment of the requirements for the degree of

Master of Philosophy

by

Thanh Dat Pham

Lead Supervisor

Dr Naisana Seyedasli

Faculty of Medicine and Health

The University of Sydney

2025

Declaration

This is to certify that the content of this thesis is my own work. This thesis has not been submitted for any other degree or purpose.

I certify that the intellectual content of this thesis is the product of my own work and that all assistance received in preparing this thesis and all sources have been acknowledged.

Thanh Dat Pham

28/02/2025

Acknowledgements

First, I want to acknowledge the Gadigal people of the Eora Nation as the traditional custodians of the University of Sydney's land. I honour their elders, both past and present, along with the emerging leaders. Their rich cultural heritage has profoundly influenced this place, and I appreciate the chance to learn here.

I wish to express my profound gratitude to my supervisor, Dr. Naisana Seyedasli, for her unwavering support and guidance, which have been instrumental in the completion of this thesis. Her mentorship has played a crucial role throughout my academic journey toward this degree.

I would also like to extend my appreciation to my mentor, Rabia Zafar, for her resolute support during the course of this study. Additionally, I acknowledge the significant contributions of Joey Lai and Ali Afrasiabi in the RNA sequencing analysis pertinent to this research.

I convey my heartfelt gratitude to the staff at WIMR, my colleagues, and friends within the biotechnology laboratory – Rabia Zafar, Lupeuea Vakafua, Mitchell Lockwood, Sachchit Ghosh, Michelle Angela Tanro, Teana Reed, Marie-elle Ajaka, and Elizabeth Kelly. Their continual support, invaluable assistance, and insightful guidance have greatly enriched my academic pursuits.

Finally, I would like to extend my deepest gratitude to my family and friends for their unwavering emotional support and steadfast belief in my capabilities.

Abstract

Remodelling along the epithelial-mesenchymal (E-M) axis is crucial in carcinomas and is strongly linked to tumour invasion, metastasis, and radiation resistance. Research indicates hyperglycaemia, which refers to chronic exposure to high glucose levels, significantly increases cancer risk and impacts key features of tumour development, including the epithelial-mesenchymal transition (EMT). This research seeks to explore the effects of hyperglycaemia on the phenotypic remodelling of oral squamous cell carcinoma (OSCC) in the context of metabolic stress and ionising radiation, while investigating the potential molecular mechanisms involved.

In this study, we utilised the 3D tumour spheroid models generated from the OSCC cells subjected to a 7-day hyperglycaemic stress and performed different cellular, molecular, and high-level transcriptome analyses to investigate the cellular and molecular dynamics of hyperglycaemia and its effects on the tumour remodelling as part of the response to ionising radiation.

The immunohistochemical analysis of epithelial and mesenchymal markers, E-cadherin and Vimentin, revealed a notably higher abundance of both hybrid EMT and mesenchymal-like subpopulations in OSCC spheroids subjected to hyperglycaemic stress. This phenotypic remodelling, triggered by metabolic stress and ionising radiation, is shown to be influenced by the regulation and transition among different EMT transcription factors. Transcriptional profiling and pathway analyses have pinpointed several molecular components that may link hyperglycaemia, EMT, and radioresistance in OSCC spheroids, including integrins, MMPs, and laminins.

This study provides a better understanding of the intricate dynamics involved in OSCC progression and treatment responses, offering essential knowledge for future therapeutic approaches. It may also enlighten new therapeutic possibilities for radioresistant carcinomas, thus enriching the ongoing advancements in cancer research.

Table of Contents

Table of Figures

Table of Figures

Chapter 1 – Introduction

1.1. Oral Squamous Cell Carcinoma (OSCC)

Cancer has emerged as the second leading cause of death globally, resulting in over 10 million deaths in 2020. This underscores the critical demand for more extensive and in-depth research on disease detection, management, and treatment approaches. Carcinoma is the predominant type of tumour, representing over 85% of all cancer diagnoses. This term describes malignant tumours that develop from epithelial tissues, which comprise the skin, line internal organs, and form glands and passageways in various biological systems, including the circulatory, urinary, respiratory, and gastrointestinal systems (1).

Oncogenesis, carcinogenesis, or tumorigenesis constitute a multifaceted process where normal cells undergo transformation into cancerous cells, involving alterations in their genetic structure. This transformation encompasses cellular changes, epigenetic modifications, and genetic mutations. Mutations in oncogenes and tumour suppressor genes disrupt the balance of cell production and death, leading to uncontrolled cell growth. Furthermore, cancerous cells gain various capabilities, known as the hallmarks of cancer, which facilitate and sustain cell growth, the ability to resist cell death, invade surrounding tissues, migrate to new sites, and initiate the formation of new tumours. The tumour cells also acquire other additional features, including but not limited to phenotypic plasticity and deregulating cellular metabolism (Figure 1) (2).

Oral cavity cancer (OCC) is ranked as the 16th most prevalent cancer worldwide, with roughly 390,000 new diagnoses and about 190,000 fatalities (3). The terms oral cavity cancer and oral cancer (OC) encompass all malignant neoplastic tissues developed from premalignant lesions on the lips or any part of the inner oral cavity, including the cheeks, tongue, gingiva, floor of the mouth, and hard palate. Squamous cell carcinoma is the most prevalent type of oral cancer, accounting for more than 90% of diagnosed cases (4). Oral squamous cell carcinoma (OSCC) often originates from premalignant lesions in the oral mucosa exhibiting atypical histological characteristics indicative of epithelial dysplasia (5). These abnormalities include nuclear pleomorphism, increased mitotic activity, and loss of cellular polarity (6). However, not all dysplastic lesions are guaranteed to progress to

invasive cancer, and this variability adds complexity to early diagnosis and accurate risk assessment of malignant potential (7). Consequently, OSCC is often overlooked in its early stages, resulting in delays in detection and poorer clinical outcomes. OSCC is strongly associated with heavy smoking and high alcohol consumption. Additional causes of OSCC include immune deficiencies, nutritional deficiencies, and viral infections, especially those caused by human papillomavirus (HPV). Continuous exposure to these factors can lead to genetic and epigenetic changes, along with disturbances in the tumour microenvironment, which together result in the overexpression of oncogenes and the disruption of tumour suppressor genes, thereby facilitating carcinogenesis.

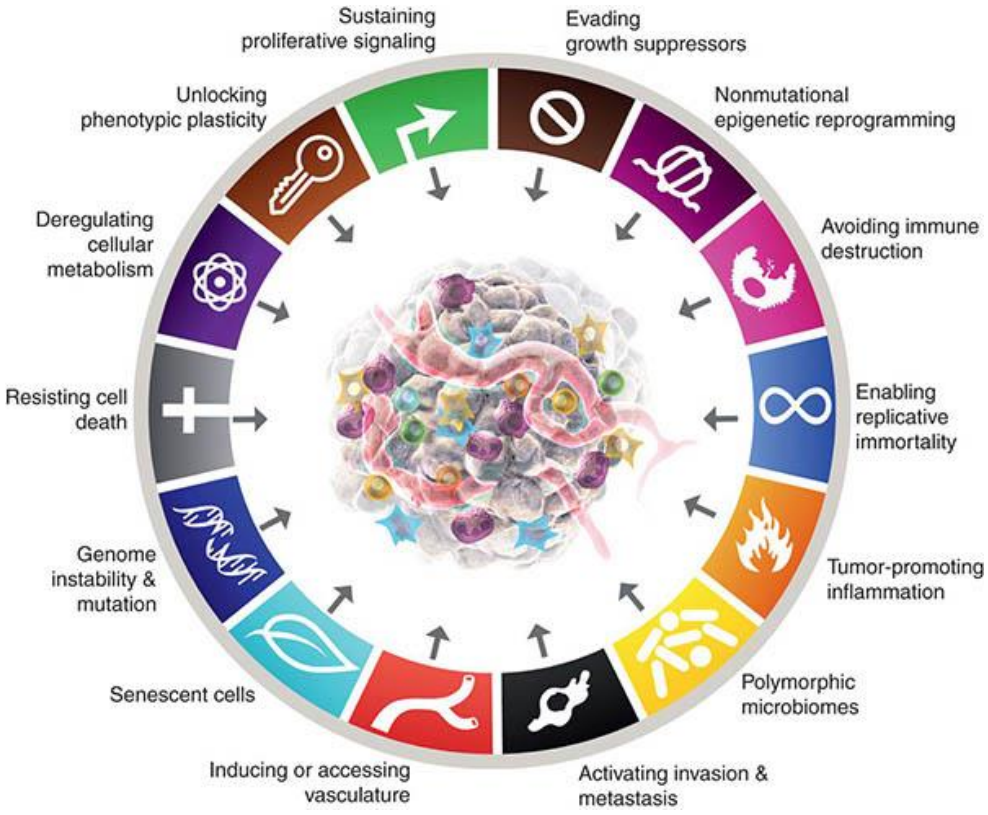

Figure 1. The Hallmark of Cancer (Updated 2022) with the addition of four emerging features: Unlocking phenotypic plasticity, nonmutational epigenetic reprogramming, senescent cells, and polymorphic microbiome.

Management strategies for OSCC involve multidisciplinary decisions influenced by factors, including the clinical TNM stages of the disease, the current underlying health conditions, and the histological characteristics of the tumour. Surgical resection is typically used to

excise early-stage OSCC tumours, often followed by additional treatments such as radiation (RT) or chemoradiation (CRT). In more severe cases where the tumours are highly invasive, OSCC patients are at high risk for relapse or cannot undergo surgery, radiotherapy and/or chemotherapies are employed as the primary treatment strategy. In recent years, immunotherapy has emerged as a treatment since OSCC was recognised as an immunosuppressive disease that can evade immune detection (8). Unfortunately, despite advancements in cancer therapies, the survival rates for patients with advanced-stage OSCC remain relatively low (9, 10). Frequent misdiagnoses, combined with the aggressive and invasive characteristics of OSCC, as well as high rates of local invasion and distant metastasis, diminish the effectiveness of cancer treatments. This leads to an increased risk of tumour recurrence and the emergence of therapeutic resistance (11).

1.2. Radiation Therapy and Radioresistance

After Wilhelm Rontgen discovered X-rays in 1895 and Henri Becquerel discovered radioactivity in 1896, ionising radiation (IR) has been utilised alongside surgery and other treatments for various cancers. Typically, radiation therapy is administered post-surgery in daily doses of 1.8 to 2.0 Gy (Gray). For oral cancer patients, the total cumulative dose typically reaches 66-72 Gy, delivered over 5 to 7 consecutive weeks to effectively eliminate tumour cells (4, 12). Radiation therapy employs high-energy X-rays or gamma rays to directly cause lesions in the DNA of cancer cells, leading to base damage, interstrand crosslinks, single-stranded breaks (SSBs), and double-stranded breaks (DSBs). Among all forms of DNA damage, DSB is the most deleterious. Additionally, radiation can indirectly damage the genetic material of cancer cells by exciting or ionising the cellular water molecules, resulting in the formation of free radicals. These radiation-induced DNA lesions decelerate cancer cell growth and hinder the replication of affected cells. In addition to damaging the genetic material, radiation can disrupt cancer cell organelles, including the plasma membrane, mitochondria, cytoskeleton, nucleus, and endoplasmic reticulum (13). When the damage to genetic and cellular components is irreparable, critical signalling pathways like ATM/ATR, p53, and Bcl-2 family are activated to trigger various forms of cell death, thereby preventing the spread of genetic mutations (14, 15). While IR has proven effective in treating and managing different cancer types, it has also been established to

initiate various downstream signalling pathways that contribute to the development and acquisition of radioresistance.

Radiation resistance, often referred to as radioresistance, is a multifaceted process comprised of a sophisticated signalling network, enabling cancer cells to endure and diminish the damaging impact of ionising radiation, thereby decreasing radiosensitivity and enabling tumours to develop resistance to IR. It encompasses various genes, signalling pathways, and regulatory factors that facilitate and sustain tumour proliferation, invasion, and metastasis in different carcinomas, ultimately resulting in treatment failure and disease recurrence (16).

IR exposure inflicts severe damage to cancer cell DNA, initiating the DNA damage response (DDR) mechanisms that identify the locations of DNA lesions. This process triggers various repair mechanisms tailored to the specific type of IR-induced damage. For double-strand breaks (DSBs), which are particularly lethal and typically irreparable, the non-homologous end-joining (NHEJ) and homologous recombination (HR) pathways are engaged to resolve DSBs caused by IR exposure. Furthermore, research indicates that IR exposure simultaneously activates various prosurvival signalling pathways, such as phosphatidylinositol-3-kinase (PI3K)/protein kinase B (AKT), ATM, ATR, nuclear factor kappa B (NF-κB), Sirtuin 1 (SIRT1), and mitogen-activated protein kinase (MAPK) (17-20). These pathways orchestrate several cancer hallmarks, aiding post-IR survivability of tumour cells, acquiring radioresistance, and enhancing invasion and metastasis.

Moreover, the excessive production of reactive oxygen species (ROS) and the heightened hypoxic tumour microenvironment (TME) following radiation exposure trigger the HIF-1 signalling network, facilitating tumour angiogenesis, alteration in cellular metabolism, and enhancing DNA repair processes (21, 22). Additionally, epithelial-to-mesenchymal transition (EMT) is concomitantly activated during radiation therapy for cancer treatment. This phenotypic remodelling has been linked to reduced efficacy of radiation, increased invasiveness, and metastasis, leading to treatment failure and tumour recurrence (23-25).

1.3. Epithelial to mesenchymal transition (EMT)

Intratumor heterogeneity refers to the existence of diverse subpopulations of cells within a single tumour, each exhibiting unique functional and phenotypic traits. These variations encompass gene expression patterns, potential for invasion and metastasis, metabolic profiles, morphology, plasticity, and differing reactions to treatments, which pose substantial obstacles in formulating effective cancer treatment approaches (26-28). This phenomenon is influenced by a complex network, incorporating variations in cancer stem cells, genetic mutations, epigenetic modifications, changes in the TME caused by environmental stressors, and the detrimental impacts of cancer therapies (29, 30). These factors collectively influence tumour recurrence, metastasis, and sensitivity to treatments, leading to poor prognoses and resistance to therapies (31).

Unlocking phenotypic plasticity is one of the emerging hallmarks of cancer cells. Cellular plasticity refers to the capacity of a cell to reprogram itself and adopt various molecular and phenotypic identities in response to different stimuli, stressors, or changes in its microenvironment. This capability is vital for normal cells, especially during embryonic differentiation, and plays a significant role in the intratumor heterogeneity observed during cancer progression. A fundamental aspect of this adaptive mechanism is the morphological transition along the epithelial-mesenchymal (E-M) spectrum, known as epithelial-to-mesenchymal transition (EMT), where epithelial cells are transformed into mesenchymal cells (32). EMT is classified into three primary types according to their biological functions. Type I EMT, or developmental EMT, mainly takes place during implantation, embryogenesis, and organ formation (33). In contrast, Type II EMT relates to fibrosis and wound healing, occurring during tissue repair and organ fibrosis following traumas and injuries (34). Lastly, Type III EMT plays a critical role in carcinogenesis and tumour progression across various cancers, notably in cancer metastasis, enhancing migratory and invasive abilities, which contribute to tumour advancement and resistance to treatment (35). Our study will primarily focus on Type III EMT during the cancer progression of OSCC.

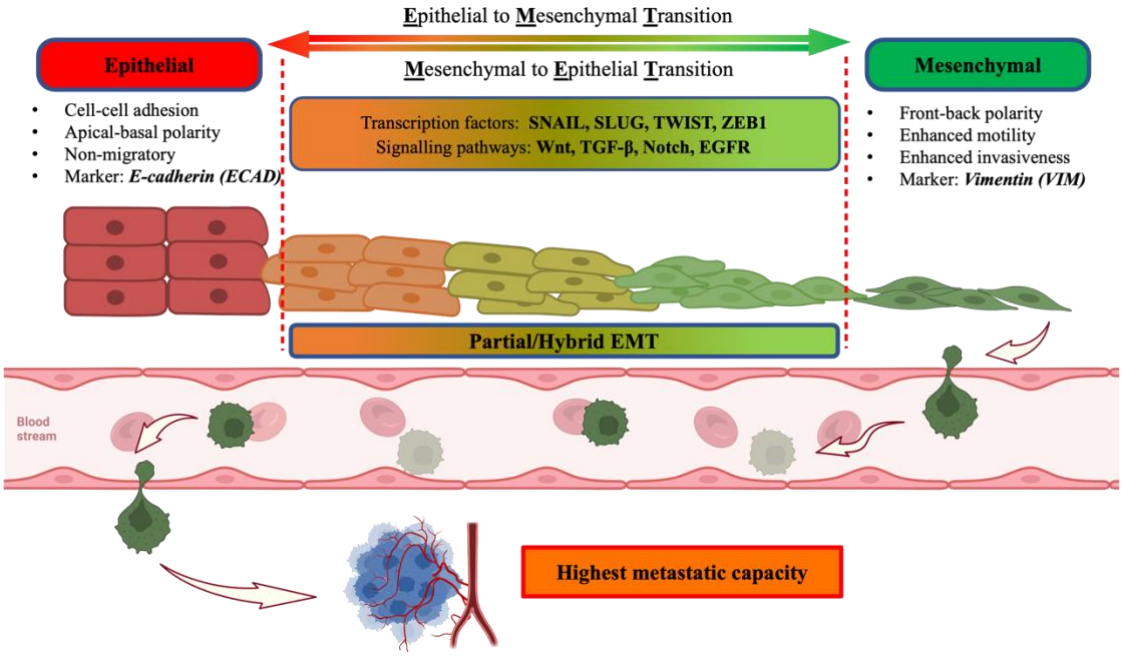

Figure 2. An overview of the epithelial-to-mesenchymal transition (EMT) and its reverse, the mesenchymal-to-epithelial transition (MET), during cancer progression. This includes the regulatory network of EMT driven by EMT transcription factors (TFs) and pathways. Throughout the EMT process, epithelial cells progressively diminish their unique features and take on mesenchymal properties. The schematic was created using Biorender.com.

The epithelial-mesenchymal transition (EMT) process is intricate, dynamic, and reversible, unfolding in multiple stages during cancer development and tumour progression. Studies indicate a strong link between EMT and poor outcomes for cancer patients, including tumour invasion, metastasis, and resistance to treatment. As epithelial cells undergo phenotypic remodelling along the epithelial-mesenchymal (E-M) axis, they enter a highly adaptable state, gradually losing their distinct molecular characteristics. This transformation includes alterations in cell adhesion molecules and cytokeratin, along with a decrease in E-cadherin (ECAD) markers. Consequently, these molecular changes lead to various morphological adaptations, such as the loss of apical-basal polarity, disruption of cell-cell junctions, and reduced cellular adhesion. In contrast, cells start expressing mesenchymal markers like N-cadherin, Vimentin, and fibronectin, giving them an irregular spindle-like shape with front-back polarity (36-39). This transition boosts their invasiveness and migratory abilities while heightening resistance to anti-cancer therapies. Several mechanisms have been recognised as initiators of EMT during cancer progression. Alarmingly, some cancer therapies have also been shown to inadvertently induce EMT (40, 41). Ionising radiation, commonly used as a cancer treatment, can provoke EMT by elevating hypoxic conditions in the TME, activating

multiple oncogenic signalling pathways, including HIF-1, Wnt, EGFR, PI3K/AKT, NF-kB, and Notch pathways, as well as influencing EMT-related transcription factors like SNAIL, ZEB, TWIST, and SLUG (Figure 2) (32, 37, 42-45).

Our laboratory's previous studies on EMT in OSCC, along with existing literature, have discovered subpopulations of carcinoma cells that express both epithelial and mesenchymal markers – namely, E-cadherin (ECAD) and Vimentin (VIM) – at varying levels (46-48). This indicates mixed molecular and morphological phenotypes, which allows these cells to achieve increased motility while still preserving their adhesion properties. Increasing evidence suggests that the phenotypic shift along the E-M axis encompasses a spectrum of intermediate states, known as partial or hybrid EMT, rather than merely existing as a binary system. The increased plasticity observed in these hybrid cells is strongly linked to collective metastasis, tumour invasion, cancer stemness, and resistance to therapies (49). Although the molecular mechanisms and regulatory factors underlying EMT states have been extensively identified and studied across various carcinomas, effectively targeting this phenotypic remodelling to potentially reverse it and re-sensitise tumour cells to cancer treatments remains inadequately understood.

1.4. Glucose metabolism in cancer cells and exposure to hyperglycaemic conditions

1.4.1. Cellular glucose metabolism and cancer progression

Cellular respiration, commonly referred to as the metabolic breakdown of glucose, is an essential catabolic process. It breaks down glucose, generating adenosine triphosphate (ATP), which serves as a primary energy source for cells, along with other essential biomaterials that support the systems necessary for cell growth and the maintenance of both normal and cancerous cells (Figure 3). The deregulation of cellular metabolism is a critical feature of cancer, and researchers have extensively investigated the roles of glucose metabolism during carcinogenesis and tumour progression in various types of epithelial

malignancies. To survive the metabolically challenging environment while fulfilling the high demands for energy and biomaterials required for their uncontrolled growth, tumour cells are shown to engage in a reprogrammed type of cellular metabolism (50).

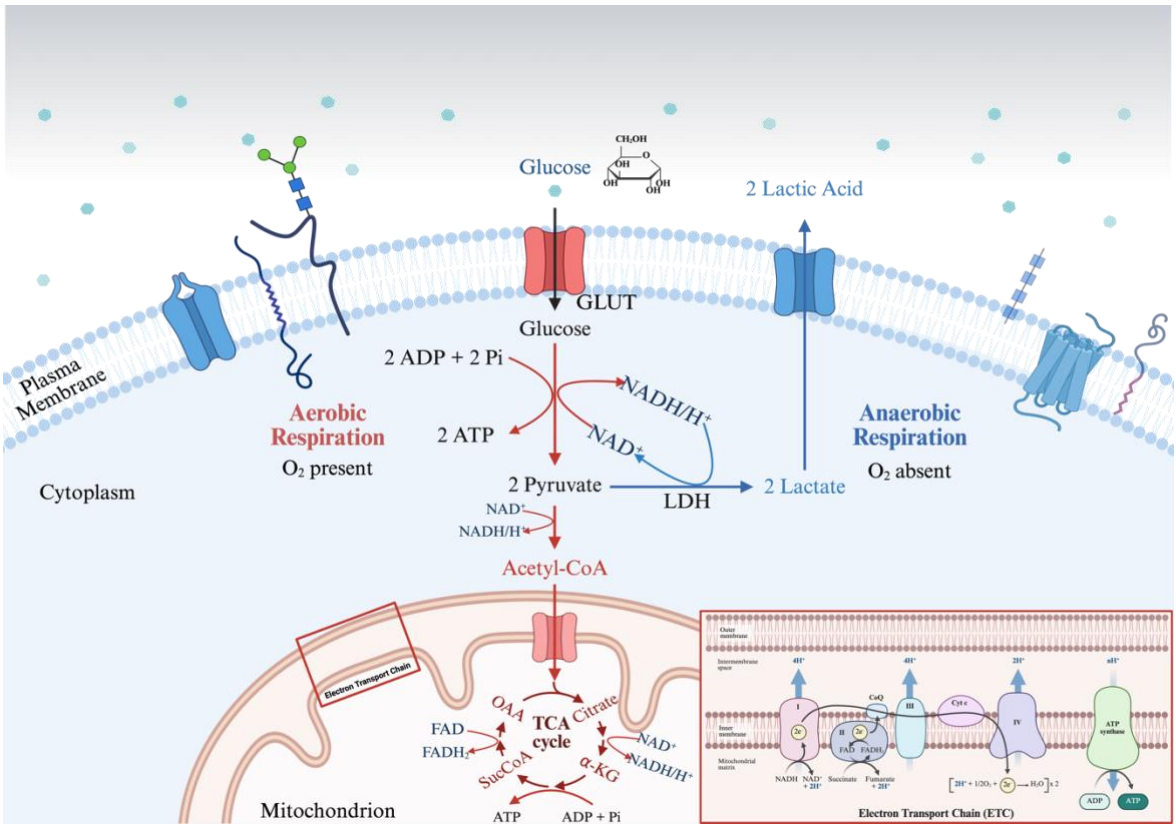

Figure 3. Cellular respiration or glucose metabolism in normal cells. Red arrows denote the aerobic respiration process under oxygen-rich conditions. Blue arrows illustrate anaerobic respiration that occurs in low-oxygen environments. Key abbreviations: ADP = Adenosine diphosphate; ATP = Adenosine triphosphate; ETC = Electron Transport Chain; FAD = Flavin adenine dinucleotide; GLUT = Glucose transporter; NAD = Nicotinamide adenine dinucleotide; OAA = Oxaloacetate; TCA = Tricarboxylic Acid Cycle. This schematic was designed using BioRender.com, based on adaptations from (51).

In normal cells, glucose molecules enter through glucose transporters (GLUTs) and are converted to pyruvates. Their subsequent processing depends on the cellular oxygen (O_2) conditions (Figure 3). Under O_2-deprived conditions, glucose undergoes anaerobic respiration; pyruvate is transformed into lactic acid catalysed by lactate dehydrogenase (LDH), which also helps oxidise NADH to NAD^+. Conversely, in the presence of ample oxygen, pyruvate is transformed into acetyl Coenzyme A and enters the Krebs cycle for

oxidation, producing additional energy as well as NADH and FADH2, which then donate electrons during the Electron Transport Chain (ETC) (52). A newly identified concept called "aerobic glycolysis", or the Warburg effect, describes how tumour cells primarily utilise anaerobic respiration to produce ATP, even in the presence of oxygen, distinguishing them from normal cells (53). This metabolic reprogramming goes beyond just glucose metabolism, encompassing lipid and amino acid metabolisms in tumour cells. While glycolysis is less efficient than aerobic respiration via oxidative phosphorylation, the byproducts of this process are essential for the uncontrolled proliferation of cancer cells. Consequently, to make up for inadequate energy production, cancer cells significantly increase glucose uptake by enhancing the expression of glucose transporters and glycolytic activity (50).

While the Warburg effect is recognised as a cornerstone of cancer cell metabolism, and cancer cells typically prefer it for energy production, not every cancer cell or type of tumour will choose this path (54). Mitochondrial and oxidative phosphorylation (OXPHOS) respiration is still utilised for ATP generation and other macromolecular byproducts (54).

Under hyperglycaemic conditions, glucose uptake and metabolism rates significantly increase, leading to heightened production of reactive oxygen species (ROS) and hypoxic environments (55). These elevated hypoxic conditions can harm the genetic material of cancer cells and trigger various oncogenic signalling pathways that govern key features of tumorigenesis and mechanisms behind therapeutic resistance. This includes processes such as cellular proliferation, tumour angiogenesis, invasion, and metastasis.

Growing evidence indicates a connection between hyperglycaemic conditions in diabetes patients and an increased risk of various cancers. Meta-analysis focusing on oral cancer in individuals with type 2 diabetes mellitus (T2DM) found that cancer incidence and mortality rates were higher in diabetic patients compared to non-diabetics (56, 57). Furthermore, hyperglycaemia is associated with more extended hospital stays and more advanced clinical stages of oral squamous cell carcinoma (OSCC). It also contributes to more frequent local

recurrences and distant metastasis, leading to diminished effectiveness of cancer therapies and poorer survival outcomes (Figure 4) (58).

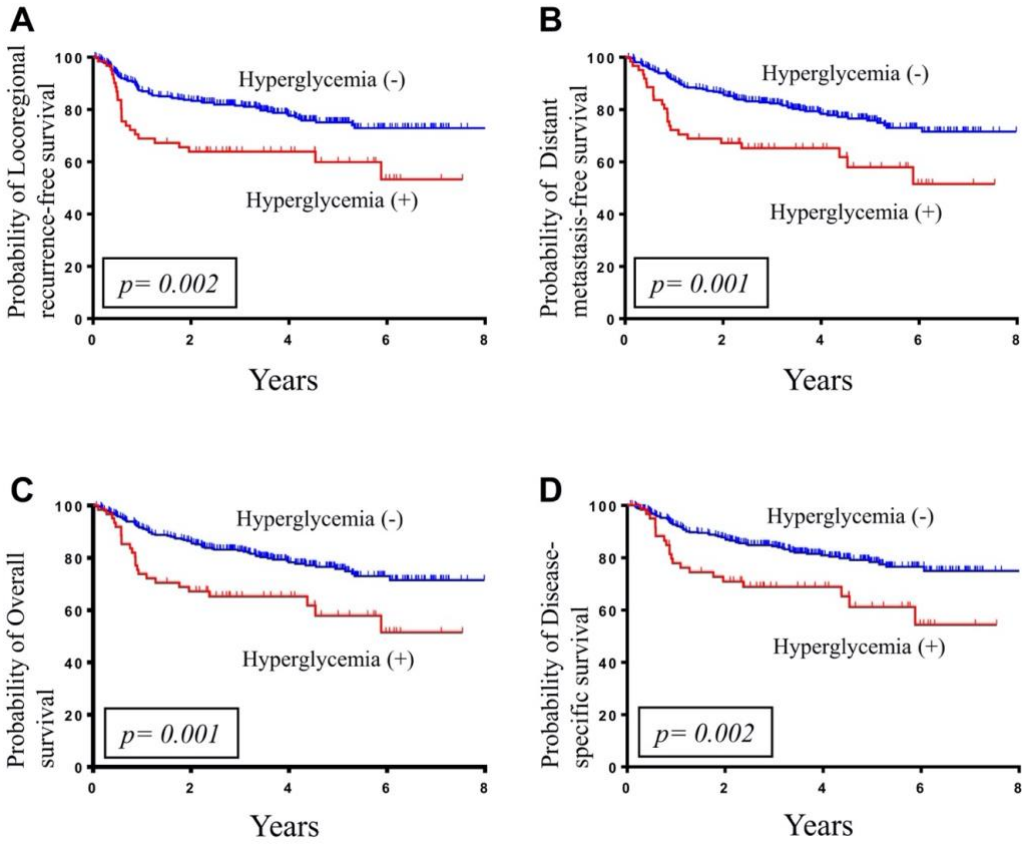

Figure 4. Survival outcomes over five years for OSCC patients, comparing those with hyperglycaemia to those without. The red line indicates hyperglycaemic patients, while the blue line shows non-hyperglycaemic patients. **(A)** Locoregional recurrence-free survival. **(B)** Distant metastasis-free survival. **(C)** Overall survival. **(D)** Disease-specific survival. (58)

1.4.2. Hyperglycaemia and EMT remodelling

The adaptability of tumour glucose metabolism plays a crucial role in the epithelial-to-mesenchymal transition (EMT). Researchers have been actively exploring the link between prolonged hyperglycaemic exposure and tumour development as well as cancer metastasis. The subsequent downstream effects of metabolism changes in cancer cells, induced by hyperglycaemia, such as increased reactive oxygen species (ROS), oxidative stress, and hypoxia, have been shown to trigger EMT (59-61). The heightened production of ROS and

the hypoxic conditions within the tumour microenvironment (TME), driven by increased glucose uptake by cancer cells in hyperglycaemic settings, have been demonstrated to activate EMT in several types of carcinomas (62, 63). This activation promotes tumour invasion, metastasis, and resistance to treatment. Moreover, the exacerbated hypoxia stimulates various signalling pathways that facilitate the phenotypic shift along the E-M axis by boosting the expression of EMT transcription factors (42, 64). In pancreatic cancer, excessive production of ROS, particularly H_2O_2, facilitates EMT by downregulating ECAD and increasing levels of VIM, N-cadherin (NCAD), and the EMT transcription factor SNAIL (65). Furthermore, SNAIL has been demonstrated to trigger EMT in gastric cancer under hyperglycaemic conditions by promoting the expression of enolase 1 (ENO1) via the activation of the TGF/Smad signalling pathway (66). Additionally, the molecular mechanisms underlying hyperglycaemia-induced EMT differ among various carcinomas. In the case of bladder cancer, hyperglycaemia triggers the activation of YAP1/TAZ signalling, resulting in the downregulation of ECAD and the upregulation of NCAD, VIM, and fibronectin (67). In contrast, the increased secretion of VEGF mediated by ER/GLUT4 contributes to hyperglycaemia-induced EMT in uterine cancer (68).

While extensive research has explored the relationship between tumour exposure to hyperglycaemic conditions and the induction of epithelial-mesenchymal transition (EMT) in various carcinomas, this link remains undefined in oral squamous cell carcinoma (OSCC). Additionally, the molecular mechanisms that enable this association between hyperglycaemia and EMT involve a complex interplay of various signalling pathways and regulatory factors, which still need further investigation.

1.5. Rationale for the Project and Objectives of the Study

1.5.1. Project rationale

Current literature emphasises that intratumor phenotypic heterogeneity along the epithelial-mesenchymal (E-M) axis is critical for tumour initiation, invasiveness, metastasis, and

resistance to radiation therapy. Conversely, the link between hyperglycaemia and heightened cancer risk, as well as tumour progression, has been well-documented across various human carcinomas, including OSCC. Additionally, several retrospective studies have shown that chronic high glucose exposure in diabetic patients can affect how different cancer types respond to radiation therapy, leading to increased rates of treatment failure and cancer recurrence. Nonetheless, few studies have actually explored how hyperglycaemia impacts tumour cellular responses to radiotherapy. Given the high metastatic rates and frequent local recurrences after treatment for epithelial carcinoma, a thorough understanding of the intricate mechanisms involved is essential for enhancing the therapeutic effectiveness of treatment.

Our previous lab data indicate that OSCC cell lines show significantly higher radiation resistance (S.F.) under hyperglycaemia-induced metabolic stress (Figure 5). Although the link between hyperglycaemia, EMT and cancer progression is well-known, the specific effects of these factors on the response of epithelial carcinoma to ionising radiation (IR) and subsequent dynamic remodelling are not fully understood. To gain a deeper insight into the *in vivo* effects of hyperglycaemia, IR exposure, and intratumoral phenotypic heterogeneity along the E-M axis, we cultivated OSCC cells in a 3D spheroid system rather than the standard 2D monolayer cell culturing. This approach mimics the 3D architecture of tumours, in vivo exposure to external stressors, and factors affecting tumour cell radiosensitivity, such as cell-to-cell interactions and hypoxia.

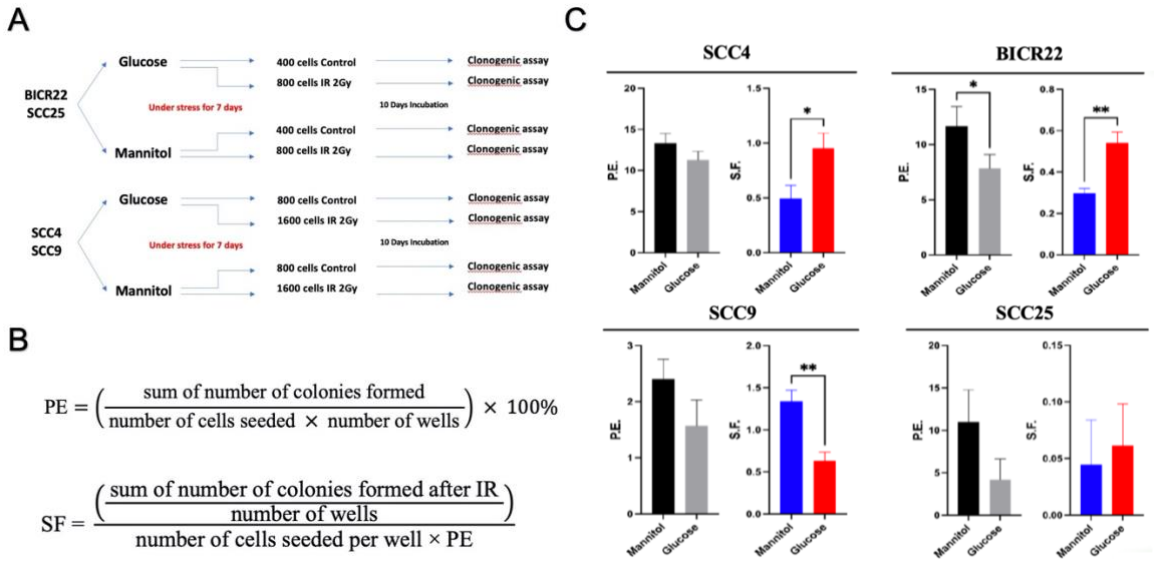

Figure 5. Levels of radioresistance in OSCC cell lines influenced by hyperglycaemic stress. **(A)** This section outlines the experimental design for **(C)**. Cells from four distinct OSCC cell lines were cultured for seven days under hyperglycaemic conditions (+ 20 mM glucose) and a normal-glucose control (+ 20 mM mannitol) before being subjected to ionising irradiation (IR- 2 Gy). The clonogenic assay was carried out on day 10 post-irradiation. **(B)** Here are the formulas used to calculate Plating Efficiency (P.E.) and Survival Fraction (S.F.). **(C)** Bar graphs depict the P.E. and S.F. of OSCC cell lines. Statistical analysis was performed using an unpaired two-tailed t-test (*$p < 0.05$, **$p < 0.01$). The values presented are *mean* ± *SD*.

1.5.2. Hypothesis and objectives of the study

We hypothesised that exposure to hyperglycaemic conditions would promote EMT remodelling in OSCC-derived spheroids and further accelerate the process of EMT as a response to ionising radiation.

To address this hypothesis, our objectives are:

- To perform molecular analyses to evaluate the expression of EMT canonical markers and the regulation of EMT transcription factors following exposure to hyperglycaemic conditions and ionising radiation.
- To assess and validate the key transcriptional signatures obtained from existing RNA sequencing data.

Chapter 2 – Methods

2.1. General tissue culture

This study utilised two well-characterised tongue carcinoma cell lines: SCC4, acquired from the American Type Culture Collection (ATCC), and BICR22, sourced from the European Collection of Authenticated Cell Cultures (ECACC). These two cell lines were cryopreserved in dimethyl sulfoxide (DMSO), a cryoprotective agent, and stored in liquid nitrogen at -196°C to ensure long-term viability. The cells were expanded in an oral culture medium, which consisted of filtered Dulbecco's Modified Eagle's Medium/Nutrient Mixture F-12 (DMEM/F12) (Sigma-Aldrich, Cat. # D8437) supplemented with 10% foetal bovine serum (Gibco, Cat. # 26140079) and 1% GlutaMAX (Gibco, Cat. # 35050079).

The cryopreserved cryovials containing SCC4 and BICR22 cells were rapidly thawed in the 37°C water bath until only a small ice core remained and then transferred into 15 mL Falcon tubes containing 2 mL of oral medium and centrifuged at 1500 r.p.m for 5 min at 4°C to pellet the cells. After discarding the supernatant, the cell pellet was resuspended in 1 mL of oral medium and transferred into 10 cm tissue culture dishes containing 7 mL of oral medium. The cells were expanded in a humidified incubator with 5% CO_2 at 37°C. The culturing medium was replaced every two or three days to remove metabolic waste and provide fresh nutrients. Once the cell confluency had reached approximately 70-80%, the cells were passaged at a 1:2 ratio.

For cell passaging, SCC4 and BICR22 culture plates were washed with Dulbecco's phosphate-buffered saline (DPBS) (Gibco, Cat. # 14190136) to remove residual serum and debris. The cells were then incubated with TrypLE enzyme (Gibco, Cat. # 12605010) for 5 to 7 min to dissociate the adherent cells. An equal volume of oral media was added to the dishes to neutralise the TrypLE enzyme. The cell suspension was collected into the Falcon tubes, which were then centrifuged to pellet the cells, and the supernatant was discarded. The cell pellets were then resuspended in the fresh oral medium and transferred into two or three new 10 cm culture dishes at the desired ratio. The plates were kept in the incubator for expansion until they reached 80-90% confluency. Depending on the experimental requirements, the cells were then passaged again at the appropriate ratio.

The extra culturing dishes were cryopreserved again for future experiments. In this process, the cells were washed with DPBS, incubated with the TrypLE enzyme to dissociate adherent cells, and centrifuged at 1500 r.p.m for 5 min at 4°C. The cell pellets were resuspended in oral media containing 10% DMSO and aliquoted into cryovials. These vials were placed in an insulated box and stored at -80°C overnight to allow gradual cooling before being transferred to liquid nitrogen for long-term storage.

Every step of these protocols was executed with sterile equipment under strict aseptic conditions to avoid any potential contamination.

2.2. Hyperglycaemia-induced metabolic stress of OSCC cells

The glucose medium was formulated using filtered Dulbecco's Modified Eagle's Medium/Nutrient Mixture F-12 (DMEM/F12) (Sigma-Aldrich, Cat. # D8437), 10% foetal bovine serum (FBS) (Gibco, Cat. # 26140079), 2 mM GlutaMAX (Gibco, Cat. # 35050079), and 20 mM filtered D-(+)-Glucose solution (Sigma). In the preparation of the mannitol medium, the equivalent concentration of mannitol (Sigma) was added in place of glucose.

After at least two passages, once the plates had reached 80-90% confluence, the cells were harvested and resuspended in 1 mL oral medium per two collected plates. Eight to ten culture dishes containing 8 mL oral medium were prepared for each cell line. The plates were divided into two experimental groups: (1) glucose for inducing hyperglycaemic metabolic stress (glucose group) and (2) mannitol as the control (mannitol group). In the glucose group, 100 µL of the resuspended cells were added to each plate, whereas in the mannitol group, 80 µL was added per plate. The plates were incubated in a humidified environment with 5% CO_2 at 37°C for 3 to 4 h, allowing the cells to settle at the bottom of the plates. When the cells had adhered and settled, 20 mM of either filtered D-(+)-Glucose or filtered mannitol solution was distributed to the respective plates. The cells were then incubated for seven days, with the glucose and mannitol media replenished every three to four days.

2.3. Generation of 3D tumour spheroid model and irradiation

Following the seven days of expansion under metabolic stress, the cells were harvested and resuspended in their respective sugar-containing medium. Drops of 25-30 μL of the resuspended cells were carefully deposited onto the inverted lids of the culture dishes. These lids were then gently reverted and placed onto the dishes filled with 4 – 5 mL of DPBS to prevent evaporation of the hanging drops. The plates with the hanging drops were incubated overnight in a humidified environment at 37°C and 5% CO_2, allowing the cell sheets to form without adhering to the lid surface. The cell sheets were then individually transferred to the 12-well plates containing 1-2 mL of the corresponding sugar medium using P1000 pipette tips with clipped ends to reduce the pressure suction pressure. The 12-well plates were placed on an orbital shaker in a humidified incubator supplemented with 5% CO_2 at 37°C overnight, allowing the cell sheets to form a spherical shape.

The next day, the glucose and mannitol media from the 12-well plates were replaced with the standard oral culture medium before irradiation. Subsequently, the spheroids were irradiated with 200 cGy X-rays in the enclosed chamber of the X-RAD 320 irradiator (Precision X-Ray) at a dose rate of 90.77 cGy/min. The control samples remained on the orbital shaker in the incubator without radiation exposure. The irradiated spheroids were placed in the incubator and collected at 2 and 24 h after irradiation for subsequent experiments.

2.4. Tumour tissues

The fresh, frozen tumour tissues dissected from diabetic and non-diabetic patients were obtained from the Head and Neck Tumour Banking (Table 1). Once the fresh specimens were brought from the operating theatre to the Tissue Pathology Area in Lifehouse or Royal Prince Alfred Hospital (RPA), they were processed following the procedures outlined in the RPA Tissue Pathology Surgical Dissection Manual (DOCID-530-31):

(1) Identification checks were conducted, including verifying specimen demographics, matching request form details with those on the specimen containers, and confirming the consent form for tumour banking had been obtained, signed, dated, witnessed, and attached. Preoperative pathology and radiology reports were also attached along with the specimens.

(2) The specimens were examined to ensure that tumour banking would not compromise histopathological assessment. The primary goals were to achieve an accurate diagnosis, assess margins, and identify prognostic factors. Tumours must be at least 15 mm in the largest diameter before sampling.

(3) When sampling for the tumour bank, macroscopic findings were documented, a sterile technique was used, and margins were differentially inked and documented with diagrams and photographs. The specimens were incised through the tumour to assess its size and location relative to margins, and a thin slice through the centre of the tumour was taken, avoiding necrotic, keratinous, haemorrhagic, mucoid, or otherwise non-cellular areas. Tumour tissues were placed into a sterile cryotube, and 2x3 mm normal tissue away from the tumour and margins were also collected into a cryotube. The time and date of sampling were noted on the specimen data form, and the TBO prepared the specimen.

(4) Any remaining tissue was placed in formalin and processed routinely.

Table 1. TNM Staging of the tumour tissues dissected from tongue cancer patients with/without diabetes. (*) Tumour and normal tissues used in the Immunohistochemistry experiment assessing ECAD and VIM expression. (**) Tumour and normal tissues used in the qRT-PCR to validate the expression of the genes of interest.

Sample	T-Stage	N-Stage	M-Stage	Staging	Diabetes Dx	HbA1c	BGL Fasting	BGL Random	Diabetic rx	Outcome
SP-20-032134(**)	4a	3b	0	4	T2DM	7	4.4	15.7	Nil, previously gliclazide 160mg BD	Died of metastatic lung cancer and metastatic HNC.
SP-20-022014(**)	3	0	0	3	T2DM	N/A	N/A	9.7	Metformin XR 500mg BD	Died of unresectable locally advanced tongue SCC.
SP-20-006784(*)(**)	2	0	0	2	T2DM	6.9	N/A	19.3	Empagliflozin 25mg mane, Novomix 36/32	Died of metastatic buccal SCC.
SP-20-017562(**)	3	2B	0	3	No Diabetes	N/A	N/A	N/A	-	Alive, no disease
SP-20-007297(*)(**)	3	0	0	3	No Diabetes	N/A	N/A	N/A	-	Alive, no disease
SP-20-022392(**)	2	1	0	3	No Diabetes	N/A	N/A	N/A	-	Died, with Head and Neck Cancer

2.5. Total protein extraction and Western Blotting

The spheroids were harvested from the 12-well plates and transferred into RIPA buffer (Thermo Fisher Scientific, Cat. # 89900) with 1% protease/phosphatase inhibitors (Thermo Fisher Scientific, Cat. # 78440). The spheroids were lysed on ice using the sonication pulses from the VEVOR FS-450N Ultrasonic Homogeniser Sonicator. The resulting cell lysates were then centrifuged at 14,000 r.p.m for 10 min at 4°C and then mixed with Laemmli buffer (Bio-rad, Cat. # 1610747) and β-mercaptoethanol (BME) (Sigma, Cat. # M7154).

For the Western blotting run, the cell lysates were heated to 95°C for 5 min before being loaded onto the 4-15% Tris-Glycerine extend precast polyacrylamide gels (Bio-Rad). The samples were subjected to denaturing electrophoresis in 1X running buffer (25 mM Tris, 192 mM glycine, and 0.1% sodium dodecyl sulphate (SDS)) (Bio-Rad). Initially, the voltage was set to 150V for the first 5 min, then increased to 200V until the protein bands reached the bottom of the gels. Afterwards, the gels were transferred onto 0.2 mm nitrocellulose membranes using the Trans-Blot Turbo Transfer System (Bio-Rad) for 7 min, set at 2.5 A and 25 V.

The membranes were blocked for 15 min using 5% milk powder in 1X TRIS-buffered saline (TBS) (1M Tris-HCl, 0.8% NaCl, pH 7.5) and 0.1% Tween-20 (TBST). The membranes were then washed three times with TBST, each for 5 min, before the overnight incubation at 4°C with the primary antibodies: 1/5000 anti-γH2AX (Abcam, Cat. # ab81299) and 1/2000 anti-Vinculin (Sigma-Aldrich, Cat. # V9131) diluted in 5% bovine serum albumin (BSA) (Sigma-Aldrich, Cat. # A4919) in TBST.

On the next day, after three 5-minute washes with TBST, the membranes were incubated for 1 hour in the dark at room temperature with 1/10000 fluorescent secondary antibodies, including IRDye 680RD (LI-COR Biosciences, Cat. # 926-68073) and 1/10000 secondary antibody IRDye 800CW (LI-COR Biosciences, Cat. # 926-32212) diluted in 5% BSA in TBST. Throughout the incubations with both primary and secondary antibodies, the

membranes were gently rocked or placed on an orbital shaker at low speed to ensure even coverage with the antibody mixtures.

The fluorescent signals from the targeted proteins were detected by the Odyssey Fc Imaging System (LI-COR Biosciences), and the images were captured using the Image Studio software (LI-COR Biosciences).

2.6. Immunohistochemistry, Haematoxylin and eosin staining and fluorescence microscopy

2.6.1. Preparation of tumour spheroids, human tumour tissues and cryosection

The oral medium in the plates was discarded, and the tumour spheroids were rinsed with ice-cold DPBS and subsequently fixed with 4% paraformaldehyde (PFA) for 10 min at room temperature. Following fixation, the spheroids were dehydrated in a 25% sucrose solution for 15–30 min, or until they sank to the bottom of the plates. They were subsequently transferred into cryomolds filled with Optimal Cutting Temperature (O.C.T.) compound.

The fresh, frozen tongue cancer tumour tissues were cut into small pieces and washed with PBS before being fixed with 4% PFA overnight at 4°C. The fixed tumour tissues underwent a gradient dehydration process with 10% and 20% sucrose (one hour each at 4°C), followed by 30% sucrose overnight at 4°C. They were then transferred into cryomolds containing the O.C.T. compound. These O.C.T. blocks, containing tumour spheroids and tumour tissue, were initially frozen on dry ice before being transferred to and stored at -80°C.

The frozen O.C.T. blocks containing tumour spheroids and tumour tissues were sectioned into 6 – 8 μm slices using a cryostat (Leica Biosystems) and collected onto poly–L–Lysine–

coated slides, prepared for the subsequent immunohistochemistry and haematoxylin and eosin staining procedures.

2.6.2. Immunohistochemistry staining and fluorescent microscopic imaging

The sections of tumour spheroids and tissues collected on glass slides were fixed with 4% PFA for 10 min. Following the fixation, the sections were blocked and permeabilised with 3% donkey serum (Sigma, Cat. # D9663), 0.1% BSA, and 0.1% Triton X-100 in PBS for one hour at room temperature. Afterwards, the sections were incubated with primary antibodies in 1% BSA/PBS overnight at 4°C. The primary antibodies used were anti-E-cadherin (ECAD) (R&D Systems Cat. # AF748) at a 1/200 dilution and anti-Vimentin (VIM) (Abcam, Cat. # 92547) at a 1/1000 dilution.

The following day, the slides were washed with 0.1% Tween-20 in PBS (PBST) before incubation with secondary antibodies in 1% BSA/PBS for one hour in the dark at room temperature. The secondary antibodies used were 1/500 Alexa Fluor 555-conjugated donkey anti-goat (Invitrogen, Cat. # A31572) and 1/500 Alexa Fluor 488-conjugated donkey anti-rabbit (Invitrogen, Cat. # A11055). To protect the fluorescent signals from light damage, the slides were kept in the dark after this step. Subsequently, the slides were washed with PBST, and the cell nuclei were stained with 1/8000 Hoechst (Invitrogen, Cat. # H3569) in PBS for 5 min. Finally, the slides were mounted with ProLong™ Gold Antifade Mountant (Invitrogen, Cat. # P36930) and covered with coverslips.

2.6.3. Fluorescence microscopic imaging and quantification

The fluorescent signals on tumour spheroids and tissue sections were captured using the Olympus U-RFL-T fluorescent microscope, and images were processed through Leica Application Suite (LAS) software. For each biological replicate, five random, identical-sized areas were selected from the fluorescent images, which showed only nuclei. The quantification was then conducted on the overlaid images with the other biomarker

fluorescent channels. The average percentage for each biological replicate was calculated from the number of cells positive for either or both biomarker fluorescent signals relative to the total number of nuclei in the selected areas.

2.7. Total RNA extraction, Quantitative Reverse Transcription Polymerase Chain Reaction (qRT-PCR), and RNA Sequencing

2.7.1 Total RNA Extraction from OSCC tumour spheroids and human tumour tissues

The metabolic-stressed and irradiated OSCC tumour spheroids were collected, washed with DPBS and transferred into RNase-free 1.5 mL Eppendorf tubes. The fresh frozen tumour tissues were dissected into 20 mg pieces and then frozen in liquid nitrogen. The frozen tissues were ground into fine powder and transferred into RNase-free Eppendorf tubes. The tumour spheroids and ground tissues were lysed in Lysis buffer RLY and β-mercaptoethanol (BME) and subsequently proceeded to RNA extraction using the Isolate II RNA Mini kit (Bioline, Cat. # BIO-52072), following the protocol provided by the manufacturer. The concentration and quality of the extracted total RNA samples were assessed using a NanoPhotometer (Integrated Science).

2.7.2 cDNA synthesis and qRT-PCR

The extracted total RNA samples were reverse-transcribed into complementary DNA (cDNA) using the SensiFAST cDNA Synthesis Kit (Bioline, Cat. # BIO-65054) according to the provided protocol from the manufacturer. In brief, the total RNA sample was mixed with 4x TransAmp buffer, reverse transcriptase and RNase-free water. The mixtures were subsequently placed in the thermal cycler with the following steps: annealing at 25°C for 10 min, reverse transcription at 42°C for 30 min, enzyme inactivation at 85°C for 5 min, and then holding at 4°C.

Table 2. Forward and reverse primer sequences used for qRT-PCR

Gene	Forward primer	Reverse primer
ECAD	GCAGAACTGTCCCTGTCCCAG	GAACAGCACGTACACAGCCCT
VIM	TCTCTGAGGCTGCCAACCG	CGAAGGTGACGAGCCATTTCC
SNAIL	ACCACTATGCCGCGCTCTT	GGTCGTAGGGCTGCTGGAA
TWIST	GGACAAGCTGAGCAAGATTCAGA	TCTGGAGGACCTGGTAGAGGAA
SLUG	TGTTGCAGTGAGGGCAAGAA	GACCCTGGTTGCTTCAAGGA
ZEB1	GCACCTGAAGAGGACCAGAG	TGCATCTGGTGTTCCATTTT
GUSB	CCACCAGGGACCATCCAAT	AGTCAAAATATGTGTTTCTGGACAAAGTAA
GAPDH	GGATTTGGTCGTATTGGG	GGAAGATGGTGATGGGATT
β-Actin	CACCATTGGCAATGAGCGGTTC	AGGTCTTTGCGGATGTCCACGT
ITGA3	GCCTGACAACAAGTGTGAGAGC	GGTGTTCGTCACGTTGATGCTC
ITGAV	AGGAGAAGGTGCCTACGAAGCT	GCACAGGAAAGTCTTGCTAAGGC
ITGB4	AGGATGACGACGAGAAGCAGCT	ACCGAGAACTCAGGCTGCTCAA
MMP2	AGCGAGTGGATGCCGCCTTTAA	CATTCCAGGCATCTGCGATGAG
MMP9	GCCACTACTGTGCCTTTGAGTC	CCCTCAGAGAATCGCCAGTACT
LAMB1	GAGGTGTCTCAAGTGCCTGTAC	ACTGGCAGTCAGAGCCGTTACA
LAMC1	CTGTGAGGTCAACCACTTTGGG	AGCCTTCTCTGCATTCACAGCG
FN1	ACAACACCGAGGTGACTGAGAC	GGACACAACGATGCTTCCTGAG
IRS1	AGTCTGTCGTCCAGTAGCACCA	ACTGGAGCCATACTCATCCGAG

The real-time RT-PCR (qRT-PCR) was conducted employing the SensiFAST SYBR Lo-ROX Kit (Bioline, Cat. # BIO-94020). The primers that amplify the target genes for assessing EMT states and for RNA Sequencing validation are listed in Table 2. GAPDH, β-Actin, and GUSB were utilised as housekeeping genes. A master mix was prepared for each targeted gene containing its forward and reverse primers, H_2O, and the SensiFAST SYBR Lo-ROX mix containing SYBR® Green I dye, dNTPs, stabilisers and enhancers. After distributing the master mix into the PCR 96-well plate, the cDNAs were added and subject to the BioRad CFX96 PCR machine for the PCR measurement, starting with polymerase activation at 95°C for 2 min and then 40 cycles of denaturation at 95°C for 5 s, annealing at 60°C for 10 s, and extension at 72°C for 20 s.

The resulting Ct values obtained from the PCR machine were subsequently analysed to investigate the relative change in gene transcript level using the delta-delta Ct (ΔΔCt) method. The ΔCt values were first calculated based on the gene transcript Ct and the geometric mean Ct of the three housekeeping genes. The ΔCt values of the control and treated samples were then used to determine the ΔΔCt. The transcript expression analysis of each gene was performed in three experimental replicates. Statistical analysis was performed and evaluated using analysis of variance (ANOVA) in GraphPad Prism V10.4.1.

2.7.3 RNA Sequencing

The total RNAs isolated from the irradiated glucose- and mannitol-treated spheroids at 2 h and 24 h after radiation exposure and their respective control samples were subjected to an RNA integrity check. The integrity of the extracted RNA was measured with an Agilent 4200 TapeStation (Agilent Technologies, Santa Clara, CA, USA) using RNA screentapes (Agilent Technologies, 5067-5576). RNA purity was assessed using a spectrophotometer (Eppendorf, Hamburg, Germany).

For each sample, 400ng of RNA was used for library preparation at the Westmead Genomics Facility (The Westmead Institute for Medical Research, Sydney, Australia). The Illumina® Stranded mRNA Prep, Ligation kit (Illumina, San Diego, CA, USA) was used following the

protocol provided by the manufacturer. Libraries were then quantified with a 4200 TapeStation (Agilent Technologies, Santa Clara, CA, USA) and their integrity was assessed with the Agilent D1000 ScreenTape System (Santa Clara, CA, USA).

RNA sequencing was conducted at the Australian Genome Research Facility (Melbourne, Victoria, Australia) using an Illumina NovaSeq 6000 sequencer (Illumina, San Diego, CA, USA). The sequencing generated 50-base-pair (bp) paired-end reads, with around 20 million paired reads per sample, which were successfully mapped to the reference genome.

To analyse the obtained data, the FASTQ files were downloaded using the KARAJ Unix toolset, chosen for its efficiency in managing large-scale batch downloads due to its multithreading capabilities (69). Adapter sequences (e.g., Illumina Nextera) were removed using Cutadapt, and the quality of reads was assessed with BBMap, excluding reads with a Phred score < 30 (70, 71). These steps ensured the removal of technical artifacts and low-quality data.

Reads were aligned to the T2T genome assembly CHM13v2.0 using STAR, a splicing-aware aligner optimised for handling repetitive and complex regions of the T2T CHM13v2.0 genome assembly (72, 73). STAR was selected for its robust support of the ability to improve alignment accuracy in spliced regions. The T2T CHM13v2.0 genome assembly represents the most complete and recently characterised version of the human genome (72). Gene-level read counts were generated using FeatureCounts, restricting the analysis to reads covering at least 90% of exon regions (74). This threshold was applied to ensure an accurate representation of gene expression, minimising biases from partial alignments.

Differential gene expression analysis was conducted using DESeq2 and R, which normalised read counts across conditions and applied variance-stabilising transformations (75). Genes with total counts across all samples of at least 10 were excluded before normalisation, ensuring cleaner input for normalisation, model fitting, and hypothesis testing. Genes were considered significantly expressed if they met the FDR threshold of less than 0.01. Biological replicates were included to improve statistical power and reliability.

Chapter 3 – Results

Research has demonstrated that hyperglycaemia amplifies cancer aggressiveness across various types and worsens disease-free survival rates, including in patients with oral cancer (76). Additionally, our previous clonogenic assay experiment conducted on irradiated, hyperglycaemic-stressed models of four OSCC lines (SCC4, BICR22, SCC9, and SCC25) showed that elevated glucose levels affected the radiosensitivity of the SCC4 and BICR22 lines, enhancing their survival rates after irradiation (Figure 5) (77).

On the other hand, several studies have explored the association between hyperglycaemia and cancer EMT, observing that elevated glucose levels can enhance EMT via different mechanisms, thereby mediating tumour progression, aggressiveness, and therapeutic resistance (65, 66, 78-82). The phenotypic shift toward mesenchymal traits is linked with radioresistance and invasive capacity.

This study focuses on exploring the potential relationship between metabolic stress induced by hyperglycaemia and EMT, as well as identifying the underlying molecular mechanisms. To achieve this, we chose SCC4 and BICR22 cell lines, which demonstrated high survivability after 7 days of hyperglycaemic stress during the clonogenic assay, as our primary study models.

To explore the effects of hyperglycaemia on OSCC and their response to ionising radiation, SCC4 and BICR22 cells were exposed to metabolic stress for seven days in 20 mM glucose. Another set of these two cell lines was subjected to metabolic stress with mannitol at the same concentration, which served as an osmolarity control (Figures 6A and B). The metabolic-stressed cells were then cultured as hanging drops, and the resulting cell sheets were developed into 3D tumour spheroids, which were then irradiated for further analyses (Figure 6C).

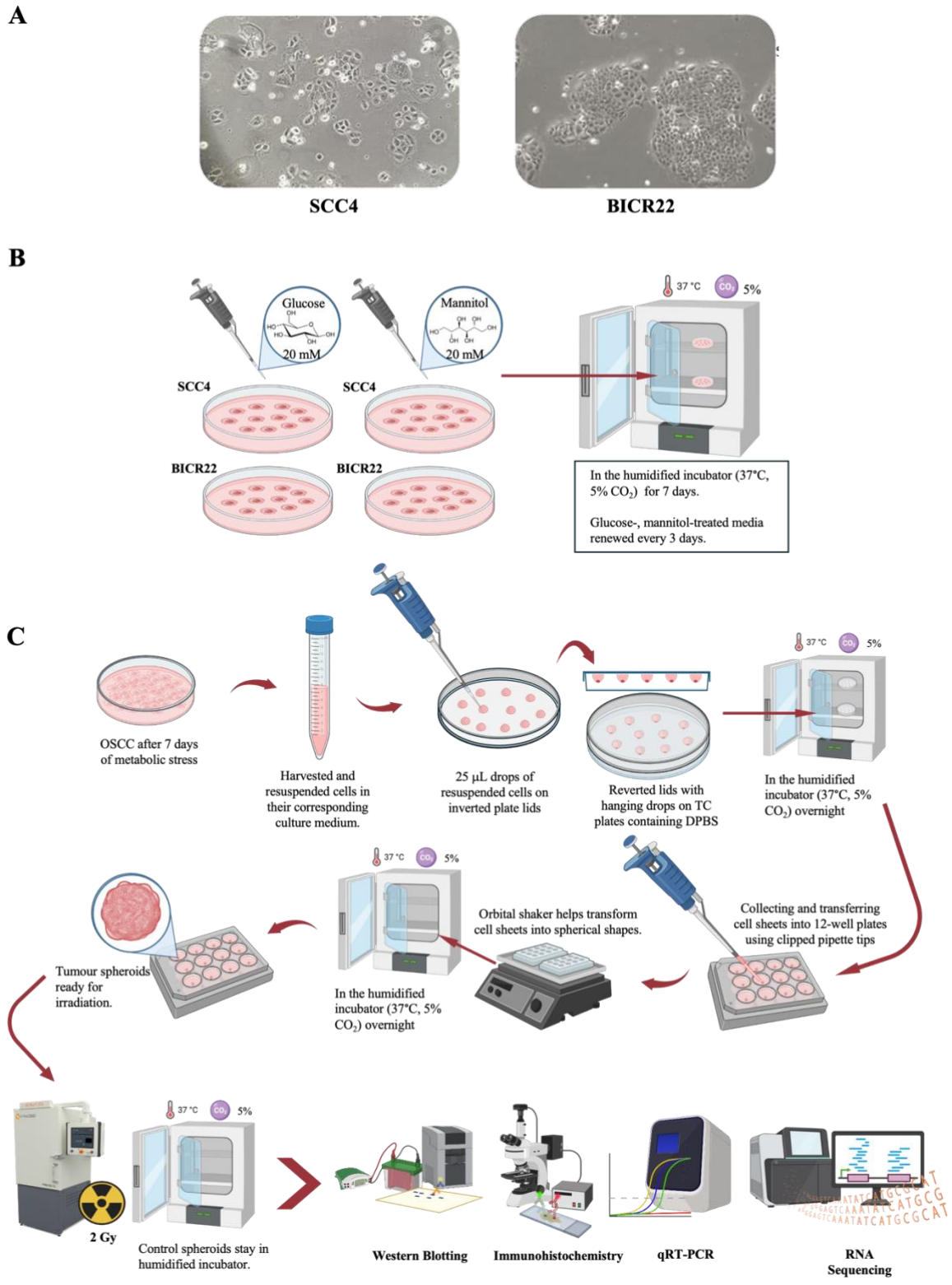

Figure 6. In vitro study of hyperglycaemic stress and irradiation in 3D tumour model derived from Oral Squamous Cell Carcinoma. **(A)** Two OSCC cell lines, SCC4 and BICR22, were utilised in the study. **(B)** Hyperglycaemic metabolic stress in OSCC. **(C)** The generation of 3D tumour spheroids and the analysis of hyperglycaemic stress in the OSCC 3D model. (Created with Biorender.com)

3.1. Hyperglycaemic metabolic stress has no significant effect on the accumulation of radiation-induced DNA double-stranded breaks (DSBs) in OSCC tumour spheroids.

Ionising radiation has been employed as an effective treatment for various types of cancer, including advanced-stage OSCC. This therapeutic approach induces a range of lethal damage to the cellular and genetic structures of cancer cells. High-energy X-rays inflict direct damage on the DNA strands of cancer cells and generate reactive oxygen species (ROS), which further compromise genetic integrity, leading to genomic instability and, ultimately, cell death (83). H2AX is a variant of histone protein H2A, when, as an early response to DNA double-stranded breaks (DSBs), phosphorylated at serine 139, is designated as γ-H2AX. γ-H2AX is recruited at the site of DNA damage to initiate the DNA repair processes (84, 85).

To assess the effect of hyperglycaemia on the accumulation of radiation-induced DNA damage, total protein was extracted from both irradiated and non-irradiated hyperglycaemic-stressed OSCC spheroids at 2 h and 24 h post-IR for western blotting experiment against γ-H2AX, a sensitive marker for DNA DSBs, with Vinculin as loading control (Figure 7A).

γ-H2AX expression was observed in both non-irradiated SCC4 spheroids treated with glucose and mannitol (Figure 7B). The level of γ-H2AX was elevated in hyperglycaemic-stressed spheroids; however, it notably declined after radiation exposure. This might indicate early activation of DNA damage response (DDR) mechanisms. However, this DDR was possibly suppressed after activation, as the reduction was offset at 24 h post-IR, with all bands maintaining a similarly elevated γ-H2AX level, indicating high levels of accumulated DSBs.

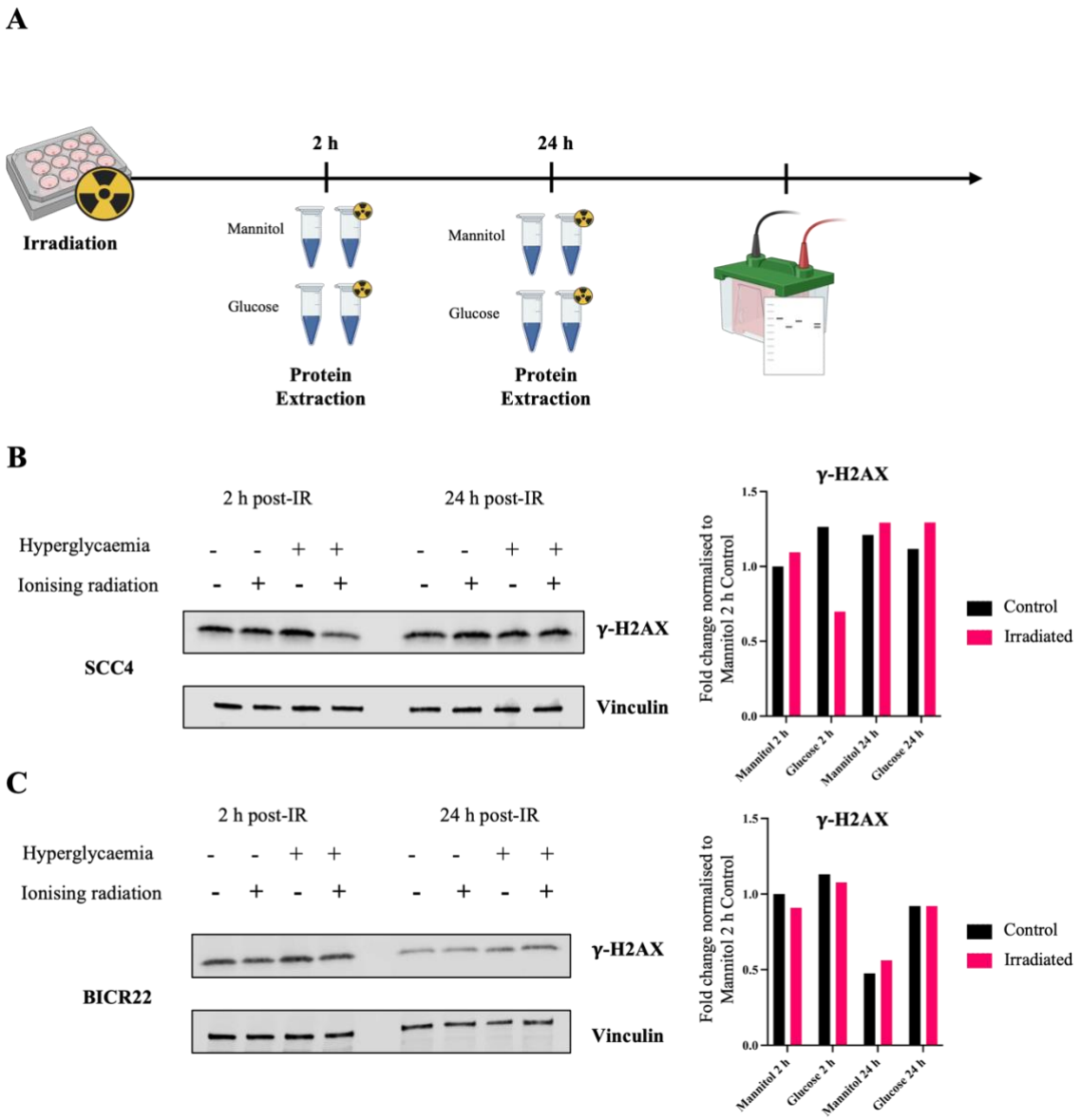

Figure 7. The effect of hyperglycaemic metabolic stress on OSCC-derived spheroids in response to ionising radiation. **(A)** Timeline of total protein extraction from irradiated spheroids for the experiment. (Created with Biorender.com) **(B)** γ-H2AX expression levels in SCC4 spheroids in response to hyperglycaemia and IR. **(C)** γ-H2AX expression levels in BICR22 spheroids in response to hyperglycaemia and IR. Vinculin was utilised as the loading control. Bar graphs in **(B)** and **(C)** represent the quantification of the γ-H2AX band density.

Tumour spheroids from BICR22 cells also exhibited an elevated level of γ-H2AX expression in glucose- and mannitol-treated samples (Figure 7C). Unlike the SCC4-derived spheroids, there was no significant radiation-induced change in γ-H2AX expression in either group. This pattern persisted for up to 24 hours post-IR in both glucose- and mannitol-treated

samples, despite an overall decline in γ-H2AX levels. This reduction may indicate the activation of DDR and DNA repair mechanisms, thereby resolving the DNA DSBs.

In summary, although observation on γ-H2AX expression varies between SCC4 and BICR22, these findings indicate that hyperglycaemia does not significantly affect the occurrence of radiation-induced DNA double-strand breaks (DSBs) or their subsequent resolution.

3.2. OSCC tumour spheroids exposed to hyperglycaemic conditions demonstrate a higher abundance of intermediate hybrid EMT states along the E-M axis.

EMT has been a key focus in cancer research due to its significant role in tumour metastasis and resistance to therapies. On the other hand, hyperglycaemic conditions have been extensively studied and demonstrated to have substantial impacts on cancer progression, treatment strategies, and survivability. Hyperglycaemia promotes inflammation and oxidative stress through various signalling pathways, including TGF-β/Smad, Wnt/β-catenin, and NF-κB pathways, which also have the potential to alter the expression of EMT markers such as E-cadherin, N-cadherin, and Vimentin (86-88).

In order to investigate the impact of hyperglycaemia on cancer EMT, we obtained spheroids generated from metabolically stressed OSCC cells that were cultivated in a medium containing 20 mM glucose (or 20 mM mannitol as an osmolarity control) and exposed them to 2 Gy of ionising radiation. The spheroids were subsequently cryo-sectioned into 8-µm sections, which were subjected to immunohistochemistry utilising antibodies directed against E-cadherin (ECAD, an epithelial marker) and Vimentin (VIM, a mesenchymal marker) (Figure 8A). The representative images of the resulting immunofluorescent staining, which illustrate ECAD and VIM in the spheroid sections derived from SCC4 and BICR22, are presented in Figures 8B and 9A, respectively.

3.2.1. Hyperglycaemic metabolic stress promotes EMT remodelling toward hybrid EMT states in SCC4 spheroids.

Research on EMT remodelling has revealed that this phenotypic transition is not a simple binary transformation of epithelial into mesenchymal cells (38, 39, 47). Instead, it is a multi-step process that transits through intermediate states with high plasticity, known as partial or hybrid EMT. Cells exhibiting hybrid EMT characteristics show traits of both epithelial and mesenchymal cells and express their respective canonical markers (48).

The immunohistochemical staining of antibodies against ECAD and VIM on sections of tumour spheroids derived from metabolically stressed SCC4 cells demonstrated the expression and precise localisation of both markers at the single-cell level (Figure 8B). Here, we observed the presence of a hybrid EMT cell subpopulation expressing both ECAD and VIM ($ECAD_{Pos}$-VIM_{Pos}) in both mannitol- and glucose-stressed spheroids, with varying levels of ECAD expression. The quantitative analysis of this cellular subpopulation reveals a higher abundance of hybrid EMT cells in spheroids cultivated under hyperglycaemic conditions, highlighting the impact of hyperglycaemia on the EMT process (***$p < 0.001$) (Figure 8C).

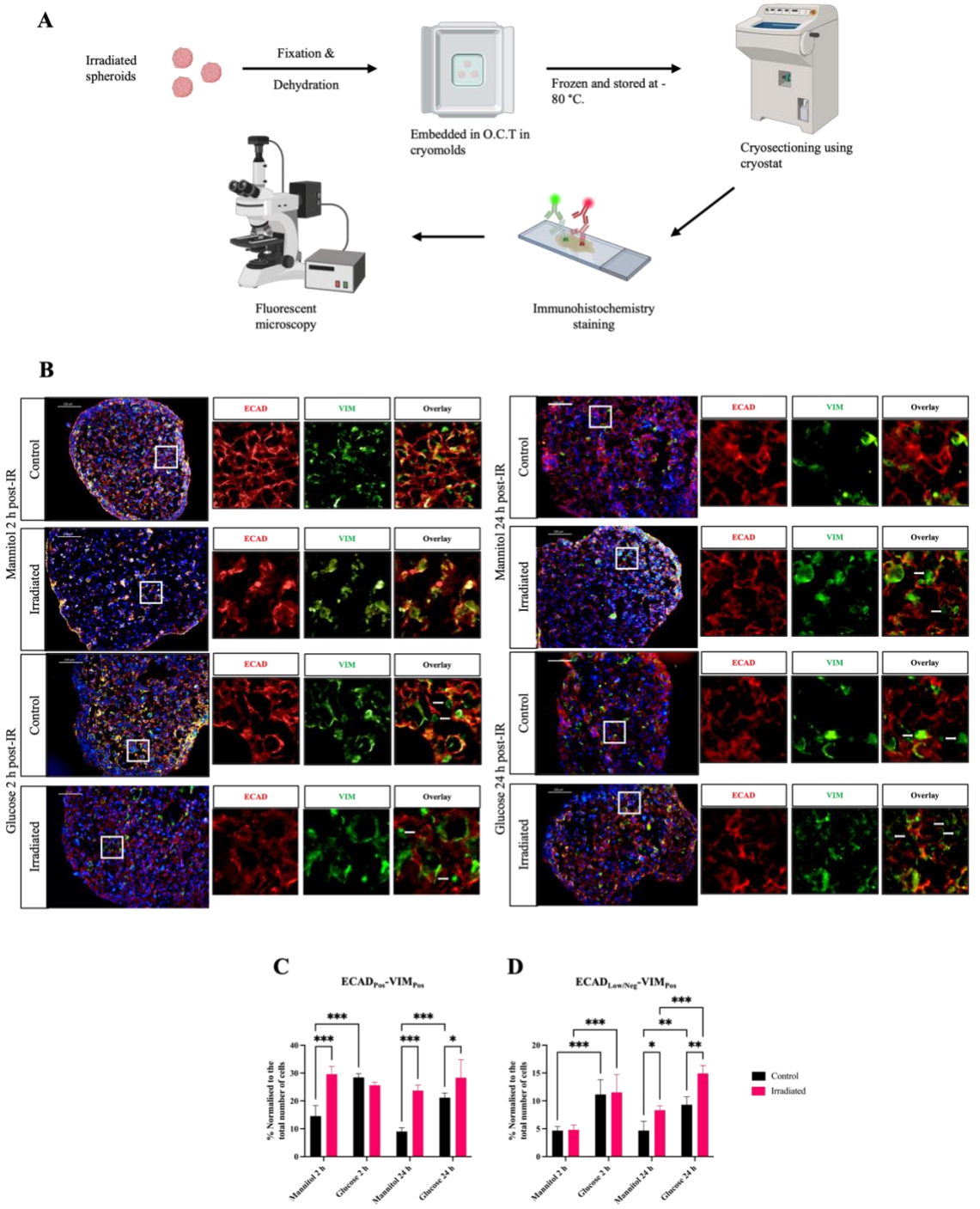

Figure 8. The hyperglycaemia-induced phenotypic switch along the epithelial-mesenchymal axis in SCC4-derived tumour spheroids with and without exposure to IR. **(A)** The collection and preparation of OSCC-derived tumour spheroids at 2 h and 24 h post-irradiation for immunohistochemistry. **(B)** The representative images of immunohistochemical stained with antibodies against the canonical epithelial and mesenchymal markers, E-cadherin (ECAD, red) and Vimentin (VIM, green), respectively, on irradiated (2 Gy) and non-irradiated SCC4-derived spheroids, with and without hyperglycaemic stress, collected at 2 h and 24 h post-irradiation (scale bar: 10 µm). The cell nuclei were counterstained with Hoechst (blue). Arrows indicate cells with $ECAD_{Low/Neg}$-VIM_{Pos} phenotype. **(C)** Bar graph demonstrating the quantification of hybrid EMT cells ($ECAD_{Pos}$-VIM_{Pos}). **(D)** Bar graph demonstrating the quantification of $ECAD_{Low/Neg}$-VIM_{Pos} cells. The quantification was performed on experimental triplicates. Statistical analysis was conducted with two-way ANOVA (*$p < 0.05$, **$p < 0.01$, ***$p < 0.001$). Values represent *mean ± SD*.

The spheroids were exposed to 2 Gy of ionising radiation to assess the potential effects of hyperglycaemia on EMT remodelling in response to radiation. Following irradiation, a notable early elevation in the hybrid cell population was observed in mannitol-stressed spheroids just 2 h post-IR (***$p < 0.001$). In contrast, hyperglycaemic spheroids did not show a comparable increase until the 24-hour timepoint; however, the increase was not as significant as in mannitol samples (*$p < 0.05$) due to a much higher baseline of hybrid EMT cell abundance in non-irradiated spheroids (***$p < 0.001$). Altogether, these findings suggest that hyperglycaemic metabolic stress promotes the phenotypic shift toward the hybrid EMT states in OSCC cells.

3.2.2. Exposure to hyperglycaemic conditions promotes the generation of the $ECAD_{Low/Neg}$-VIM_{Pos} cell subpopulation in SCC4 3D tumour spheroids.

Our data confirms the presence of the hybrid EMT state in OSCC spheroids and the effect of hyperglycaemia on the generation of this subpopulation. However, the hybrid E-M state has been demonstrated to exhibit high plasticity and can shift along the E-M axis in response to environmental stresses (89, 90). Our previous study on EMT remodelling in OSCC revealed the emergence of a new subpopulation expressing low to negative ECAD levels while still exhibiting high levels of VIM, referred to as $ECAD_{Low/Neg}$-VIM_{Pos}, in response to radiation (37). The generation of this phenotypic subpopulation was linked with increased invasive capacity and resistance to radiation.

Immunohistochemistry analyses of SCC4 tumour spheroid sections indicated the presence of $ECAD_{Low/Neg}$-VIM_{Pos} (Figure 8B). Quantitative analysis of this subpopulation demonstrated a significant increase in the number of $ECAD_{Low/Neg}$-VIM_{Pos} cells in spheroids exposed to hyperglycaemic conditions, regardless of the effects of irradiation (***$p < 0.001$) (Figure 8D). Following exposure to IR, no immediate change was noted in both mannitol- and glucose-treated spheroids (at 2 h post-IR). However, this increased in both groups at 24 h after irradiation. Metabolic stress in hyperglycaemic conditions seems to have shifted more cells in the spheroids toward the $ECAD_{Low/Neg}$-VIM_{Pos} in response to ionising radiation (mannitol: *$p < 0.05$, glucose: **$p < 0.01$) (Figure 8D).

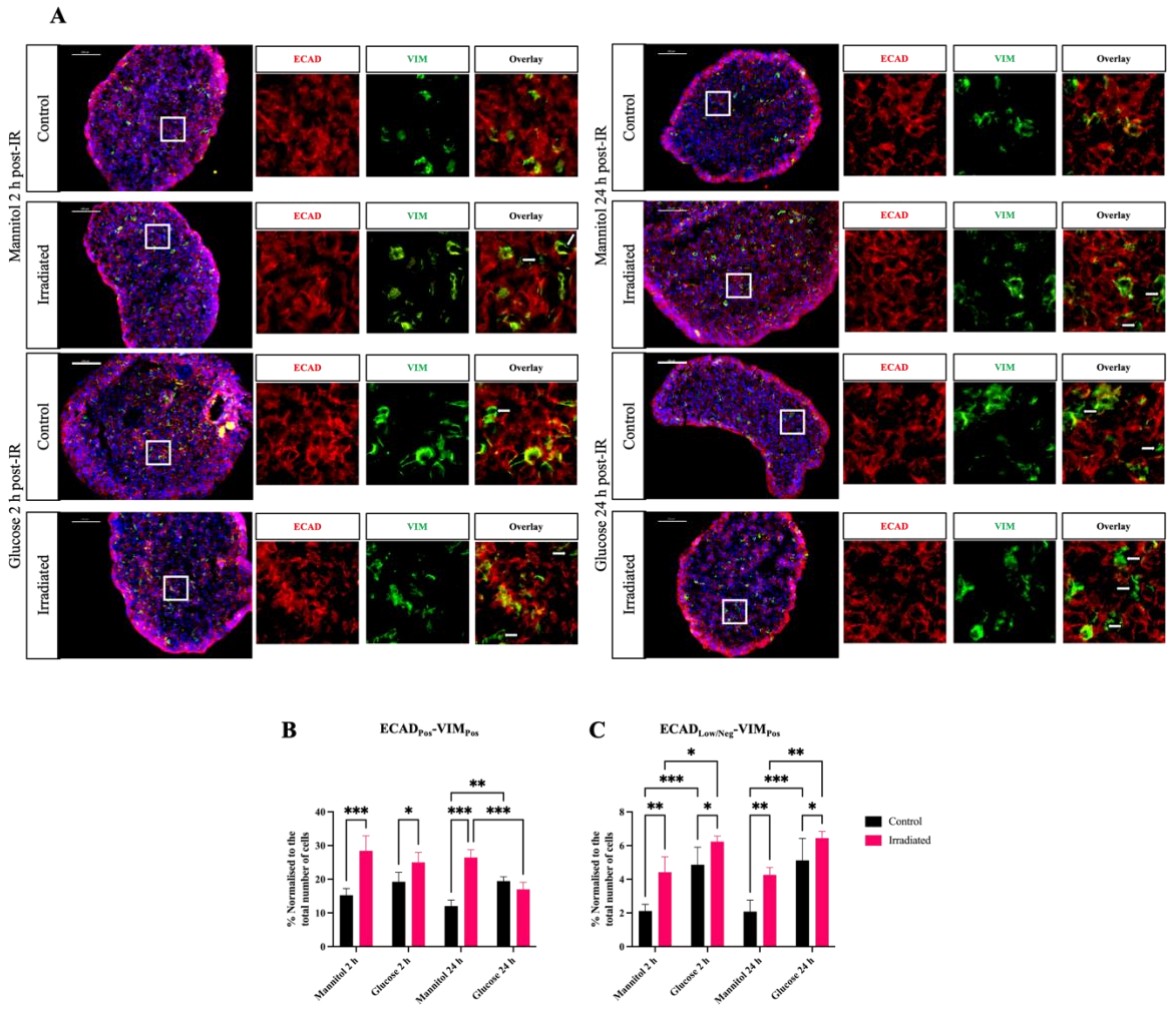

Figure 9. The hyperglycaemia-induced phenotypic switch along the epithelial-mesenchymal axis in BICR22-derived tumour spheroids with and without exposure to IR. **(A)** The representative images of immunohistochemical stained with antibodies against the canonical epithelial and mesenchymal markers, E-cadherin (ECAD, red) and Vimentin (VIM, green), respectively, on irradiated (2 Gy) and non-irradiated BICR22-derived spheroids, with and without hyperglycaemic stress, collected at 2 h and 24 h post-irradiation (scale bar: 10 µm). The cell nuclei were counterstained with Hoechst (blue). Arrows indicate cells with $ECAD_{Low/Neg}$-VIM_{Pos} phenotype. **(B)** Bar graph demonstrating the quantification of hybrid EMT cells ($ECAD_{Pos}$-VIM_{Pos}). **(C)** Bar graph demonstrating the quantification of $ECAD_{Low/Neg}$-VIM_{Pos} cells. The quantification was performed on experimental triplicates. Statistical analysis was conducted with two-way ANOVA *(*p < 0.05, **p < 0.01, ***p < 0.001*). Values represent *mean ± SD*.

To ensure that these findings are not limited to a single cell line, we performed experiments using a different OSCC cell line, BICR22, which also expressed a notable level of radioresistance following exposure to hyperglycaemic conditions. The immunohistochemistry and quantitative analyses of the sections from hyperglycaemic-stressed BICR22 tumour spheroids confirmed the presence of both $ECAD_{Pos}$-VIM_{Pos} and $ECAD_{Low/Neg}$-VIM_{Pos} subpopulations and the effect of hyperglycaemic condition on their

abundance (Figure 9). In summary, our data strongly indicate that hyperglycaemic treatment notably accelerates the phenotypic shift towards E-M hybrid states and leads to a marked transition towards a mesenchymal-like phenotype following exposure to ionising radiation.

3.2.3. Tongue tumour tissues from diabetic patients exhibit a high abundance of hybrid epithelial-mesenchymal phenotype and mesenchymal-like $ECAD_{Low/Neg}$-VIM_{Pos} subpopulations.

Recognising that tumour structures exhibit greater cellular and molecular complexity than 3D tumour spheroids, we investigated whether the phenotypic transition along the E-M axis occurs in tongue tumour tissues and whether hyperglycaemic conditions in diabetic patients influence this cellular transition.

Figure 10A displays representative images of haematoxylin and eosin (H&E) staining, along with immunohistochemistry staining of tongue cancer tissue sections from diabetic and non-diabetic patients. The immunofluorescent images reveal the existence of the hybrid E-M cell population in both diabetic and non-diabetic tumour tissues (Figure 10A). Additionally, these images indicate a more significant presence of $ECAD_{Low/Neg}$-VIM_{Pos} cells in the tissues from diabetic tumours. Quantification of these subpopulations reaffirmed this observation and further supported our findings about the impact of hyperglycaemic conditions on the phenotypic transition (Figure 10B).

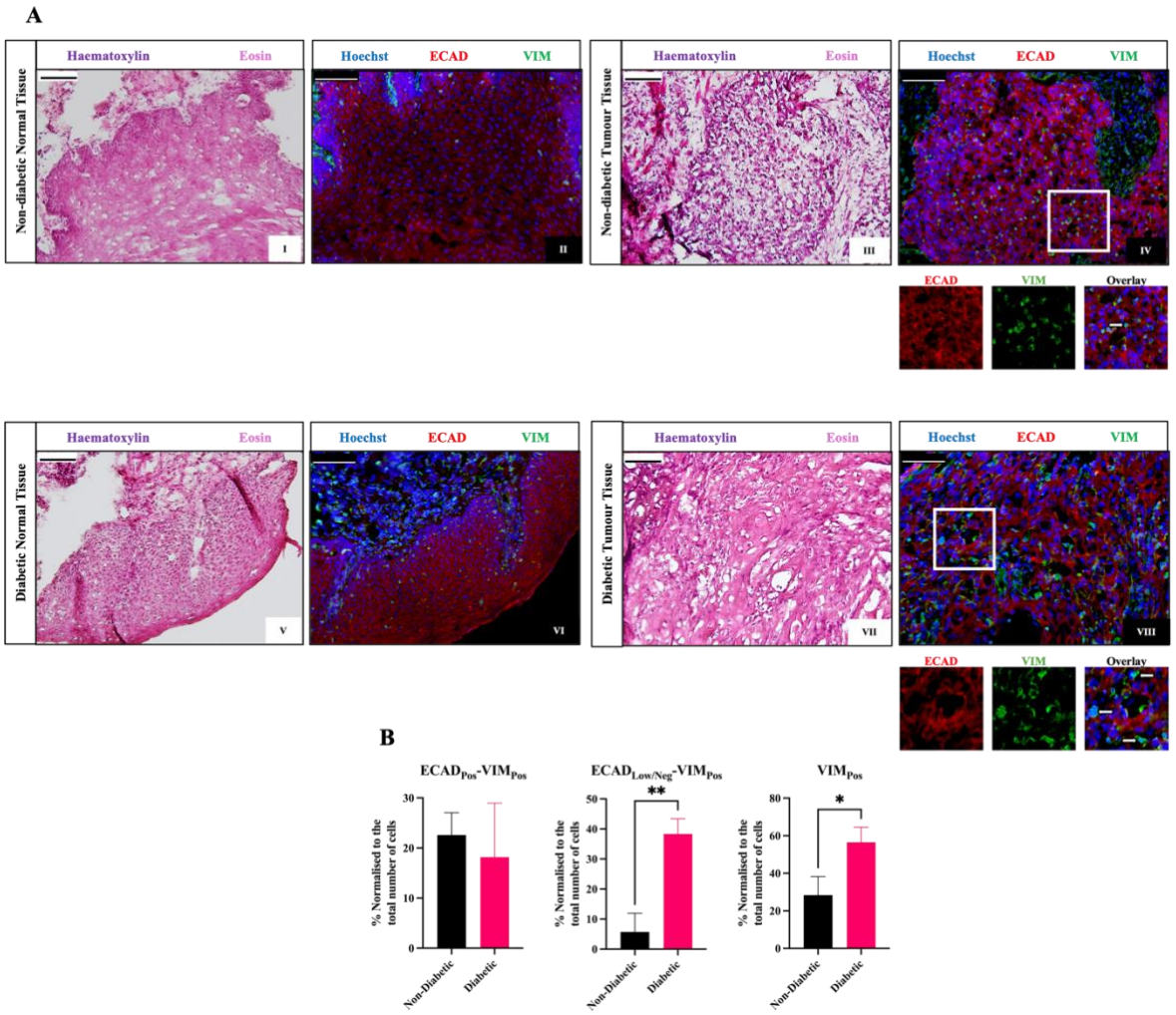

Figure 10. The states of EMT in tumour tissues from cancer patients with diabetes. **(A)** I, III, V, and VII: Haematoxylin (blue) and eosin (red) staining on normal and tumour tissue samples from non-diabetic and diabetic patients (scale bar: 100 µm). II, IV, VI, and VIIII: Immunofluorescent staining on the normal tongue and tongue tumour tissue samples from non-diabetic and diabetic patients with antibodies against E-cadherin (ECAD, epithelial marker, red) and Vimentin (VIM, mesenchymal marker, green) counterstained with Hoechst (nuclei, blue) (scale bar: 100 µm). Arrows indicate cells with $ECAD_{Low/Neg}$-VIM_{Pos} phenotype. **(B)** Bar graph demonstrating the quantitative analysis on non-diabetic and diabetic tumour tissues. The quantification was performed on experimental triplicates. Statistical analysis was conducted with two-way ANOVA *(*p < 0.05, **p < 0.01, ***p < 0.001*). Values represent *mean ± SD*.

3.3. The influence of hyperglycaemic conditions on EMT-inducing transcription factor regulation during the phenotypic transition along the E-M axis in OSCC spheroids.

The phenotypic transition along the E-M axis is primarily driven by the active modulation of EMT transcription factors (TFs), including ZEB1, SNAIL, SLUG, and TWIST. These factors facilitate the transformation of epithelial cells through various intermediate hybrid states with high levels of plasticity, ultimately progressing towards a mesenchymal state that shows enhanced invasiveness and resistance. In order to evaluate the regulation of these transcription factors under hyperglycaemic conditions and in response to exposure to ionising radiation, a quantitative reverse transcription polymerase chain reaction (qRT-PCR) analysis was conducted on the total RNA samples extracted from the metabolic-stressed SCC4 and BICR22-derived tumour spheroids. This analysis included an assessment of the transcriptional expression of four EMT-driving transcription factors alongside the expression levels of E-cadherin and Vimentin.

In SCC4-derived spheroids without radiation exposure, both SNAIL and SLUG exhibited a significant reduction in hyperglycaemic samples (SNAIL: $***p < 0.001$ at 24 h; SLUG: $*p < 0.05$ at 2 h and $***p < 0.001$ at 24 h) (Figure 11A). Two hours after exposure to 2 Gy of radiation, an upregulation of SLUG expression level was detected in both mannitol- and glucose-stressed samples; however, the significance was less pronounced in glucose ($*p < 0.05$) than in mannitol ($***p < 0.001$). In contrast, SNAIL was upregulated at 24 h after irradiation in hyperglycaemic spheroids ($***p < 0.001$), while downregulated in mannitol-treated spheres ($***p < 0.001$). No notable differences were observed in the transcriptional expression levels of ZEB1 and TWIST in SCC4 spheroids treated with glucose versus those treated with mannitol without irradiation. Following IR exposure, the expression levels of both factors increased in hyperglycaemic-stressed spheroids compared to the irradiated mannitol-stressed spheroids (ZEB1: $*p < 0.05$ and TWIST: $**p < 0.01$). Lastly, there were alterations in the expression levels of ECAD and VIM in response to hyperglycaemic conditions and irradiation, yet these changes lacked statistical significance.

In spheroids originating from BICR22, the hyperglycaemic conditions heightened the expression of TWIST (***$p < 0.001$); conversely, SNAIL levels in all hyperglycaemic samples were notably diminished regardless of irradiation (***$p < 0.001$) (Figure 11B). Two hours following IR exposure, both SNAIL and TWIST levels in hyperglycaemic spheroids were reduced compared to control samples. However, no notable changes were detected in the transcriptional level of ZEB1 and SLUG. Both ECAD (***$p < 0.001$) and VIM (**$p < 0.01$) exhibited an increased expression in the BICR22 spheroids when subjected to hyperglycaemic conditions. After IR, VIM expression level remained relatively unchanged across both treatments. Conversely, ECAD was downregulated in spheroids treated with glucose (**$p < 0.01$), in contrast to its upregulation in those treated with mannitol (***$p < 0.001$). The decrease in ECAD expression in glucose-treated spheroids persisted 24 h after IR (*$p < 0.05$).

In summary, our qRT-PCR analysis has highlighted the influence of hyperglycaemic conditions on the expression of EMT transcription factors and both epithelial and mesenchymal markers. This demonstrates their involvement in the E-M phenotypic transition in OSCC and provides valuable insights into the response to metabolic stress and radiation exposure.

3.4. The transcriptional profiling analysis in irradiated spheroids under hyperglycaemic conditions explores some potential underlying molecular players

The observed changes in E-M phenotypes and transcription factor regulation suggest hyperglycaemia enhances dynamic molecular remodelling in OSCC spheroids during the first 24 h after ionising radiation exposure. To further investigate the transcriptional dynamics of OSCC spheroids in response to environmental stimuli, we conducted RNA sequencing on total RNA obtained from irradiated glucose- and mannitol-treated SCC4-derived spheroids exposed to 2 Gy of radiation at both 2 h and 24 h, alongside their control samples (Figure 12A).

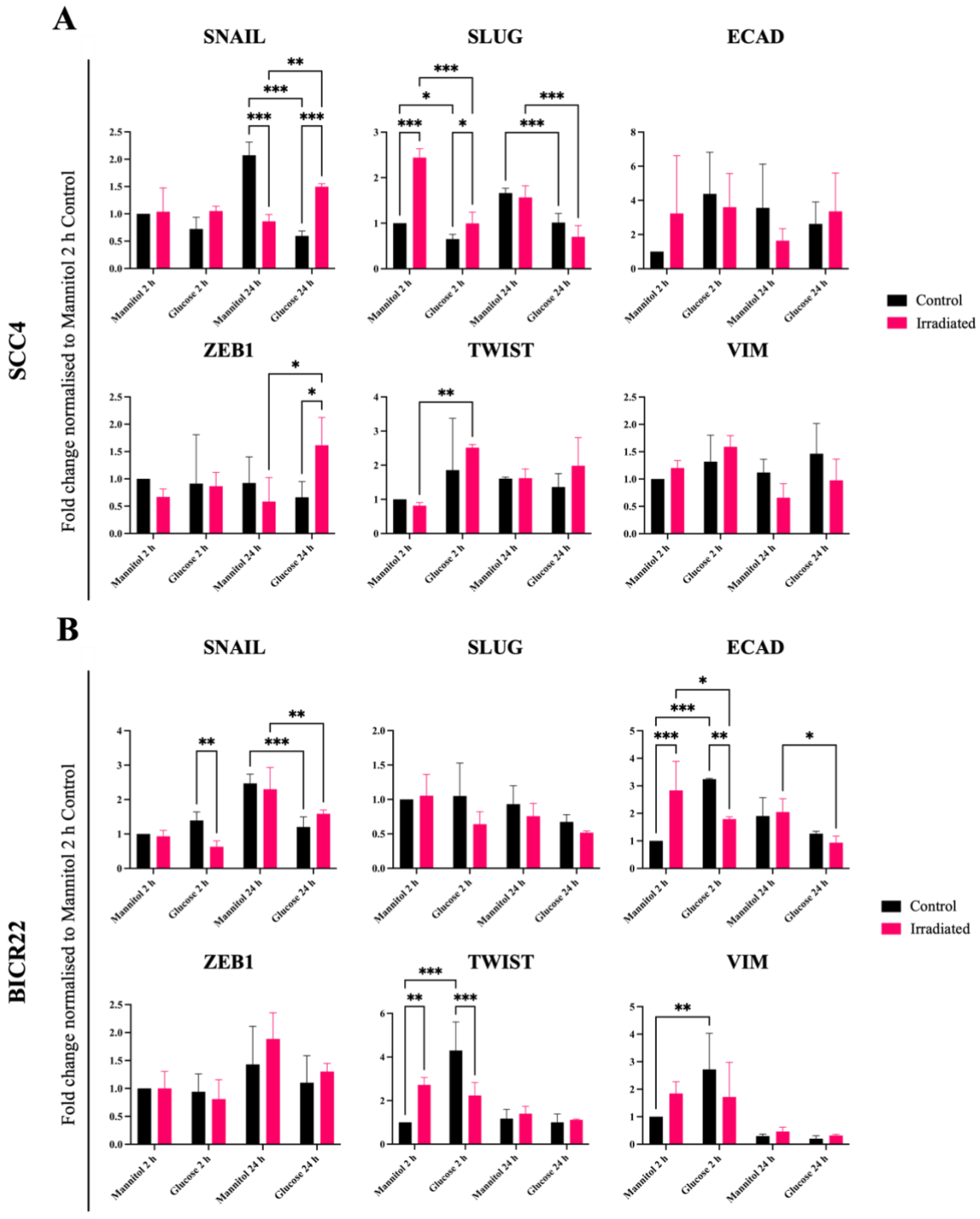

Figure 11. The hyperglycaemia-induced regulation of EMT Transcription Factors in OSCC-derived tumour spheroids in response to IR. Quantitative RT-PCR analysis was conducted on total RNA extracted from hyperglycaemic and non-hyperglycaemic **(A)** SCC4- and **(B)** BICR22-derived spheroids with and without being exposed to 2 Gy IR to assess the regulation of EMT TFs (SNAIL, SLUG, ZEB1, and TWIST), E-cadherin (ECAD, epithelial marker), and Vimentin (VIM, mesenchymal marker) in response to hyperglycaemic metabolic stress and IR. The results shown are representative of experimental triplicates. Values represented *mean ± SD* (*$p < 0.05$, **$p < 0.01$, ***$p < 0.001$).

In elaborating the effects of hyperglycaemia, the transcriptional analysis of differentially expressed genes (DEGs) was assessed between hyperglycaemic stressed samples and mannitol-treated samples. At the 2-hour mark, 643 DEGs were identified, while 494 DEGs were recorded at 24 h. Notably, 105 DEGs were common to both groups, indicating the baseline impact of hyperglycaemic metabolic stress on SCC4 cells (Figure 12B). Among these DEGs, we noticed an upregulation of Lactate Dehydrogenase A (LDHA), which catalyses the conversion of pyruvate to lactate, confirming the glucose uptake of the cells under hyperglycaemic conditions. Subsequently, we conducted a pathway enrichment analysis on the DEGs that were common across both time points, using the comprehensive gene set enrichment analysis tool developed by the Ma'ayan Lab (https://maayanlab.cloud/Enrichr/#) (Figure 12C). Hyperglycaemic metabolic stress affected the organisation of the extracellular matrix (ECM), focal adhesion, and the interactions between the membrane and the ECM (Figure 12C). Moreover, hyperglycaemic conditions affected SCC4 cells across various cancer-related pathways, such as PI3K/Akt/mTOR, TNF, Integrins, and WNT signalling. The effects of hyperglycaemia on EMT-related molecular signalling were also observed, suggesting possible molecular pathways that might clarify how hyperglycaemic conditions are associated with phenotypic remodelling along the E-M axis (Figure 12C).

An in-depth analysis of the transcriptional changes in SCC4 spheroids treated with glucose and mannitol, both with and without irradiation, identified 1467 DEGs in hyperglycaemic spheroids at 2 h and 1058 DEGs at 24 h post-irradiation. For mannitol-treated samples, 1001 DEGs were detected at 2 h and 632 DEGs at 24 h after irradiation (see Figure 12D). Although the count of DEGs in both conditions at 24 h following exposure to ionising radiation, glucose-treated samples consistently showed a higher DEG count than mannitol-treated samples, indicating that irradiation induces greater genomic instability in the glucose-treated spheroids.

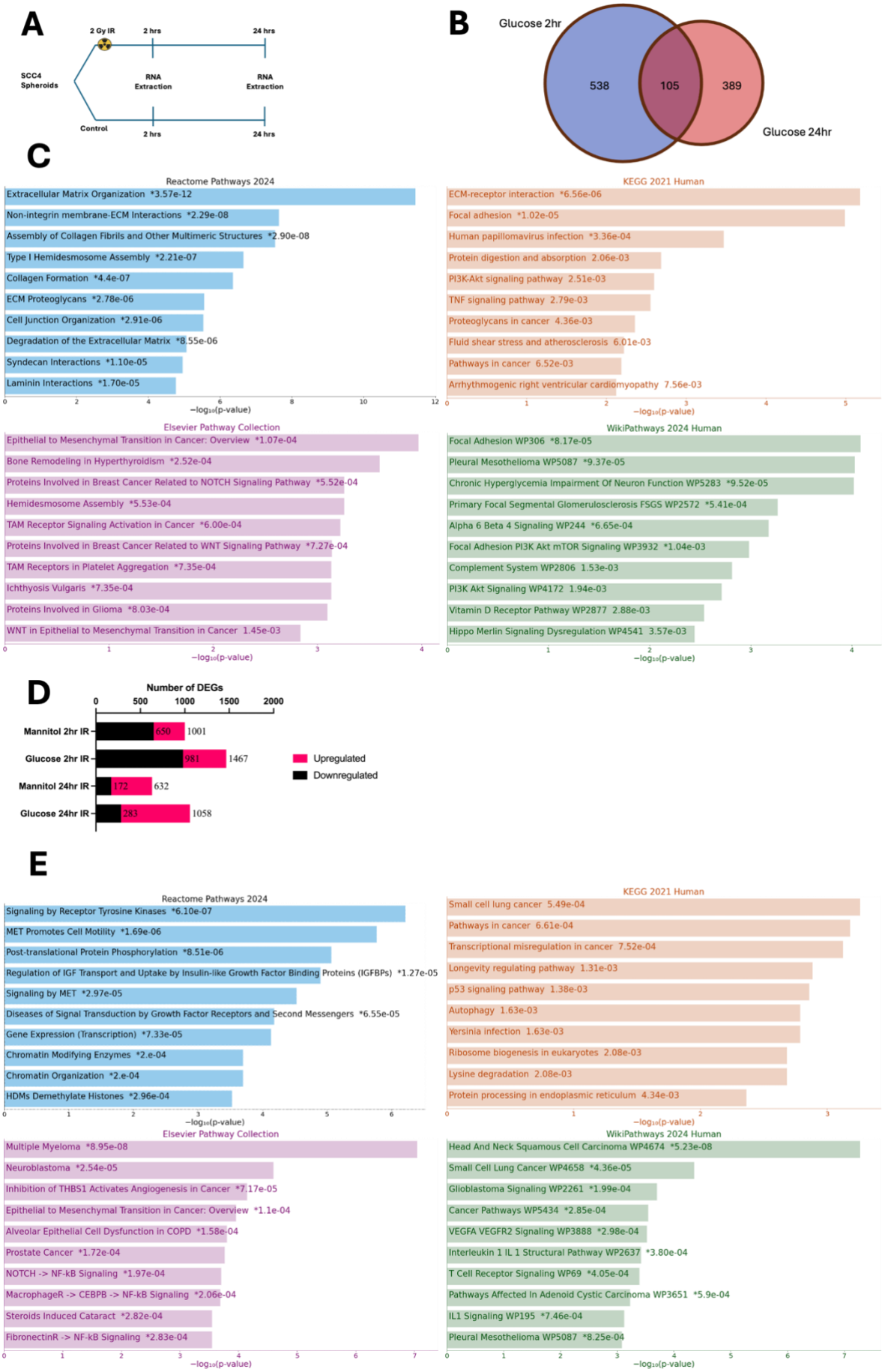
A
2 Gy IR
2 hrs
24 hrs
SCC4 Spheroids
RNA Extraction
RNA Extraction
Control
2 hrs
24 hrs
B
Glucose 2hr
538
105
389
Glucose 24hr
C
Reactome Pathways 2024
Extracellular Matrix Organization *3.57e-12
Non-integrin membrane-ECM Interactions *2.29e-08
Assembly of Collagen Fibrils and Other Multimeric Structures *2.90e-08
Type I Hemidesmosome Assembly *2.21e-07
Collagen Formation *4.4e-07
ECM Proteoglycans *2.78e-06
Cell Junction Organization *2.91e-06
Degradation of the Extracellular Matrix *8.55e-06
Syndecan Interactions *1.10e-05
Laminin Interactions *1.70e-05
−log10(p-value)
KEGG 2021 Human
ECM-receptor interaction *6.56e-06
Focal adhesion *1.02e-05
Human papillomavirus infection *3.36e-04
Protein digestion and absorption 2.06e-03
PI3K-Akt signaling pathway 2.51e-03
TNF signaling pathway 2.79e-03
Proteoglycans in cancer 4.36e-03
Fluid shear stress and atherosclerosis 6.01e-03
Pathways in cancer 6.52e-03
Arrhythmogenic right ventricular cardiomyopathy 7.56e-03
−log10(p-value)
Elsevier Pathway Collection
Epithelial to Mesenchymal Transition in Cancer: Overview *1.07e-04
Bone Remodeling in Hyperthyroidism *2.52e-04
Proteins Involved in Breast Cancer Related to NOTCH Signaling Pathway *5.52e-04
Hemidesmosome Assembly *5.53e-04
TAM Receptor Signaling Activation in Cancer *6.00e-04
Proteins Involved in Breast Cancer Related to WNT Signaling Pathway *7.27e-04
TAM Receptors in Platelet Aggregation *7.35e-04
Ichthyosis Vulgaris *7.35e-04
Proteins Involved in Glioma *8.03e-04
WNT in Epithelial to Mesenchymal Transition in Cancer 1.45e-03
−log10(p-value)
WikiPathways 2024 Human
Focal Adhesion WP306 *8.17e-05
Pleural Mesothelioma WP5087 *9.37e-05
Chronic Hyperglycemia Impairment Of Neuron Function WP5283 *9.52e-05
Primary Focal Segmental Glomerulosclerosis FSGS WP2572 *5.41e-04
Alpha 6 Beta 4 Signaling WP244 *6.65e-04
Focal Adhesion PI3K Akt mTOR Signaling WP3932 *1.04e-03
Complement System WP2806 1.53e-03
PI3K Akt Signaling WP4172 1.94e-03
Vitamin D Receptor Pathway WP2877 2.88e-03
Hippo Merlin Signaling Dysregulation WP4541 3.57e-03
−log10(p-value)
D
Number of DEGs
0
500
1000
1500
2000
Mannitol 2hr IR
650
1001
Glucose 2hr IR
981
1467
Mannitol 24hr IR
172
632
Glucose 24hr IR
283
1058
Upregulated
Downregulated
E
Reactome Pathways 2024
Signaling by Receptor Tyrosine Kinases *6.10e-07
MET Promotes Cell Motility *1.69e-06
Post-translational Protein Phosphorylation *8.51e-06
Regulation of IGF Transport and Uptake by Insulin-like Growth Factor Binding Proteins (IGFBPs) *1.27e-05
Signaling by MET *2.97e-05
Diseases of Signal Transduction by Growth Factor Receptors and Second Messengers *6.55e-05
Gene Expression (Transcription) *7.33e-05
Chromatin Modifying Enzymes *2.e-04
Chromatin Organization *2.e-04
HDMs Demethylate Histones *2.96e-04
−log10(p-value)
KEGG 2021 Human
Small cell lung cancer 5.49e-04
Pathways in cancer 6.61e-04
Transcriptional misregulation in cancer 7.52e-04
Longevity regulating pathway 1.31e-03
p53 signaling pathway 1.38e-03
Autophagy 1.63e-03
Yersinia infection 1.63e-03
Ribosome biogenesis in eukaryotes 2.08e-03
Lysine degradation 2.08e-03
Protein processing in endoplasmic reticulum 4.34e-03
−log10(p-value)
Elsevier Pathway Collection
Multiple Myeloma *8.95e-08
Neuroblastoma *2.54e-05
Inhibition of THBS1 Activates Angiogenesis in Cancer *7.17e-05
Epithelial to Mesenchymal Transition in Cancer: Overview *1.1e-04
Alveolar Epithelial Cell Dysfunction in COPD *1.58e-04
Prostate Cancer *1.72e-04
NOTCH -> NF-kB Signaling *1.97e-04
MacrophageR -> CEBPB -> NF-kB Signaling *2.06e-04
Steroids Induced Cataract *2.82e-04
FibronectinR -> NF-kB Signaling *2.83e-04
−log10(p-value)
WikiPathways 2024 Human
Head And Neck Squamous Cell Carcinoma WP4674 *5.23e-08
Small Cell Lung Cancer WP4658 *4.36e-05
Glioblastoma Signaling WP2261 *1.99e-04
Cancer Pathways WP5434 *2.85e-04
VEGFA VEGFR2 Signaling WP3888 *2.98e-04
Interleukin 1 IL 1 Structural Pathway WP2637 *3.80e-04
T Cell Receptor Signaling WP69 *4.05e-04
Pathways Affected In Adenoid Cystic Carcinoma WP3651 *5.9e-04
IL1 Signaling WP195 *7.46e-04
Pleural Mesothelioma WP5087 *8.25e-04
−log10(p-value)

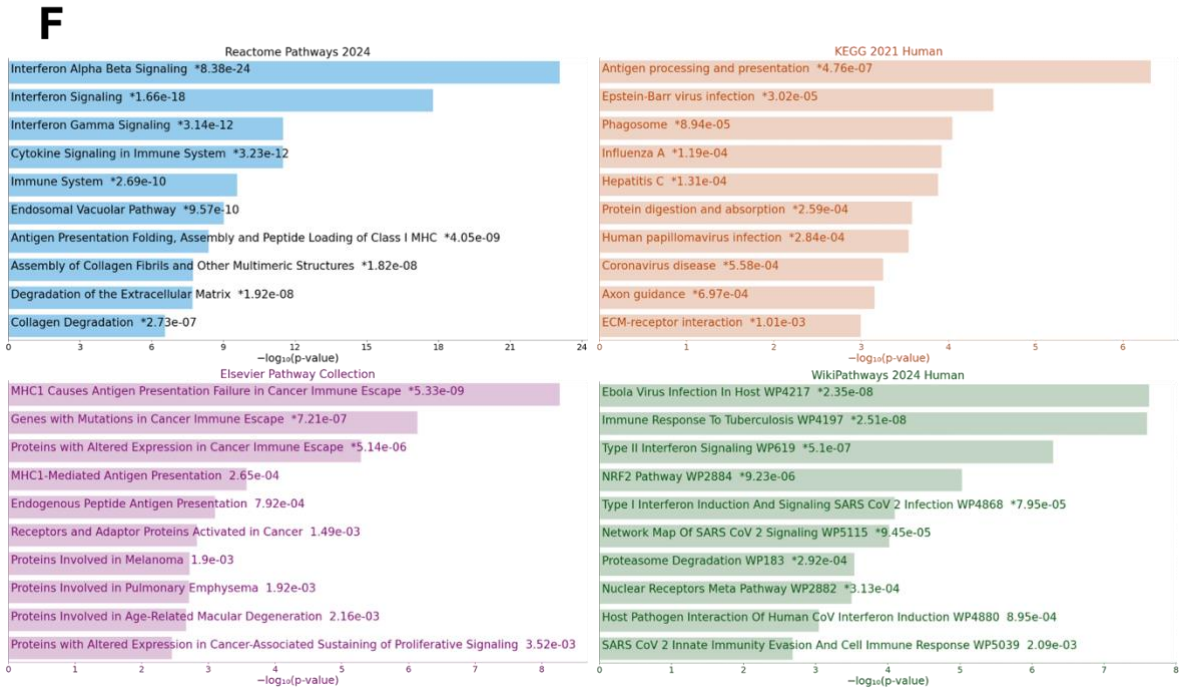

Figure 12. The transcriptomic profiling and pathway analyses of irradiated SCC4 spheroids under metabolic stress induced by hyperglycaemic condition. **(A)** The experimental design and timeline of sample extraction from SCC4 spheroids for RNA Sequencing analysis. **(B)** Venn diagram showing the number of differentially expressed genes (DEGs) in response to the hyperglycaemic condition. **(C)** Pathway enrichment analyses from the common DEGs in **(B)**. **(D)** Number of DEGs in irradiated mannitol- and glucose-treated spheroids vs respective control (non-irradiated). **(E)** Pathway enrichment analyses from the DEGs in irradiated glucose-treated spheroids at 2 h vs the non-irradiated in **(D)**. **(F)** Pathway enrichment analyses from the DEGs in irradiated glucose-treated spheroids at 24 h vs the non-irradiated in **(D)**. In **(C), (E), and (F),** only the top 10 differentially expressed pathways from each database are demonstrated.

Two hours after IR, over half of the differentially expressed genes (DEGs) were downregulated (65% in glucose, 67% in mannitol), suggesting (Figure 12D). Ionising radiation influenced numerous cancer-related pathways, including MET signalling, Receptor Tyrosine Kinase (RTK), NOTCH, NF-κB signalling, and pathways connected to epithelial-mesenchymal transition (EMT) in hyperglycaemic samples (Figure 12E). Furthermore, pathways associated with immune responses, such as Interleukin-1 (IL-1) and Tumour Necrosis Factor (TNF), were also affected in response to hyperglycaemic conditions and irradiation (Figure 12E).

Twenty-four hours after radiation exposure, the total number of DEGs in samples treated with glucose and mannitol decreased but remained high in glucose-treated spheroids (Figure 12D). Most radiation-induced DEGs were upregulated in both treatment groups, with 460 out of 632 DEGs in mannitol and 775 out of 1058 in glucose-treated spheroids (Figure 12D). The pathway enrichment analysis of DEGs from irradiated hyperglycaemic-stressed spheroids showed significant dysregulation in immune response and immune escape signalling pathways, indicated by the upregulation of human leukocyte antigens (HLAs) (Figure 12F). Furthermore, the analysis of pathways ranked below the top 10 displayed in Figure 12F revealed several pathways linked to cancer progression, including the AKT, MAPK, and MET signalling pathways. Based on the transcriptional expression of DEGs between samples and the pathway enrichment analyses, we selected genes involved in various potential cancer- and EMT-related signalling pathways that were differentially regulated under hyperglycaemic conditions in response to irradiation for further investigation (Figure 13A). The analyses of protein interactions and co-expression conducted with the online tool STRING (https://string-db.org/) presented in Figures 13A and B uncovered a complex network of interactions among the selected genes, highlighting their correlated expressions. The potential functions of these genes in contributing to cancer progression and EMT will be thoroughly elaborated in the Discussion chapter.

To assess how hyperglycaemia affects the expression of selected genes, we conducted a qRT-PCR analysis on total RNA extracted from normal tongue tissues and tongue tumour samples from diabetic and non-diabetic oral cancer patients (Figure 13C). The integrins ITGA3, ITGAV, and ITGB4 showed increased expression in tumour tissues relative to normal tongue tissues. Additionally, the transcriptional expressions of these three integrins were considerably higher in tumour tissues from diabetic patients *(***$p < 0.001$)*, indicating that hyperglycaemic conditions may impact their linked molecular signalling, potentially affecting EMT remodelling. LAMB1, LAMC1, MMP2, and FN1 were also found to be upregulated in diabetic tumour samples when compared to diabetic normal tissues and non-diabetic tumour tissues. Although MMP9 levels were significantly greater in tongue cancer tissues from non-diabetic patients (***$p < 0.001$*), only a minor increase was noted in diabetic tumour samples, which was not statistically significant. Lastly, no notable difference in IRS1 expression was observed between the samples.

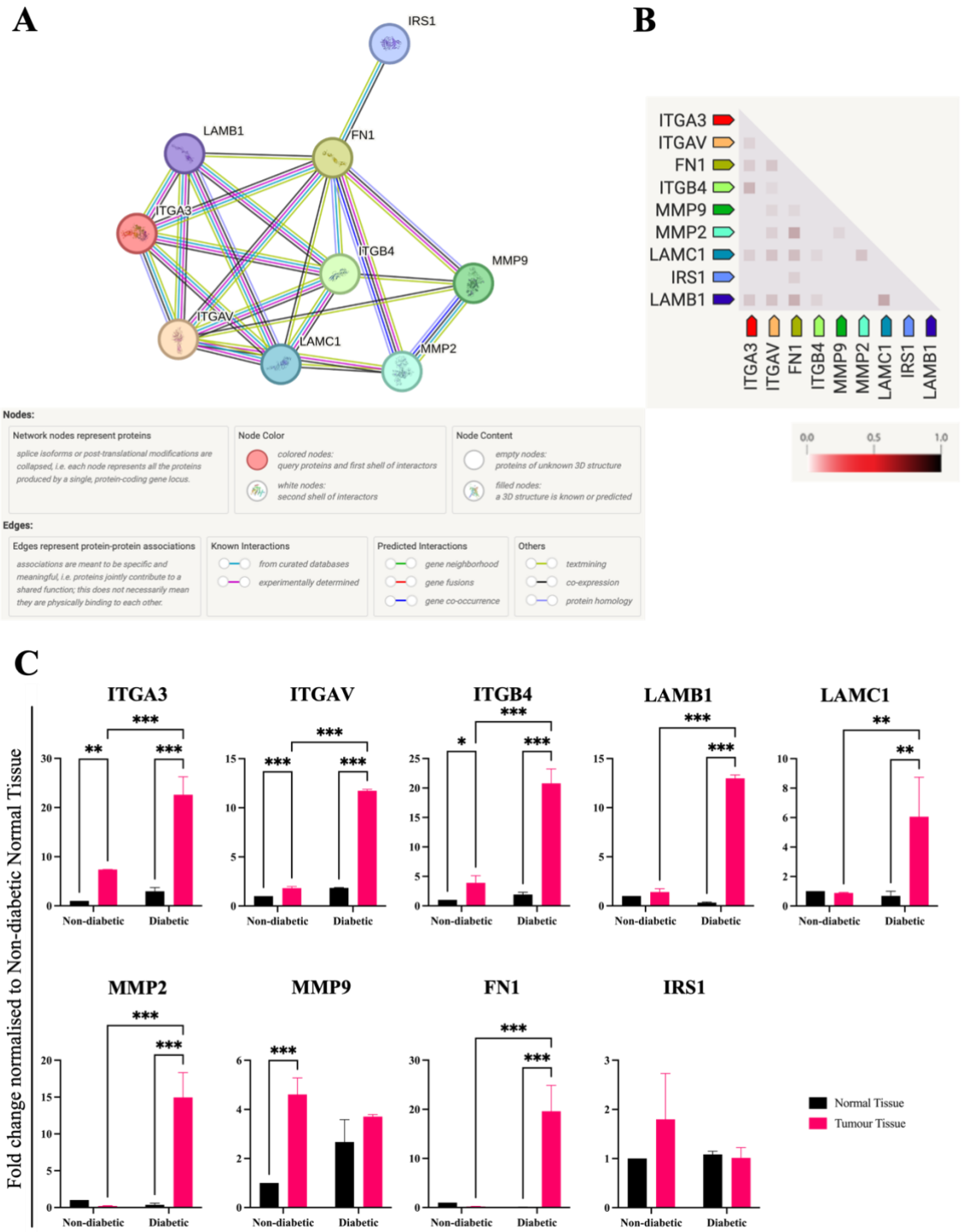

Figure 13. Potential molecular players regulating EMT remodelling and radiosensitivity of OSCC under the hyperglycaemic condition and in response to ionising radiation. **(A)** The protein interactions between the selected DEGs using the online analysis tool STRING V12.0 (https://string-db.org/). **(B)** Protein co-expression analysis of the selected DEGs using the online analysis tool STRING V12.0 (https://string-db.org/). **(C)** qRT-PCR analysis of total RNA isolated from healthy tongue and tumour samples of tongue cancer patients with and without diabetes, assessing transcriptional expression of the selected DEGs. The results shown are representative of experimental triplicates. Values represented *mean* ± *SD* (*$p < 0.05$, **$p < 0.01$, ***$p < 0.001$).

Overall, these findings confirmed the differential expression of the chosen genes under hyperglycaemic conditions identified through RNA Sequencing. This provides strong evidence to support further exploration of their potential involvement in EMT remodelling as a response to hyperglycaemic metabolic stress and ionising radiation.

Chapter 4 – Discussion and Conclusion

Because of their substantial interrelation, cancer and diabetes are subjects of intensive research. This connection has emerged as one of the major concerns worldwide due to its high prevalence. The underlying mechanisms of this connection are complex and multifaceted, including insulin resistance, chronic inflammation, hyperglycaemia, and alteration in cellular metabolism (91-93). Deregulating cellular metabolism, resisting cell death, genomic instability and mutation, and unlocking phenotypic plasticity are some of the well-recognised hallmarks of cancer that have been demonstrated to have strong connections with hyperglycaemic conditions (2, 94-96). Epidemiological studies have established a connection between prolonged hyperglycaemic states in diabetes mellitus and higher mortality and recurrence rates for various cancers, such as hepatocellular, pancreatic carcinoma, oral, ovarian, and kidney cancer (91, 97-99).

Previous research from our lab, detailed in the Introduction chapter, demonstrated increased radioresistance in OSCC cells following exposure to hyperglycaemic conditions. Additionally, Zolghadr *et al.* validated in their study on epithelial-to-mesenchymal transition (EMT) remodelling in OSCC the significant links between radiation-induced EMT changes and enhanced invasive potential and radiation resistance (37). In the context of this study, limited evidence exists to confirm if the E-M phenotypic transition is the primary mechanism linking hyperglycaemic metabolic stress to radioresistance in OSCC, as well as identifying the potential key molecular players involved in this process.

The previous study established an *in vitro* model simulating hyperglycaemic metabolic stress using both 2D monolayer and 3D spheroid cultures from four OSCC cell lines (Figure 5). A clonogenic assay was conducted to evaluate the survival of hyperglycaemic stressed OSCC cells after exposure to 2 Gy of ionising radiation. Since SCC4 and BICR22 showed greater survival rates, we chose these two cell lines to explore further how hyperglycaemia affects their radiosensitivity, employing the same experimental protocol. In this study, however, we implemented the 3D tumour spheroid culture. Briefly, after a week of exposure to hyperglycaemic conditions (20 mM glucose), the cells were collected and incubated as hanging drops to create cell sheets. These sheets were then shaped into spheres, known as tumour spheroids. The non-hyperglycaemic group received the same concentration of mannitol.

Mannitol was employed as an osmotic control, simulating the hyperosmolar state in the glucose-treated group without introducing additional metabolic effects on the cells, thereby preventing any undesired impact of hyperosmolarity (100, 101). The tumour spheroids effectively replicate the intricate 3D structure of the tumours, capturing the *in vivo* physiological cell-cell interactions and hypoxic environment (102, 103). Furthermore, 3D spheroid cultures provide a more accurate representation of *in vivo treatment* effects, such as ionising radiation, and environmental stresses, like hyperglycaemic conditions, highlighting cellular responses more precisely than 2D monolayer cultures (102-104).

4.1. The effect of hyperglycaemic condition on γ-H2AX expression levels in response to ionising radiation

The DNA DSBs to γ-H2AX ratio is approximately 1:1; therefore, γ-H2AX is utilised as a key biomarker for DNA damage and to estimate double-stranded breaks (DSBs), and it is essential in the DNA damage response (DDR) process (105, 106). When the DSBs are induced, the DDR mechanisms are also initiated, starting with the phosphorylation of histone protein H2AX at Ser139, which accumulates at the sites of DNA damage (107). H2AX can be phosphorylated by different PI3-kinases, such as Ataxia Telangiectasia Mutated (ATM), Ataxia Telangiectasia and Rad3-related protein (ATR), DNA-protein kinase catalytic subunit (DNA-PKcs), depending on the type of DNA-damaging agent (107, 108). In this study, we used Western blotting to investigate the γ-H2AX expression levels in the SCC4 and BICR22 cell lines to evaluate the accumulation of DNA damage in OSCC cells in response to hyperglycaemic conditions and ionising radiation. In both cell lines, hyperglycaemia had a negligible effect on DSB accumulation in the spheroids. It has been shown that hyperglycaemic conditions can cause and sustain increased DSBs through various mechanisms, including hindering DNA repair, promoting DNA SSBs and DSBs, destabilising HIF1, and indirectly causing DNA damage through oxidative stress and ROS production (109-111). Although hyperglycaemia did not result in any notable change to radiation-induced γ-H2AX regulation, glucose-treated spheroids still exhibited elevated γ-H2AX accumulation.

Ionising radiation is employed as a potent therapy for various cancers, including OSCC (112-114). It utilises high-energy particles and waves to induce various destructive lesions in the cellular genome, including DSBs, contributing to genomic instability and ultimately leading to cell death (14, 115). Following DNA damage from ionising radiation, γ-H2AX accumulates at the locations of DSBs, facilitating the recruitment of DNA repair proteins like BRCA1, 53BP1, EXPAND1, and RAD18, which initiate repair processes such as homologous recombination (HR) and non-homologous end joining (NHEJ) (107, 108, 116). Once the repair process is completed, γ-H2AX is dephosphorylated, and its expression is resolved.

In our analysis of the DNA double-stranded break marker, γ-H2AX, in SCC4, an initial DNA damage repair was observed only 2 h after radiation exposure. However, it appeared to be subsequently suppressed, with γ-H2AX level peaking again at 24 h after IR. On the other hand, BICR22 showed a reduction in γ-H2AX expression in both the control and irradiated glucose groups at 24 hours post-IR; however, this reduction was not as pronounced as in the mannitol samples. Research shows that cancer cells sensitive to IR retain γ-H2AX for a longer duration compared to those that are more radioresistant (117-120). However, referring to the clonogenic assay (Figure 5), both SCC4 and BICR22 cells that were expanded in a hyperglycaemic condition expressed high survival rates after radiation exposure, suggesting that hyperglycaemia promotes resistance to radiation while maintaining high levels of genomic instability.

4.2. The impact of hyperglycaemic metabolic stress on phenotypic remodelling along the E-M axis in response to ionising radiation

The phenotypic transition along the epithelial-mesenchymal (E-M) axis is essential for cancer progression and advancement. It facilitates metastasis and invasive capability, significantly aiding in the emergence of resistance to anti-cancer treatments (35, 121).

Extensive research has investigated the role of EMT in drug and therapeutic resistance across various cancer types, underscoring its association with a complex array of molecular pathways. In skin squamous cell carcinoma, EMT is driven by RHOJ, allowing cancer cells to endure replicative stress and DNA damage from cisplatin and 5-fluorouracil (5FU), thereby developing chemotherapy resistance (122). Additionally, EMT is shown to be regulated by the PI3K/Akt/mTOR signalling pathway, which is activated by PDK1, promoting motility and invasiveness in hepatocellular carcinoma cells, as well as enhancing post-IR relapse (123). Moreover, EMT-induced local lymph node metastasis and tumour invasiveness diminish treatment effectiveness, resulting in poorer prognoses and higher relapse rates in patients with advanced oral cancer (10, 35, 124).

The epithelial-mesenchymal transition (EMT) is defined by the gradual loss of epithelial traits and gain of mesenchymal features, which enhances their metastatic and invasive potential. During this transition, various hybrid E-M phenotypes have been observed in various cancers, which display both epithelial and mesenchymal markers. Cancer cells in these transient states gain characteristics of both cell types and demonstrate different levels of plasticity, stemness, metastasis, and invasiveness (48, 125-129). Our research indicates that hybrid E-M cells, indicated by the co-expression of positive levels of ECAD and VIM, are present in tumour spheroids derived from OSCC and tongue tumour tissues. As interest grows in the relationship between diabetes and cancer, researchers are extensively investigating how hyperglycaemia influences EMT, which affects the progression and advancement of epithelial tumours (79-82, 96). Notably, hyperglycaemic conditions have been found to shift the metabolism of pancreatic and bladder cancer cells towards a glycolytic phenotype and promote EMT through the YAP/TAZ/Hedgehog signalling pathway (67, 96). Moreover, hyperglycaemia is known to promote invasion and migration by accelerating EMT in lung cancer. Administration of Mogroside V reversed hyperglycaemia, leading to the reversal of EMT and, consequently, metastasis inhibition (78). Our findings are consistent with the previous studies, which showed that hyperglycaemic conditions significantly promote the phenotypic remodelling towards hybrid E-M cells ($ECAD_{Pos}$-VIM_{Pos}). It was only after 2 Gy exposure to ionising radiation that the hybrid E-M population in normoglycaemic OSCC spheroids matched the abundance found in hyperglycaemic stress spheroids.

Prior research conducted in our laboratory by Zolghadr et al. showed the post-IR emergence of a distinct phenotypic subpopulation that adopts a more mesenchymal-like EMT state, marked by a notable reduction in ECAD expression while retaining positive VIM expression ($ECAD_{Low/Neg}$-VIM_{Pos}) (37). This subpopulation exhibits enhanced invasive properties and resistance to ionising radiation. E-cadherin has been implicated as a prognostic predictor in various cancers (130-133). Generally, elevated ECAD levels correlate with improved prognosis, whereas diminishing ECAD expression is significantly linked to aggressive characteristics in later stages of tumours and unfavourable disease outcomes (131, 132). The induction of the low-ECAD EMT states by ionising radiation was also noted in other cancer types (134-137). Acquiring mesenchymal characteristics enhances cancer cell movement, enabling them to escape the detrimental effects of anti-cancer therapies and increase metastasis rates.

In our study, the IR-induced generation of the $ECAD_{Low/Neg}$-VIM_{Pos} subpopulation at the early time point was only observed in BICR22. In fact, both cell lines under the hyperglycaemic conditions exhibited a significantly higher presence of this subpopulation, both prior to and after radiation exposure. Furthermore, while there was no notable difference in hybrid E-M cell levels between the tumour tissues from diabetic and non-diabetic tongue cancer patients, the abundance of $ECAD_{Low/Neg}$-VIM_{Pos} was significantly elevated in the tumour tissue of diabetic cancer patients. These results underscore how hyperglycaemic metabolic stress influences the phenotypic shift along the E-M axis in epithelial cells, promoting the development of hybrid E-M cells and their progression towards a mesenchymal-like phenotype. Consequently, this enhances the aggressiveness of tumours and strengthens their resistance to radiation in OSCC.

Furthermore, diabetic tongue cancer patients, from whom the tumour tissues were retrieved, exhibited persistently elevated pre-operative random blood glucose levels and suboptimal HbA1c values, despite receiving anti-diabetic treatment. These findings suggest that pharmacological interventions may not fully mitigate hyperglycaemic stress within the tumour microenvironment. Importantly, these patients consistently experienced poorer

outcomes, including metastasis and unresectable disease, highlighting a potential link between metabolic dysregulation and tumour progression.

Our findings support this model by showing that metabolic stress, even with the use of anti-diabetic medications, correlates with enhanced tumour aggressiveness in OSCC. Although previous studies and the findings from our study have demonstrated the impact of hyperglycaemia on the EMT states of epithelial cancer cells and in response to irradiation, the precise molecular mechanisms underlying this association remain to be fully elucidated, warranting further investigation into glucose-mediated signalling in cancer cell plasticity.

4.3. The influence of hyperglycaemic condition on EMT Transcription Factor regulation in response to metabolic stress and ionising radiation.

The vital functions of EMT in tumour invasion, metastasis, and resistance to therapy have been emphasised across different cancers, indicated by the reduced expression of epithelial markers. At the transcriptional level, EMT is orchestrated by several transcription factors associated with EMT, including members of the ZEB (ZEB1 and ZEB2), TWIST, and SNAIL (SNAIL1 and SNAIL2/SLUG) families, which enhance cellular adhesion, motility, and invasiveness. These master regulators function distinctly to suppress epithelial markers like E-cadherin, β-catenin, and cytokeratin while promoting the expression of mesenchymal markers such as Vimentin, Fibronectin, and N-cadherin (138). Numerous studies have shown that hyperglycaemic conditions enhance the levels of EMT transcription factors; however, this relationship has yet to be thoroughly elucidated.

Our previous clonogenic assay experiments using irradiated, hyperglycaemic-stressed models of four OSCC cell lines (SCC4, BICR22, SCC9, and SCC25) demonstrated that elevated glucose levels selectively enhanced post-irradiation survival in SCC4 and BICR22 cells (Figure 5). This differential radiosensitivity under hyperglycemic conditions informed the selection of these two lines for further mechanistic investigation. However, the real-time

RT-PCR revealed divergent regulation patterns of EMT-associated transcription factors in SCC4 and BICR22, despite the comparable final expression of ECAD and VIM in both cell lines.

E-cadherin (ECAD) plays a crucial role in cell-cell adhesion. A decrease in its expression indicates a worse prognosis for cancer patients, linking it to the initiation of EMT, which enhances tumour invasion and metastasis. Notably, our research revealed ECAD was upregulated in both SCC4 and BICR22, contrasting with our immunofluorescent analysis that indicated increased EMT remodelling toward hybrid E-M and mesenchymal-like phenotypes in both cell lines. While the loss of ECAD is commonly associated with EMT, some studies have indicated that losing E-cadherin is not essential for EMT, as its expression can persist in late-stage carcinomas (139-141). Following irradiation exposure to irradiation, BICR22 spheroids under hyperglycaemic stress exhibited a significant reduction in ECAD levels, in contrast to those treated with mannitol. While hyperglycaemic spheroids demonstrated higher ECAD expression before irradiation compared to the mannitol-treated counterparts, their post-irradiation ECAD expression declined and continued to decrease 24 h later.

Vimentin is well established as a key indicator of mesenchymal phenotypes in cancer-related EMT studies. The transition of epithelial cells to adopt mesenchymal traits involves heightened Vimentin expression, which aids tumour invasion and metastasis and enhances resistance to environmental stressors. The ratio of the mesenchymal marker Vimentin to the epithelial marker E-cadherin is elevated in diabetic tumours and decreases when treated with insulin (142). This indicates a connection between diabetic hyperglycaemia, increased EMT, and more aggressive tumours. Furthermore, research into the relationship between EMT and hyperglycaemia across different cancers has demonstrated that Vimentin expression increases in cells under hyperglycaemic stress (65, 96, 143). The literature observations match our results from BICR22-derived spheroids, where hyperglycaemic stress leads to increased VIM expression. However, we did not observe any upregulation of VIM due to IR nor any significant alteration in VIM expression between the irradiated spheroids treated with glucose and mannitol in both cell lines.

SNAIL and SLUG are zinc-finger transcription factors from the SNAIL family, which acts as an inducer of the EMT process by downregulating the epithelial marker ECAD and upregulating mesenchymal markers. Both factors are found to be overexpressed in OSCC, facilitating EMT-associated tumour invasion, metastasis, and resistance to therapy. Additionally, SNAIL levels rise under hyperglycaemic stress due to ENO1, a glycolysis-related gene, which further drives EMT in gastric cancer. Inhibition of ENO1 can block the SNAIL-induced EMT and the activation of TGF-β signalling (66). Moreover, cholangiocarcinoma cells subjected to high glucose show increased FOXM1 expression; blocking FOXM1 significantly reduces SLUG-mediated migration and invasion (144). Ionising radiation is known to increase SNAIL and SLUG levels, which contribute to tumour invasiveness and radiation resistance in various cancers, including OSCC (37, 145-149). However, in contrast to previous studies, SNAIL expression decreased in SCC4 and BICR22 cells subjected to hyperglycaemic stress. Integrating this finding with the immunohistochemical analysis of the E-M hybrid phenotype and considering that SNAIL acts as a transcriptional repressor of ECAD and is not directly linked to a mesenchymal-like phenotype, lowering SNAIL expression levels may be a necessity for maintaining a high prevalence of the hybrid E-M cell population (138, 150, 151). Following exposure to 2 Gy of ionising radiation, SCC4 spheroids exhibited increased SNAIL levels, unlike the decrease observed in mannitol-treated spheroids. For BICR22 spheroids, SNAIL expression decreased at 2 h post-radiation, without any recovery at the 24-hour mark, remaining lower than in mannitol-treated spheroids. Conversely, SLUG levels in SCC4 spheroids were diminished under hyperglycaemic conditions compared to mannitol-treated spheroids, independent of ionising radiation effects. Notably, while IR prompted an increase in SNAIL in hyperglycaemic spheroids 24 h post-exposure, SLUG was elevated sooner. This indicates a potential switch between these two factors in facilitating hybrid E-M phenotype in response to hyperglycaemic stress and IR in SCC4-derived spheroids.

TWIST functions as an EMT regulator in different carcinomas associated with tumour progression and aggressiveness. It facilitates EMT by downregulating the epithelial marker E-cadherin and increasing VIM expression (152-154). In SCC4, IR did not lead to any significant changes in TWIST expression levels. However, after IR, TWIST expression was markedly higher under hyperglycaemic conditions than mannitol-treated spheroids. Conversely, BICR22-derived spheroids showed increased TWIST expression levels due to

hyperglycaemia before IR, which is positively correlated with the upregulation of VIM. While IR increased TWIST levels in mannitol-treated spheroids, it decreased TWIST expression in glucose-treated tumour spheroids. Interestingly, when examining the regulation of EMT TFs and markers, we observed a similar regulatory pattern between TWIST and ECAD in response to hyperglycaemic stress and irradiation, despite the expectation that these two should be inversely regulated since TWIST downregulates ECAD to facilitate the EMT process (37, 155). Additionally, although TWIST overexpression is associated with the downregulation of ECAD, it is not always correlated with the mesenchymal markers or EMT (150, 156-158). Further research is required to fully elucidate the exact role of TWIST during EMT remodelling and its contribution to cancer progression and tumour advancement.

Zinc finger E-box binding homeobox 1 (ZEB1) serves as a potent regulator of EMT. It plays a crucial role in the phenotypic shift along the E-M axis, significantly enhancing tumour invasion, metastasis, and resistance to anti-cancer therapies. Our investigation into EMT TF regulation revealed no significant change in ZEB1 expression in BICR22 in response to metabolic stress and irradiation. Conversely, ionising radiation increased the ZEB1 expression level in SCC4-derived spheroids subjected to hyperglycaemic stress. Furthermore, ZEB1 expression after irradiation was significantly elevated in hyperglycaemic spheroids relative to those exposed to mannitol. This increase, in conjunction with SNAIL, correlates positively with the IR-induced phenotypic change towards hybrid E-M and mesenchymal-like phenotypes identified in the IHC analysis. The partnership between ZEB1 and SNAIL in promoting EMT has been shown in non-small cell lung cancer, where SNAIL overexpression alone proves insufficient (151, 159). The mesenchymal-like cell populations in different carcinomas show elevated ZEB1 levels, correlating with aggressive cancer behaviour (64, 128, 150, 160, 161). This highlights ZEB1's role in enhancing cancer cell invasiveness, metastatic ability, and radioresistance development. Overall, these results emphasise the distinct functions of EMT transcription factors in cancer progression and tumour aggressiveness. They point to a potential functional transition from SLUG and TWIST early on to SNAIL and ZEB1, which promote E-M phenotypes in response to hyperglycaemic metabolic stress and ionising radiation.

The inconsistency in EMT-TF regulation between these two cell lines emphasises that EMT is governed by multiple transcription factors (162). Rather than a single switch, various regulator combinations can lead to similar phenotypes (163). EMT is increasingly recognised as a spectrum with intermediate states, where cells can exhibit hybrid epithelial–mesenchymal traits that have distinct transcriptional architectures but share functional similarities (164). Therefore, the misregulation of different EMT transcription factors in SCC4 and BICR22 likely reflects cell line–specific regulatory landscapes, yet both lines undergo comparable EMT remodelling in response to hyperglycemic stress and irradiation.

4.4. The potential molecular players driving EMT remodelling and resistance to radiation in SCC4-derived spheroids under hyperglycaemic conditions.

In this study, we conducted an RNA-sequencing analysis of spheroids from SCC4 cells to examine transcriptional changes associated with cellular responses to hyperglycaemic metabolic stress and ionising radiation. The results indicated a dynamic pattern of transcriptional remodelling due to hyperglycaemia in control samples (non-irradiated). However, a decrease was observed at the 24-hour post-irradiation time point compared to the 2-hour mark. Several factors could be taken into consideration to explain this observation. Tumour spheroids were withdrawn from hyperglycaemic and mannitol-treated media before exposure to ionising radiation, potentially reversing the hyperglycaemic-induced metabolic changes in the tumour microenvironment. Such changes may gradually affect the spheroid transcriptome, explaining the differences noted between transcriptomes of spheroids collected 2 and 24 h after irradiation. However, various studies indicate that cancer cells experiencing extended hyperglycaemic stress can retain gene profile alterations induced by hyperglycaemia even after being withdrawn from these conditions, a phenomenon known as “hyperglycaemic memory” (165-168). Another potential factor is the amount of time culturing in 3D spheroid form that can affect the spheroid size and alter their hypoxic environment, causing alteration in transcriptional dynamic (169-172). Therefore, having time-equivalent non-hyperglycaemic and non-irradiated samples is vital

for accurate comparisons and analyses of the transcriptional dynamic in response to metabolic stress and ionising radiation.

The impacts of hyperglycaemic conditions and radiation exposure on the transcriptomic profile of cancer cells have been well-documented across various cancers. In the present study, employing RNA-sequencing and pathway analyses of the differentially expressed genes among the samples, we have noticed several potential molecular players that have also been investigated for their functions during cancer progression.

Integrins are transmembrane glycoprotein receptors that operate in both directions and are found on cell surfaces, responsible for transmitting signals between the extracellular matrix (ECM) and the intracellular cytoskeleton (173). The integrin family includes 24 distinct heterodimer molecules made up of 18 α and 8 β subunits, which are vital for governing numerous biological functions (174). In cancer cells, integrins play a crucial role in proliferation, angiogenesis, tumour invasion, and metastasis. Integrin subunits α3 (ITGA3), αV (ITGAV), and β4 (ITGB4) are found to be overexpressed in various cancers, correlating with poor prognoses and advanced tumour stages (175-182). This indicates their crucial role in tumour progression, invasion, and metastasis. In oral squamous cell carcinoma (OSCC), ITGAV overexpression is linked to increased perineural invasion and tumour budding (177). Meanwhile, the overexpression of ITGA3 correlates with high rates of lymph node metastasis, more invasive histopathology, and elevated recurrence rates, while higher levels of ITGB4 are associated with distant metastasis (178). The RNA-sequencing analysis in the present study only demonstrated an upregulation of ITGA3 and ITGB4 in the control samples under hyperglycaemic stress. Furthermore, the validation of the identified DEGs through qRT-PCR showed significant overexpression of all three integrins in tongue tumour tissues from patients with diabetes. However, there is insufficient research exploring their significance in the association between cancer and hyperglycaemia.

ITGA3 only forms heterodimer laminin receptors with subunit β1, activated when interacting with extracellular laminin ligands, shown to be involved in different aspects of cancer hallmarks, including polymorphic microbiomes and activating invasion and

metastasis (173). Within the framework of cancer epithelial-mesenchymal transition (EMT), overexpression of ITGA3 was linked to aggressive breast cancer and the expression of ZEB1, an EMT transcription factor, through the MEK-ERK signalling pathway (183). In cervical cancer, ITGA3 was shown to influence EMT via the PI3K/AKT pathways (184). In addition, cells that overexpress ITGA3 showed heightened levels of VIM, MMP2, and MMP9. However, the potential connection between ITGA3, MMP2, and MMP9 remains to be thoroughly explored. Conversely, in some cancers, ITGA3 evidently appears to also function as a tumour suppressor, and its downregulation results in EMT remodelling, thereby facilitating tumour invasion and both local and distant metastases (185-192). A study on the CD151-ITGA3 functional connection in breast cancer has demonstrated that knocking down ITGA3 enhanced tumour growth and EMT via upregulating the EMT transcription factor SLUG and the canonical Wnt pathway (192). The β4 integrin subunit (ITGB4) exclusively pairs with the α6 subunit to form the α6β4 integrin receptor that interacts with laminin. This interaction is vital for establishing and preserving the integrity of epithelial adhesion and enabling communication between the ECM and intracellular cytoskeletal components through binding with laminins and epidermal integral ligand proteins (193). This regulatory mechanism impacts several key biological processes, such as cell death, angiogenesis, autophagy, and cell differentiation (194). ITGB4 has been identified as a tumour-associated antigen overexpressed in various cancers (195). It plays a crucial role in tumorigenesis traits, including cell proliferation, evasion of apoptosis, tumour invasiveness, and metastasis, by interacting with the growth factor receptor signalling network. This interaction regulates downstream pathways such as the PI3K/AKT and MAPK pathways (196, 197). ITGAV forms transmembrane heterodimer arginine-glycine-aspartic (RGD) receptors with 5 β-subunits (β1, β3, β5, β6, β8). It reduces ECAD expression by interacting with TGF-β signalling pathways, promoting EMT as cancer progresses and tumours advance (180). In addition, the crosstalk between αV-pairing heterodimer integrins and TGF-β signalling can also trigger various downstream pathways, including MAPK, PI3K/AKT, Ras, and SMAD signalling, facilitating tumour invasion and migration (180, 198, 199). Currently, there is insufficient research on the regulation of ITGA3 and ITGAV in response to irradiation. Our RNA-sequencing analysis revealed that irradiation induces an elevation in ITGA3 and ITGAV. Given their crucial roles in cancer EMT, this elevation could play a part in the radioresistance seen in epithelial tumours under hyperglycaemic conditions; however, further functional analyses are required to validate this hypothesis. ITGB4 levels were found

to be increased in irradiated SCC4-derived spheroids in our study and also shown to be upregulated in radioresistant colorectal HCT116 and esophageal squamous carcinoma cells, indicating that ITGB4 may be another critical factor in regulating cancer cells radiosensitivity in hyperglycaemic conditions (200, 201).

Matrix metalloproteinase-2 (MMP2) and Matrix metalloproteinase-9 (MMP9) are zinc-dependent gelatinases produced by tumour and stromal cells. They play crucial roles in degrading type IV collagen and gelatin in the extracellular matrix (ECM). These enzymes are overexpressed in various carcinomas, where they significantly facilitate cancer cell proliferation, angiogenesis, tumour invasion, and metastasis, ultimately resulting in poor prognosis and survival outcomes (202-206). In the setting of hyperglycaemia, cholangiocarcinoma cells experience metabolic stress, resulting in heightened expression of MMP2 and vimentin, a process that occurs downstream of increased FOXM1 levels (144, 207). Inhibiting FOXM1 subsequently reduces the expression of SLUG and MMP2, suggesting that MMP2 is involved in the hyperglycaemia-triggered epithelial-mesenchymal transition (EMT), which is regulated by SLUG and influenced by FOXM1 (144). Additionally, MMP9 has been found to be overexpressed in hyperglycaemic pancreatic cancer cells, consistent with our findings of increased MMP2 and MMP9 expression in hyperglycaemic SCC4-derived spheroids (55). However, analysis of diabetic tumour tissues via qRT-PCR revealed that only MMP2 expression was elevated in diabetic patients, while no significant change in MMP9 levels was observed. Additionally, irradiation also upregulates MMP2 and MMP9 levels, suppressing the radiosensitivity of adenocarcinoma and neuroblastoma cells (208-211). Using adenovirus expressing siRNA targeting MMP2 (Ad-MMP-2-Si) effectively inhibits MMP2, which in turn suppresses Checkpoint-2/1 and reverses the radiation-induced G2 cell cycle arrest, thereby increasing apoptosis in cancer cells (208). Conversely, the downregulation of MMP-9 overexpression induced by radiation via Ad-MMP-9 infection has been shown to inhibit HIF-1 and NF-κB signalling pathways, leading to a reduction in breast cancer progression (209). Together, MMP2 and MMP9 present promising targets for further research on their role in the relationship between hyperglycaemic metabolic stress, EMT, and radioresistance.

Laminin subunit beta 1 (LAMB1) and laminin subunit gamma 1 (LAMC1) play essential roles in forming large extracellular matrix (ECM) proteins called laminins. These proteins are vital for several key biological processes, including the creation of basement membranes, as well as cell adhesion, migration, and proliferation. LAMB1 and LAMC1 are frequently upregulated in various carcinomas, which correlates with adverse disease outcomes, linking them to specific oncogenic pathways and facilitating cancer cell adhesion, tumour invasion and metastasis (212-216). In our study, the RNA-sequencing analysis did not detect any upregulation or downregulation of LAMB1 and LAMC1 in the SCC4-derived spheroids due to hyperglycaemia. However, their regulation in response to the combination of hyperglycaemic metabolic stress and irradiation differed from that in mannitol-treated spheroids, and increased expression levels were observed in the diabetic tongue tumour tissues. Currently, there is limited research on the regulation of LAMB1 and LAMC1 in tumours under hyperglycaemic conditions, along with their functions during the EMT process. However, elevated levels of LAMB1 were detected in the metastatic E1 cell lines of colorectal cancer, even though LAMB1 is known not to be secreted by colorectal cancer cells at the primary sites. The pathway analysis from our study also shows the potential involvement of LAMB1 and LAMC1 in various cancer-related pathways, including focal adhesion and the PI3K/AKT/mTOR and MET signalling pathways, which are known to facilitate EMT remodelling in cancer.

Fibronectin 1 (FN1) has been demonstrated to act as a tumour promoter in various cancers, in which its overexpression is correlated with poor prognosis, enhanced proliferation and migration (217, 218). FN1 serves as a marker for EMT due to its crucial role in regulating cellular adhesion, migration, and ECM remodelling, all of which are vital during the phenotypic shift along the E-M axis. In ovarian cancer, FN1 shows a positive correlation with designated promoting transition-associated lncRNA (PTAL), which enhances metastasis by facilitating EMT through increasing the expression of SLUG and VIM while inhibiting E-cadherin (219). In head and neck squamous cell carcinoma, the overexpression of FN1 is also associated with the elevation of VIM and N-Cadherin levels, favouring EMT remodelling toward the mesenchymal-like phenotypes (220). The expression of FN1 in cancer cells under hyperglycaemic conditions has not been extensively studied. In our research, we found a substantial increase in FN1 levels in tongue tumour tissues from diabetic patients, as well as in spheroids derived from SCC4. Furthermore, FN1 levels were

notably higher in radioresistant HNSCC (220, 221). Together, these results highlight the crucial role of FN1 in the EMT remodelling of OSCC under metabolic stress and radiation exposure.

Insulin receptor substrate 1 (IRS1) is a cytoplasmic adaptor protein that plays a crucial role in insulin signalling pathways by acting as a binding site for insulin receptors and insulin-like growth factor receptors. Overexpression of IRS1 is linked to more aggressive diseases and worse clinical outcomes in various cancers, facilitating tumour progression through the PI3K/AKT and MAPK pathways (222-225). In thyroid cancer, increased IRS1 levels are associated with more significant distant metastasis and more advanced stages of the disease (226). Additionally, IRS1 has been shown to promote thyroid cancer metastasis by influencing epithelial-mesenchymal transition (EMT) remodelling through PI3K/AKT pathways (226). In OSCC, IRS1 expression levels were found to be increased, influencing proliferation and triggering EMT through p53/Line-1 signalling pathways (227). When IRS1 was inhibited, there was a decrease in the levels of SNAIL, SLUG, and VIM, which could potentially reverse EMT (227). In this study, we observed no significant increase or decrease in IRS1 due to hyperglycaemia-induced metabolic stress in both SCC4-derived tumour spheroids and tongue cancer tissues. However, evidence suggests IRS1 is overexpressed in cancer cells facing hyperglycaemic conditions, which boosts Ras and RAF1 proto-oncogene activity, leading to the phosphorylation of ERK1/2 signalling (228).

4.5. Conclusion

In summary, although significant research has examined tumour progression and how cancer cells respond to external stressors and treatments, the signalling pathways that regulate tumour formation and disease progression remain complex and require further investigation. Moreover, the relationship between hyperglycaemia and the cancer-related epithelial-to-mesenchymal transition (EMT), along with its association with radioresistance, has not been thoroughly investigated. This study aims to contribute our findings to the broader field of cancer research concerning diabetes mellitus and resistance to radiation therapy. Given our initial results showing a high post-irradiation survival fraction of SCC4 and BICR22 cells

after seven days of metabolic stress in hyperglycaemic conditions, we delve further into the mechanisms at play and identify potential key factors influencing this response to ionising radiation.

In our research, we employed 3D tumour spheroid tissue cultures and utilised various analytic techniques to investigate the impact of chronic exposure to elevated glucose levels on the EMT phenotypic changes in SCC4 and BICR22-derived spheroids, particularly concerning their response to ionising radiation. This may influence the radiosensitivity of both OSCC cell lines. Immunohistochemical analysis of OSCC-derived spheroids and tongue cancer tissues indicated increased EMT remodelling toward the mesenchymal end of the E-M axis in the spheroids stressed by hyperglycaemia, a higher abundance of hybrid or intermediate EMT and mesenchymal-like populations. Additionally, exposure to ionising radiation intensified these phenotypic changes. Transcriptional analysis of EMT transcription factors hinted at a potential shift from TWIST and SLUG to SNAIL and ZEB1 in promoting E-M phenotypes under metabolic stress and radiation exposure.

We employed high-throughput RNA sequencing and pathway analyses to identify the main molecular components that drive epithelial-mesenchymal transition (EMT) and enhance radioresistance. To gain deeper insights into the signalling network that supports cancer cell responses to hyperglycaemia and radiation, additional functional analyses, such as gain-of-function or loss-of-function studies, are necessary.

Nevertheless, our current study has certain limitations. Although the 3D spheroid system provides a more physiologically relevant model than traditional 2D monolayers, it is essential to acknowledge its constraints. Our model only consisted of a single OSCC cell type, which does not reflect the cellular heterogeneity present in the native tumour microenvironment, including stromal, immune, and endothelial cells. Therefore, while the spheroids offer insight into cell–cell interactions and hypoxia, they do not fully represent the complexity of the *in vivo* conditions. Additionally, we utilised tumour tissues from tongue cancer patients, both with and without diabetes, to validate our findings from the immunofluorescent analyses of the hybrid E-M phenotypes. These tissues also helped to

explore the expression of selected genes identified through RNA sequencing and pathway analyses in diabetic tumours. However, we lacked access to any tongue cancer tissues that had undergone radiotherapy, limiting our ability to confirm the effects of ionising radiation. Furthermore, most diabetic cancer patients would be on diabetic control medication. Therefore, to have a more relevant understanding of the association between diabetic hyperglycaemic conditions and cancer progression, these diabetic control medications should also be engaged in future studies.

In summary, we have demonstrated that exposure to both hyperglycaemic metabolic stress and ionising radiation can induce phenotypic changes along the epithelial-mesenchymal (E-M) axis, which is closely associated with the emergence of resistance to therapeutic ionising radiation. The molecular mechanisms that contribute to cancer progression, along with their connections to various factors during disease development, constitute a complex and extensive area of research; therefore, there remains a significant need for more comprehensive studies.

References

1. Kurn H, Daly DT. Histology, Epithelial Cell. Statpearls. Treasure Island (FL): StatPearls Publishing

Copyright © 2022, StatPearls Publishing LLC.; 2022.

2. Hanahan D. Hallmarks of Cancer: New Dimensions. Cancer Discovery. 2022;12:31-46.

3. Bray F, Laversanne M, Sung H, Ferlay J, Siegel RL, Soerjomataram I, et al. Global Cancer Statistics 2022: Globocan Estimates of Incidence and Mortality Worldwide for 36 Cancers in 185 Countries. CA: A Cancer Journal for Clinicians. 2024;74:229-63.

4. Chamoli A, Gosavi AS, Shirwadkar UP, Wangdale KV, Behera SK, Kurrey NK, et al. Overview of Oral Cavity Squamous Cell Carcinoma: Risk Factors, Mechanisms, and Diagnostics. Oral Oncology. 2021;121:105451.

5. Ranganathan K, Kavitha L. Oral Epithelial Dysplasia: Classifications and Clinical Relevance in Risk Assessment of Oral Potentially Malignant Disorders. Journal of Oral and Maxillofacial Pathology. 2019;23:19-27.

6. Gupta S, Jawanda MK, Madhushankari GS. Current Challenges and the Diagnostic Pitfalls in the Grading of Epithelial Dysplasia in Oral Potentially Malignant Disorders: A Review. Journal of Oral Biology and Craniofacial Research. 2020;10:788-99.

7. Wolk R, Lingen MW. Proceedings of the North American Society of Head and Neck Pathology Companion Meeting, New Orleans, LA, March 12, 2023: Oral Cavity Dysplasia: Why Does Histologic Grading Continue to Be Contentious? Head and Neck Pathology. 2023;17:292-8.

8. Sun Y, Liu N, Guan X, Wu H, Sun Z, Zeng H. Immunosuppression Induced by Chronic Inflammation and the Progression to Oral Squamous Cell Carcinoma. Mediators of Inflammation. 2016;2016:5715719.

9. Yang J, Guo K, Zhang A, Zhu Y, Li W, Yu J, et al. Survival Analysis of Age-Related Oral Squamous Cell Carcinoma: A Population Study Based on Seer. European Journal of Medical Research. 2023;28:413.

10. Wang B, Zhang S, Yue K, Wang XD. The Recurrence and Survival of Oral Squamous Cell Carcinoma: A Report of 275 Cases. Chinese Journal of Cancer Research. 2013;32:614-8.

11. Imbesi Bellantoni M, Picciolo G, Pirrotta I, Irrera N, Vaccaro M, Vaccaro F, et al. Oral Cavity Squamous Cell Carcinoma: An Update of the Pharmacological Treatment. Biomedicines. 2023;11.

12. Anderson G, Ebadi M, Vo K, Novak J, Govindarajan A, Amini A. An Updated Review on Head and Neck Cancer Treatment with Radiation Therapy. Cancers (Basel). 2021;13.

13. Somosy Z. Radiation Response of Cell Organelles. Micron. 2000;31:165-81.

14. Sia J, Szmyd R, Hau E, Gee HE. Molecular Mechanisms of Radiation-Induced Cancer Cell Death: A Primer. Frontiers in Cell and Developmental Biology. 2020;8.

15. Lewanski CR, Gullick WJ. Radiotherapy and Cellular Signalling. Lancet Oncology. 2001;2:366-70.

16. Kim BM, Hong Y, Lee S, Liu P, Lim JH, Lee YH, et al. Therapeutic Implications for Overcoming Radiation Resistance in Cancer Therapy. International Journal Of Molecular Sciences. 2015;16:26880-913.

17. Hee Park J, Hee Jung K, Jung Kim S, Fang Z, Hua Yan H, Kwon Son M, et al. Radiosensitisation of the PI3K Inhibitor Hs-173 through Reduction of DNA Damage Repair in Pancreatic Cancer. Oncotarget. 2017;8.

18. Alves-Fernandes DK, Jasiulionis MG. The Role of SIRT1 on DNA Damage Response and Epigenetic Alterations in Cancer. International Journal of Molecular Sciences. 2019;20.

19. Yacoub A, Park JS, Qiao L, Dent P, Hagan MP. MAPK Dependence of DNA Damage Repair: Ionising Radiation and the Induction of Expression of the DNA Repair Genes XRCC1 and ERCC1 in DU145 Human Prostate Carcinoma Cells in a MEK1/2 Dependent Fashion. International Journal of Radiation Biology. 2001;77:1067-78.

20. Kumar V, Vashishta M, Kong L, Wu X, Lu JJ, Guha C, et al. The Role of Notch, Hedgehog, and Wnt Signalling Pathways in the Resistance of Tumours to Anticancer Therapies. Frontiers in Cell and Developmental Biology. 2021;9.

21. Cook KM, Shen H, McKelvey KJ, Gee HE, Hau E. Targeting Glucose Metabolism of Cancer Cells with Dichloroacetate to Radiosensitise High-Grade Gliomas. International Journal of Molecular Sciences. 2021;22.

22. Meijer TW, Kaanders JH, Span PN, Bussink J. Targeting Hypoxia, HIF-1, and Tumour Glucose Metabolism to Improve Radiotherapy Efficacy. Clinical Cancer Research. 2012;18:5585-94.

23. Theys J, Jutten B, Habets R, Paesmans K, Groot AJ, Lambin P, et al. E-Cadherin Loss Associated with EMT Promotes Radioresistance in Human Tumour Cells. Radiotherapy and Oncology: Journal of the European Society for Therapeutic Radiology and Oncology. 2011;99:392-7.

24. Ribatti D, Tamma R, Annese T. Epithelial-Mesenchymal Transition in Cancer: A Historical Overview. Translational Oncology. 2020;13:100773.

25. Zhang H, Luo H, Jiang Z, Yue J, Hou Q, Xie R, et al. Fractionated Irradiation-Induced EMT-Like Phenotype Conferred Radioresistance in Esophageal Squamous Cell Carcinoma. Journal of Radiation Research. 2016;57:370-80.

26. Ramón YCS, Sesé M, Capdevila C, Aasen T, De Mattos-Arruda L, Diaz-Cano SJ, et al. Clinical Implications of Intratumor Heterogeneity: Challenges and Opportunities. Journal of Molecular Medicine (Berlin). 2020;98:161-77.

27. Marusyk A, Polyak K. Tumour Heterogeneity: Causes and Consequences. Biochimica et Biophysica Acta (BBA). 2010;1805:105-17.

28. Oh BY, Shin H-T, Yun JW, Kim K-T, Kim J, Bae JS, et al. Intratumor Heterogeneity Inferred from Targeted Deep Sequencing as a Prognostic Indicator. Scientific Reports. 2019;9:4542.

29. Evan T, Wang VM-Y, Behrens A. The Roles of Intratumour Heterogeneity in the Biology and Treatment of Pancreatic Ductal Adenocarcinoma. Oncogene. 2022;41:4686-95.

30. Hensley CT, Faubert B, Yuan Q, Lev-Cohain N, Jin E, Kim J, et al. Metabolic Heterogeneity in Human Lung Tumours. Cell. 2016;164:681-94.

31. Yu T, Gao X, Zheng Z, Zhao X, Zhang S, Li C, et al. Intratumor Heterogeneity as a Prognostic Factor in Solid Tumours: A Systematic Review and Meta-Analysis. Frontiers in Oncology. 2021;11:744064.

32. Chaffer CL, San Juan BP, Lim E, Weinberg RA. EMT, Cell Plasticity and Metastasis. Cancer and Metastasis Reviews. 2016;35:645-54.

33. Kim DH, Xing T, Yang Z, Dudek R, Lu Q, Chen Y-H. Epithelial Mesenchymal Transition in Embryonic Development, Tissue Repair and Cancer: A Comprehensive Overview. Journal of Clinical Medicine. 2017;7:1.

34. Marconi GD, Fonticoli L, Rajan TS, Pierdomenico SD, Trubiani O, Pizzicannella J, et al. Epithelial-Mesenchymal Transition (EMT): The Type-2 EMT in Wound Healing, Tissue Regeneration and Organ Fibrosis. Cells. 2021;10.

35. Ghantous Y, Mozalbat S, Nashef A, Abdol-Elraziq M, Sudri S, Araidy S, et al. EMT Dynamics in Lymph Node Metastasis of Oral Squamous Cell Carcinoma. Cancers. 2024;16:1185.

36. Fan L, Lei H, Zhang S, Peng Y, Fu C, Shu G, et al. Non-Canonical Signalling Pathway of SNAI2 Induces EMT in Ovarian Cancer Cells by Suppressing miR-222-3p Transcription and Upregulating PDCD10. Theranostics. 2020;10:5895-913.

37. Zolghadr F, Tse N, Loka D, Joun G, Meppat S, Wan V, et al. A Wnt-Mediated Phenotype Switch Along the Epithelial-Mesenchymal Axis Defines Resistance and Invasion Downstream of Ionising Radiation in Oral Squamous Cell Carcinoma. British Journal of Cancer. 2021;124:1921-33.

38. Garg M. Epithelial, Mesenchymal and Hybrid Epithelial/Mesenchymal Phenotypes and Their Clinical Relevance in Cancer Metastasis. Expert Review in Molecular Medicine. 2017;19:e3.

39. Schliekelman MJ, Taguchi A, Zhu J, Dai X, Rodriguez J, Celiktas M, et al. Molecular Portraits of Epithelial, Mesenchymal, and Hybrid States in Lung Adenocarcinoma and Their Relevance to Survival. Cancer Research. 2015;75:1789-800.

40. Shah PP, Dupre TV, Siskind LJ, Beverly LJ. Common Cytotoxic Chemotherapeutics Induce Epithelial-Mesenchymal Transition (EMT) Downstream of ER Stress. Oncotarget. 2017;8:22625-39.

41. Sun XY, Li HZ, Xie DF, Gao SS, Huang X, Guan H, et al. LPAR5 Confers Radioresistance to Cancer Cells Associated with EMT Activation Via the ERK/Snail Pathway. Journal of Translational Medicine. 2022;20:456.

42. Tam SY, Wu VWC, Law HKW. Hypoxia-Induced Epithelial-Mesenchymal Transition in Cancers: HIF-1α and Beyond. Frontiers in Oncology. 2020;10.

43. Simpson DR, Mell LK, Cohen EE. Targeting the PI3K/AKT/mTOR Pathway in Squamous Cell Carcinoma of the Head and Neck. Oral Oncology. 2015;51:291-8.

44. Wee P, Wang Z. Epidermal Growth Factor Receptor Cell Proliferation Signalling Pathways. Cancers (Basel). 2017;9.

45. Aggarwal V, Montoya CA, Donnenberg VS, Sant S. Interplay between Tumor Microenvironment and Partial EMT as the Driver of Tumor Progression. iScience. 2021;24:102113.

46. Jolly MK, Somarelli JA, Sheth M, Biddle A, Tripathi SC, Armstrong AJ, et al. Hybrid Epithelial/Mesenchymal Phenotypes Promote Metastasis and Therapy Resistance across Carcinomas. Pharmacology & Therapeutics. 2019;194:161-84.

47. Kröger C, Afeyan A, Mraz J, Eaton EN, Reinhardt F, Khodor YL, et al. Acquisition of a Hybrid E/M State Is Essential for Tumorigenicity of Basal Breast Cancer Cells. Proceedings of the National Academy of Sciences of the United States of America. 2019;116:7353-62.

48. Muralidharan S, Sahoo S, Saha A, Chandran S, Majumdar SS, Mandal S, et al. Quantifying the Patterns of Metabolic Plasticity and Heterogeneity Along the Epithelial-Hybrid-Mesenchymal Spectrum in Cancer. Biomolecules. 2022;12.

49. Pastushenko I, Brisebarre A, Sifrim A, Fioramonti M, Revenco T, Boumahdi S, et al. Identification of the Tumour Transition States Occurring During EMT. Nature. 2018;556:463-8.

50. Schiliro C, Firestein BL. Mechanisms of Metabolic Reprogramming in Cancer Cells Supporting Enhanced Growth and Proliferation. Cells. 2021;10.

51. Rigoulet M, Bouchez CL, Paumard P, Ransac S, Cuvellier S, Duvezin-Caubet S, et al. Cell Energy Metabolism: An Update. Biochimica et Biophysica Acta (BBA) - Bioenergetics. 2020;1861:148276.

52. Lee S, Tak E, Lee J, Rashid MA, Murphy MP, Ha J, et al. Mitochondrial H_2O_2 Generated from Electron Transport Chain Complex I Stimulates Muscle Differentiation. Cell Research. 2011;21:817-34.

53. Barba I, Carrillo-Bosch L, Seoane J. Targeting the Warburg Effect in Cancer: Where Do We Stand? International Journal of Molecular Sciences. 2024;25.

54. Chen CL, Lin CY, Kung HJ. Targeting Mitochondrial Oxphos and Their Regulatory Signals in Prostate Cancers. International Journal of Molecular Sciences. 2021;22.

55. Li W, Liu H, Qian W, Cheng L, Yan B, Han L, et al. Hyperglycemia Aggravates Microenvironment Hypoxia and Promotes the Metastatic Ability of Pancreatic Cancer. Computational and Structural Biotechnology Journal. 2018;16:479-87.

56. Cannata D, Fierz Y, Vijayakumar A, LeRoith D. Type 2 Diabetes and Cancer: What Is the Connection? Mount Sinai Journal of Medicine: A Journal of Translational and Personalised Medicine. 2010;77:197-213.

57. Shahid RK, Ahmed S, Le D, Yadav S. Diabetes and Cancer: Risk, Challenges, Management and Outcomes. Cancers. 2021;13:5735.

58. Lien K-H, Padua PFC, Tay ZY, Kao H-K, Hung S-Y, Huang Y, et al. Influence of Hyperglycaemia on Treatment Outcomes of Oral Cavity Squamous Cell Carcinoma. Journal of Oral and Maxillofacial Surgery. 2020;78:935-42.

59. Duan W, Shen X, Lei J, Xu Q, Yu Y, Li R, et al. Hyperglycemia, a Neglected Factor During Cancer Progression. BioMed Research International. 2014;2014:461917-.

60. Li W, Ma Q, Liu J, Han L, Ma G, Liu H, et al. Hyperglycemia as a Mechanism of Pancreatic Cancer Metastasis. Frontiers Bioscience (Landmark Edition). 2012;17:1761-74.

61. Kang H, Kim H, Lee S, Youn H, Youn B. Role of Metabolic Reprogramming in Epithelial-Mesenchymal Transition (EMT). International Journal of Molecular Sciences. 2019;20.

62. Yeo CD, Kang N, Choi SY, Kim BN, Park CK, Kim JW, et al. The Role of Hypoxia on the Acquisition of Epithelial-Mesenchymal Transition and Cancer Stemness: A Possible Link to Epigenetic Regulation. The Korean Journal of Internal Medicine. 2017;32:589-99.

63. Joseph JP, Harishankar MK, Pillai AA, Devi A. Hypoxia Induced EMT: A Review on the Mechanism of Tumour Progression and Metastasis in OSCC. Oral Oncology. 2018;80:23-32.

64. Zhang W, Shi X, Peng Y, Wu M, Zhang P, Xie R, et al. HIF-1α Promotes Epithelial-Mesenchymal Transition and Metastasis through Direct Regulation of ZEB1 in Colorectal Cancer. PLoS One. 2015;10:e0129603.

65. Li W, Zhang L, Chen X, Jiang Z, Zong L, Ma Q. Hyperglycemia Promotes the Epithelial-Mesenchymal Transition of Pancreatic Cancer Via Hydrogen Peroxide. Oxidative Medicine and Cellular Longevity. 2016;2016:5190314.

66. Xu X, Chen B, Zhu S, Zhang J, He X, Cao G, et al. Hyperglycemia Promotes Snail-Induced Epithelial-Mesenchymal Transition of Gastric Cancer Via Activating ENO1 Expression. Cancer Cell International. 2019;19:344.

67. Li S, Zhu H, Chen H, Xia J, Zhang F, Xu R, et al. Glucose Promotes Epithelial-Mesenchymal Transitions in Bladder Cancer by Regulating the Functions of YAP1 and TAZ. Journal of Cellular and Molecular Medicine. 2020;24:10391-401.

68. Gu CJ, Xie F, Zhang B, Yang HL, Cheng J, He YY, et al. High Glucose Promotes Epithelial-Mesenchymal Transition of Uterus Endometrial Cancer Cells by Increasing ER/GLUT4-Mediated VEGF Secretion. Cellular Physiology and Biochemistry. 2018;50:706-20.

69. Labani M, Beheshti A, Lovell NH, Alinejad-Rokny H, Afrasiabi A. Karaj: An Efficient Adaptive Multi-Processor Tool to Streamline Genomic and Transcriptomic Sequence Data Acquisition. International Journal of Molecular Sciences. 2022;23.

70. Martin M. CUTADAPT Removes Adapter Sequences from High-Throughput Sequencing Reads. 2011. 2011;17:3.

71. Bushnell B. Bbmap: A Fast, Accurate, Splice-Aware Aligner. Conference: 9th Annual Genomics of Energy & Environment Meeting, Walnut Creek, CA, March 17-20, 2014; United States. DE-AC02-05CH11231: Lawrence Berkeley National Lab. (LBNL), Berkeley, CA (United States); 2014. p. Medium: ED.

72. Nurk S, Koren S, Rhie A, Rautiainen M, Bzikadze AV, Mikheenko A, et al. The Complete Sequence of a Human Genome. Science. 2022;376:44-53.

73. Dobin A, Davis CA, Schlesinger F, Drenkow J, Zaleski C, Jha S, et al. Star: Ultrafast Universal RNA-Seq Aligner. Bioinformatics. 2013;29:15-21.

74. Liao Y, Smyth GK, Shi W. Featurecounts: An Efficient General Purpose Program for Assigning Sequence Reads to Genomic Features. Bioinformatics. 2013;30:923-30.

75. Love MI, Huber W, Anders S. Moderated Estimation of Fold Change and Dispersion for RNA-Seq Data with DESeq2. Genome Biology. 2014;15:550.

76. Yu J, Hu D, Wang L, Fan Z, Xu C, Lin Y, et al. Hyperglycemia Induces Gastric Carcinoma Proliferation and Migration Via the Pin1/BRD4 Pathway. Cell Death Discovery. 2022;8:224.

77. Zhong A, Chang M, Yu T, Gau R, Riley DJ, Chen Y, et al. Aberrant DNA Damage Response and DNA Repair Pathway in High Glucose Conditions. Journal of Cancer Research Updates. 2018;7:64-74.

78. Chen J, Jiao D, Li Y, Jiang C, Tang X, Song J, et al. Mogroside V Inhibits Hyperglycemia-Induced Lung Cancer Cells Metastasis through Reversing EMT and Damaging Cytoskeleton. Current Cancer Drug Targets. 2019;19:885-95.

79. Mansor R, Holly J, Barker R, Biernacka K, Zielinska H, Koupparis A, et al. IGF-1 and Hyperglycaemia-Induced FOXA1 and IGFBP-2 Affect Epithelial to Mesenchymal Transition in Prostate Epithelial Cells. Oncotarget. 2020;11:2543-59.

80. He X, Cheng X, Ding J, Xiong M, Chen B, Cao G. Hyperglycemia Induces miR-26-5p Down-Regulation to Overexpress PFKFB3 and Accelerate Epithelial-Mesenchymal Transition in Gastric Cancer. Bioengineered. 2022;13:2902-17.

81. Rahn S, Zimmermann V, Viol F, Knaack H, Stemmer K, Peters L, et al. Diabetes as Risk Factor for Pancreatic Cancer: Hyperglycemia Promotes Epithelial-Mesenchymal-Transition and Stem Cell Properties in Pancreatic Ductal Epithelial Cells. Cancer Letters. 2018;415:129-50.

82. Wu J, Chen J, Xi Y, Wang F, Sha H, Luo L, et al. High Glucose Induces Epithelial-Mesenchymal Transition and Results in the Migration and Invasion of Colorectal Cancer Cells. Experimental and Therapeutic Medicine. 2018;16:222-30.

83. Adjemian S, Oltean T, Martens S, Wiernicki B, Goossens V, Vanden Berghe T, et al. Ionising Radiation Results in a Mixture of Cellular Outcomes Including Mitotic Catastrophe, Senescence, Methuosis, and Iron-Dependent Cell Death. Cell Death and Disease. 2020;11:1003.

84. Collins PL, Purman C, Porter SI, Nganga V, Saini A, Hayer KE, et al. DNA Double-Strand Breaks Induce H2AX Phosphorylation Domains in a Contact-Dependent Manner. Nature Communications. 2020;11:3158.

85. KUO LJ, YANG L-X. Gamma-H2AX - a Novel Biomarker for DNA Double-Strand Breaks. In Vivo. 2008;22:305-9.

86. Lin Y-T, Wu K-J. Epigenetic Regulation of Epithelial-Mesenchymal Transition: Focusing on Hypoxia and TGF-β Signalling. Journal of Biomedical Science. 2020;27:39.

87. Zhao Y, Hu X, Liu Y, Dong S, Wen Z, He W, et al. ROS Signalling under Metabolic Stress: Cross-Talk between AMPK and AKT Pathways. Molecular Cancer. 2017;16:79.

88. Mossenta M, Busato D, Dal Bo M, Toffoli G. Glucose Metabolism and Oxidative Stress in Hepatocellular Carcinoma: Role and Possible Implications in Novel Therapeutic Strategies. Cancers. 2020;12:1668.

89. Saitoh M. Involvement of Partial EMT in Cancer Progression. The Journal of Biochemistry. 2018;164:257-64.

90. Sacchetti A, Teeuwssen M, Verhagen M, Joosten R, Xu T, Stabile R, et al. Phenotypic Plasticity Underlies Local Invasion and Distant Metastasis in Colon Cancer. eLife. 2021;10.

91. Zhang C, Le A. Diabetes and Cancer: The Epidemiological and Metabolic Associations. Advances in Experimental Medicine and Biology. 2021;1311:217-27.

92. Ramos-Garcia P, Roca-Rodriguez MdM, Aguilar-Diosdado M, Gonzalez-Moles MA. Diabetes Mellitus and Oral Cancer/Oral Potentially Malignant Disorders: A Systematic Review and Meta-Analysis. Oral Diseases. 2021;27:404-21.

93. Gong Y, Wei B, Yu L, Pan W. Type 2 Diabetes Mellitus and Risk of Oral Cancer and Precancerous Lesions: A Meta-Analysis of Observational Studies. Oral Oncology. 2015;51:332-40.

94. Hu X, Wu J, Xiong H, Zeng L, Wang Z, Wang C, et al. Type 2 Diabetes Mellitus Promotes the Proliferation, Metastasis, and Suppresses the Apoptosis in Oral Squamous Cell Carcinoma. Journal of Oral Pathology and Medicine. 2022;51:483-92.

95. Ramteke P, Deb A, Shepal V, Bhat MK. Hyperglycemia Associated Metabolic and Molecular Alterations in Cancer Risk, Progression, Treatment, and Mortality. Cancers. 2019;11:1402.

96. Liu Z, Hayashi H, Matsumura K, Ogata Y, Sato H, Shiraishi Y, et al. Hyperglycaemia Induces Metabolic Reprogramming into a Glycolytic Phenotype and Promotes Epithelial-Mesenchymal Transitions Via YAP/TAZ-Hedgehog Signalling Axis in Pancreatic Cancer. British Journal of Cancer. 2023;128:844-56.

97. Chang W-C, Hsieh T-C, Hsu W-L, Chang F-L, Tsai H-R, He M-S. Diabetes and Further Risk of Cancer: A Nationwide Population-Based Study. BMC Medicine. 2024;22:214.

98. Wang M, Yang Y, Liao Z. Diabetes and Cancer: Epidemiological and Biological Links. World Journal of Diabetes. 2020;11:227-38.

99. Gurney J, Stanley J, Teng A, Krebs J, Koea J, Lao C, et al. Cancer and Diabetes Co-Occurrence: A National Study with 44 Million Person-Years of Follow-Up. PLOS One. 2022;17:e0276913.

100. Abd-Rabou AA, Abd El-Salam NM, Sharada HMI, Abd El Samea GG, Abdalla MS. Thymoquinone Crosstalks with DR5 to Sensitise TRAIL Resistance and Stimulate ROS-Mediated Cancer Apoptosis. Asian Pacific Journal of Cancer Prevention. 2021;22:2855-65.

101. G. GK, Shinde PL, John S, C. SK, Mishra R. Understanding the Combined Effects of High Glucose-Induced Hyper-Osmotic Stress and Oxygen Tension in the Progression of Tumourigenesis: From Mechanism to Anti-Cancer Therapeutics. Cells. 2023;12:825.

102. Yun C, Kim SH, Kim KM, Yang MH, Byun MR, Kim JH, et al. Advantages of Using 3D Spheroid Culture Systems in Toxicological and Pharmacological Assessment for Osteogenesis Research. International Journal of Molecular Sciences. 2024;25.

103. Costa EC, Moreira AF, de Melo-Diogo D, Gaspar VM, Carvalho MP, Correia IJ. 3D Tumour Spheroids: An Overview on the Tools and Techniques Used for Their Analysis. Biotechnology Advances. 2016;34:1427-41.

104. Juarez-Moreno K, Chávez-García D, Hirata G, Vazquez-Duhalt R. Monolayer (2D) or Spheroids (3D) Cell Cultures for Nanotoxicological Studies? Comparison of Cytotoxicity and Cell Internalisation of Nanoparticles. Toxicology in Vitro. 2022;85:105461.

105. Podhorecka M, Skladanowski A, Bozko P. H2AX Phosphorylation: Its Role in DNA Damage Response and Cancer Therapy. Journal of Nucleic Acids. 2010;2010.

106. Takano S, Shibamoto Y, Wang Z, Kondo T, Hashimoto S, Kawai T, et al. Optimal Timing of a γ-H2AX Analysis to Predict Cellular Lethal Damage in Cultured Tumour Cell Lines after Exposure to Diagnostic and Therapeutic Radiation Doses. Journal of Radiation Research. 2023;64:317-27.

107. Siddiqui MS, François M, Fenech MF, Leifert WR. Persistent γH2AX: A Promising Molecular Marker of DNA Damage and Aging. Mutation Research/Reviews in Mutation Research. 2015;766:1-19.

108. Ivashkevich A, Redon CE, Nakamura AJ, Martin RF, Martin OA. Use of the γ-H2AX Assay to Monitor DNA Damage and Repair in Translational Cancer Research. Cancer Letters. 2012;327:123-33.

109. Ciminera AK, Shuck SC, Termini J. Elevated Glucose Increases Genomic Instability by Inhibiting Nucleotide Excision Repair. Life Science Alliance. 2021;4:e202101159.

110. Rahmoon MA, Elghaish RA, Ibrahim AA, Alaswad Z, Gad MZ, El-Khamisy SF, et al. High Glucose Increases DNA Damage and Elevates the Expression of Multiple DDR Genes. Genes (Basel). 2023;14.

111. Binjawhar DN, Alhazmi AT, Bin Jawhar WN, MohammedSaeed W, Safi SZ. Hyperglycemia-Induced Oxidative Stress and Epigenetic Regulation of ET-1 Gene in Endothelial Cells. Frontiers in Genetics. 2023;14.

112. Baskar R, Lee KA, Yeo R, Yeoh K-W. Cancer and Radiation Therapy: Current Advances and Future Directions. International Journal of Medical Sciences. 2012;9:193-9.

113. Gianfaldoni S, Gianfaldoni R, Wollina U, Lotti J, Tchernev G, Lotti T. An Overview on Radiotherapy: From Its History to Its Current Applications in Dermatology. Open Access Macedonian Journal of Medical Sciences. 2017;5:521-5.

114. Lin A. Radiation Therapy for Oral Cavity and Oropharyngeal Cancers. Dental Clinics of North America. 2018;62:99-109.

115. Huang R-X, Zhou P-K. DNA Damage Response Signalling Pathways and Targets for Radiotherapy Sensitisation in Cancer. Signal Transduction and Targeted Therapy. 2020;5:60.

116. Prabhu KS, Kuttikrishnan S, Ahmad N, Habeeba U, Mariyam Z, Suleman M, et al. H2AX: A Key Player in DNA Damage Response and a Promising Target for Cancer Therapy. Biomedicine & Pharmacotherapy. 2024;175:116663.

117. Taneja N, Davis M, Choy JS, Beckett MA, Singh R, Kron SJ, et al. Histone H2AX Phosphorylation as a Predictor of Radiosensitivity and Target for Radiotherapy. Journal of Biological Chemistry. 2004;279:2273-80.

118. Kao J, Milano MT, Javaheri A, Garofalo MC, Chmura SJ, Weichselbaum RR, et al. Gamma-H2AX as a Therapeutic Target for Improving the Efficacy of Radiation Therapy. Current Cancer Drug Targets. 2006;6:197-205.

119. van Oorschot B, Hovingh S, Dekker A, Stalpers LJ, Franken NA. Predicting Radiosensitivity with Gamma-H2AX Foci Assay after Single High-Dose-Rate and Pulsed Dose-Rate Ionising Irradiation. Radiation Research. 2016;185:190-8.

120. Kawashima S, Kawaguchi N, Taniguchi K, Tashiro K, Komura K, Tanaka T, et al. γ-H2AX as a Potential Indicator of Radiosensitivity in Colorectal Cancer Cells. Oncology Letter. 2020;20:2331-7.

121. Pavlič A, Urh K, Štajer K, Boštjančič E, Zidar N. Epithelial-Mesenchymal Transition in Colorectal Carcinoma: Comparison between Primary Tumour, Lymph Node and Liver Metastases. Frontiers in Oncology. 2021;11.

122. Debaugnies M, Rodríguez-Acebes S, Blondeau J, Parent MA, Zocco M, Song Y, et al. RHOJ Controls EMT-Associated Resistance to Chemotherapy. Nature. 2023;616:168-75.

123. Bamodu OA, Chang HL, Ong JR, Lee WH, Yeh CT, Tsai JT. Elevated PDK1 Expression Drives PI3K/Akt/mTOR Signalling, Promotes Radiation-Resistant and Dedifferentiated Phenotype of Hepatocellular Carcinoma. Cells. 2020;9.

124. Bugshan A, Farooq I. Oral Squamous Cell Carcinoma: Metastasis, Potentially Associated Malignant Disorders, Etiology and Recent Advancements in Diagnosis. F1000Research. 2020;9:229.

125. Brabletz S, Schuhwerk H, Brabletz T, Stemmler MP. Dynamic EMT: A Multi-Tool for Tumour Progression. The EMBO Journal. 2021;40:e108647.

126. Bornes L, Belthier G, van Rheenen J. Epithelial-to-Mesenchymal Transition in the Light of Plasticity and Hybrid E/M States. Journal of Clinical Medicine. 2021;10.

127. Norgard RJ, Stanger BZ. Isolation and Identification of EMT Subtypes. Methods in Molecular Biology. 2021;2179:315-26.

128. Jolly MK, Somarelli JA, Sheth M, Biddle A, Tripathi SC, Armstrong AJ, et al. Hybrid Epithelial/Mesenchymal Phenotypes Promote Metastasis and Therapy Resistance across Carcinomas. Pharmacology and Therapeutics. 2019;194:161-84.

129. Jia D, Li X, Bocci F, Tripathi S, Deng Y, Jolly MK, et al. Quantifying Cancer Epithelial-Mesenchymal Plasticity and Its Association with Stemness and Immune Response. Journal of Clinical Medicine. 2019;8.

130. Dai C, Cao J, Zeng Y, Xu S, Jia X, Xu P. E-Cadherin Expression as a Prognostic Factor in Patients with Ovarian Cancer: A Meta-Analysis. Oncotarget. 2017;8:81052-61.

131. Li Z, Yin S, Zhang L, Liu W, Chen B. Prognostic Value of Reduced E-Cadherin Expression in Breast Cancer: A Meta-Analysis. Oncotarget. 2017;8:16445-55.

132. Favaretto RL, Bahadori A, Mathieu R, Haitel A, Grubmüller B, Margulis V, et al. Prognostic Role of Decreased E-Cadherin Expression in Patients with Upper Tract Urothelial Carcinoma: A Multi-Institutional Study. World Journal of Urology. 2017;35:113-20.

133. Yonemura Y, Nojima N, Kaji M, Kawamura T, Fushida S, Fujimura T, et al. E-Cadherin and C-Met Expression as a Prognostic Factor in Gastric Cancer. Oncology Reports. 1997;4:743-8.

134. Theys J, Jutten B, Habets R, Paesmans K, Groot AJ, Lambin P, et al. E-Cadherin Loss Associated with EMT Promotes Radioresistance in Human Tumour Cells. Radiotherapy and Oncology. 2011;99:392-7.

135. Su H, Jin X, Zhang X, Zhao L, Lin B, Li L, et al. FH535 Increases the Radiosensitivity and Reverses Epithelial-to-Mesenchymal Transition of Radioresistant Esophageal Cancer Cell Line KYSE-150R. Journal of Translational Medicine. 2015;13:104.

136. Zhao X, Liu X, Hu S, Pan Y, Zhang J, Tai G, et al. Gdf15 Contributes to Radioresistance by Mediating the EMT and Stemness of Breast Cancer Cells. International Journal of Molecular Sciences. 2022;23.

137. Li Y, Sun C, Tan Y, Zhang H, Li Y, Zou H. Itgb1 Enhances the Radioresistance of Human Non-Small Cell Lung Cancer Cells by Modulating the DNA Damage Response and YAP1-Induced Epithelial-Mesenchymal Transition. International Journal of Biological Sciences. 2021;17:635-50.

138. Saitoh M. Transcriptional Regulation of EMT Transcription Factors in Cancer. Seminars in Cancer Biology. 2023;97:21-9.

139. Hollestelle A, Peeters JK, Smid M, Timmermans M, Verhoog LC, Westenend PJ, et al. Loss of E-Cadherin Is Not a Necessity for Epithelial to Mesenchymal Transition in Human Breast Cancer. Breast Cancer Research and Treatment. 2013;138:47-57.

140. Yang J, Weinberg RA. Epithelial-Mesenchymal Transition: At the Crossroads of Development and Tumour Metastasis. Developmental Cell. 2008;14:818-29.

141. Shamir ER, Pappalardo E, Jorgens DM, Coutinho K, Tsai WT, Aziz K, et al. TWIST1-Induced Dissemination Preserves Epithelial Identity and Requires E-Cadherin. Journal of Cell Biology. 2014;204:839-56.

142. Wang W, Hapach LA, Griggs L, Smart K, Wu Y, Taufalele PV, et al. Diabetic Hyperglycaemia Promotes Primary Tumour Progression through Glycation-Induced Tumour Extracellular Matrix Stiffening. Science Advances. 2022;8:eabo1673.

143. Topel H, Bağırsakçı E, Yılmaz Y, Güneş A, Bağcı G, Çömez D, et al. High Glucose-Induced C-Met Activation Promotes Aggressive Phenotype and Regulates Expression of Glucose Metabolism Genes in HCC Cells. Scientific Reports. 2021;11:11376.

144. Detarya M, Thaenkaew S, Seubwai W, Indramanee S, Phoomak C, Saengboonmee C, et al. High Glucose Upregulates FOXM1 Expression Via EGFR/STAT3 Dependent Activation to Promote Progression of Cholangiocarcinoma. Life Sciences. 2021;271:119114.

145. Xiao L, Mao Y, Tong Z, Zhao Y, Hong H, Wang F. Radiation Exposure Triggers the Malignancy of Non-Small Cell Lung Cancer Cells through the Activation of Visfatin/Snail Signalling. Oncology Report. 2021;45:1153-61.

146. Hu Y, Li Q, Yi K, Yang C, Lei Q, Wang G, et al. HuR Affects the Radiosensitivity of Esophageal Cancer by Regulating the EMT-Related Protein Snail. Frontiers in Oncology. 2022;12.

147. Kim R-K, Kaushik N, Suh Y, Yoo K-C, Cui Y-H, Kim M-J, et al. Radiation-Driven Epithelial-Mesenchymal Transition Is Mediated by Notch Signalling in Breast Cancer. Oncotarget. 2016;7.

148. Schinke H, Pan M, Akyol M, Zhou J, Shi E, Kranz G, et al. SLUG-Related Partial Epithelial-to-Mesenchymal Transition Is a Transcriptomic Prognosticator of Head and Neck Cancer Survival. Molecular Oncology. 2022;16:347-67.

149. Riechelmann H, Steinbichler TB, Sprung S, Santer M, Runge A, Ganswindt U, et al. The Epithelial-Mesenchymal Transcription Factor Slug Predicts Survival Benefit of Up-Front Surgery in Head and Neck Cancer. Cancers (Basel). 2021;13.

150. Horiguchi K, Sakamoto K, Koinuma D, Semba K, Inoue A, Inoue S, et al. TGF-β Drives Epithelial-Mesenchymal Transition through δEF1-Mediated Downregulation of ESRP. Oncogene. 2012;31:3190-201.

151. Sakamoto K, Endo K, Sakamoto K, Kayamori K, Ehata S, Ichikawa J, et al. EHF Suppresses Cancer Progression by Inhibiting ETS1-Mediated ZEB Expression. Oncogenesis. 2021;10:26.

152. Yang J, Mani SA, Donaher JL, Ramaswamy S, Itzykson RA, Come C, et al. Twist, a Master Regulator of Morphogenesis, Plays an Essential Role in Tumour Metastasis. Cell. 2004;117:927-39.

153. Lee TK, Poon RT, Yuen AP, Ling MT, Kwok WK, Wang XH, et al. Twist Overexpression Correlates with Hepatocellular Carcinoma Metastasis through Induction of Epithelial-Mesenchymal Transition. Clinical Cancer Research. 2006;12:5369-76.

154. Meng J, Chen S, Han J-X, Qian B, Wang X-R, Zhong W-L, et al. Twist1 Regulates Vimentin through Cul2 Circular RNA to Promote EMT in Hepatocellular Carcinoma. Cancer Research. 2018;78:4150-62.

155. Chen S, Chen J-z, Zhang J-q, Chen H-x, Yan M-l, Huang L, et al. Hypoxia Induces TWIST-Activated Epithelial–Mesenchymal Transition and Proliferation of Pancreatic Cancer Cells In vitro and in Nude Mice. Cancer Letters. 2016;383:73-84.

156. Wang Y, Liu J, Ying X, Lin PC, Zhou BP. Twist-Mediated Epithelial-Mesenchymal Transition Promotes Breast Tumour Cell Invasion Via Inhibition of Hippo Pathway. Scientific Reports. 2016;6:24606.

157. Zeng J, Zhan P, Wu G, Yang W, Liang W, Lv T, et al. Prognostic Value of Twist in Lung Cancer: Systematic Review and Meta-Analysis. Translational Lung Cancer Research. 2015;4:236-41.

158. Miura N, Yano T, Shoji F, Kawano D, Takenaka T, Ito K, et al. Clinicopathological Significance of Sip1-Associated Epithelial-Mesenchymal Transition in Non-Small Cell Lung Cancer Progression. Anticancer Research. 2009;29:4099-106.

159. Jia D, Jolly MK, Tripathi SC, Den Hollander P, Huang B, Lu M, et al. Distinguishing Mechanisms Underlying EMT Tristability. Cancer Convergence. 2017;1:2.

160. Fukagawa A, Ishii H, Miyazawa K, Saitoh M. δEF1 Associates with DNMT1 and Maintains DNA Methylation of the E-Cadherin Promoter in Breast Cancer Cells. Cancer Medicine. 2015;4:125-35.

161. Larsen JE, Nathan V, Osborne JK, Farrow RK, Deb D, Sullivan JP, et al. ZEB1 Drives Epithelial-to-Mesenchymal Transition in Lung Cancer. The Journal of Clinical Investigation. 2016;126:3219-35.

162. Georgakopoulos-Soares I, Chartoumpekis DV, Kyriazopoulou V, Zaravinos A. EMT Factors and Metabolic Pathways in Cancer. Frontiers in Oncology. 2020;10:499.

163. Cook DP, Vanderhyden BC. Context Specificity of the EMT Transcriptional Response. Nature Communications. 2020;11:2142.

164. Sinha D, Saha P, Samanta A, Bishayee A. Emerging Concepts of Hybrid Epithelial-to-Mesenchymal Transition in Cancer Progression. Biomolecules. 2020;10:1561.

165. Lee C, An D, Park J. Hyperglycemic Memory in Metabolism and Cancer. Hormone Molecular Biology and Clinical Investigation. 2016;26:77-85.

166. Zhu D, Xia J, Liu C, Fang C. Numb/Notch/PLK1 Signalling Pathway Mediated Hyperglycemic Memory in Pancreatic Cancer Cell Radioresistance and the Therapeutic Effects of Metformin. Cellular Signalling. 2022;93:110268.

167. Al-Dabet MdM, Shahzad K, Elwakiel A, Sulaj A, Kopf S, Bock F, et al. Reversal of the Renal Hyperglycemic Memory in Diabetic Kidney Disease by Targeting Sustained Tubular P21 Expression. Nature Communications. 2022;13:5062.

168. Wilson-Verdugo M, Bustos-García B, Adame-Guerrero O, Hersch-González J, Cano-Domínguez N, Soto-Nava M, et al. Reversal of High-Glucose-Induced Transcriptional and Epigenetic Memories through NRF2 Pathway Activation. Life Science Alliance. 2024;7.

169. Melissaridou S, Wiechec E, Magan M, Jain MV, Chung MK, Farnebo L, et al. The Effect of 2D and 3D Cell Cultures on Treatment Response, EMT Profile and Stem Cell Features in Head and Neck Cancer. Cancer Cell International. 2019;19:16.

170. Filipiak-Duliban A, Brodaczewska K, Majewska A, Kieda C. Spheroid Culture Models Adequately Imitate Distinctive Features of the Renal Cancer or Melanoma Microenvironment. In Vitro Cellular and Development Biology – Animal. 2022;58:349-64.

171. Turner PA, Garrett MR, Didion SP, Janorkar AV. Spheroid Culture System Confers Differentiated Transcriptome Profile and Functional Advantage to 3T3-L1 Adipocytes. Annals of Biomedical Engineering. 2018;46:772-87.

172. Rovere M, Reverberi D, Arnaldi P, Palamà MEF, Gentili C. Spheroid Size Influences Cellular Senescence and Angiogenic Potential of Mesenchymal Stromal Cell-Derived Soluble Factors and Extracellular Vesicles. Frontiers of Bioengineering and Biotechnology. 2023;11:1297644.

173. Liu F, Wu Q, Dong Z, Liu K. Integrins in Cancer: Emerging Mechanisms and Therapeutic Opportunities. Pharmacology & Therapeutics. 2023;247:108458.

174. Takada Y, Ye X, Simon S. The Integrins. Genome Biology. 2007;8:215.

175. Li R, Ji Q, Fu S, Gu J, Liu D, Wang L, et al. ITGA3 Promotes Pancreatic Cancer Progression through HIF1α- and C-Myc-Driven Glycolysis in a Collagen I-Dependent Autocrine Manner. Cancer Gene Therapy. 2024.

176. Gui J, Yang L, Liu J, Li Y, Zou M, Sun C, et al. Identifying the Prognosis Implication, Immunotherapy Response Prediction Value, and Potential Targeted Compound Inhibitors of Integrin Subunit A3 (ITGA3) in Human Cancers. Heliyon. 2024;10:e24236.

177. Martínez-Flores R, Lozano-Burgos C, Niklander SE, Fernández-Cuya M, Lopes MA, González-Arriagada WA. Relationship between Aggressive Features of Oral Squamous Cell Carcinoma and the Immunoexpression of CX3CR1, CX3CL1 and ITGAV. Oral Surgery, Oral Medicine, Oral Pathology and Oral Radiology. 2024;138:79-87.

178. Nagata M, Noman AA, Suzuki K, Kurita H, Ohnishi M, Ohyama T, et al. ITGA3 and ITGB4 Expression Biomarkers Estimate the Risks of Locoregional and Hematogenous Dissemination of Oral Squamous Cell Carcinoma. BMC Cancer. 2013;13:410.

179. Tan Z, Zhang Z, Yu K, Yang H, Liang H, Lu T, et al. Integrin Subunit Alpha V Is a Potent Prognostic Biomarker Associated with Immune Infiltration in Lower-Grade Glioma. Frontiers in Neurology. 2022;13.

180. Wang H, Chen H, Jiang Z, Lin Y, Wang X, Xiang J, et al. Integrin Subunit Alpha V Promotes Growth, Migration, and Invasion of Gastric Cancer Cells. Pathology - Research and Practice. 2019;215:152531.

181. Pan C, Wang Z, Wang Q, Wang H, Deng X, Chen L, et al. TFAP2A-Activated ITGB4 Promotes Lung Adenocarcinoma Progression and Inhibits CD4+/CD8+ T-Cell Infiltrations by Targeting NF-κB Signalling Pathway. Translational Lung Cancer Research. 2024;13:2116-38.

182. Chen P, Ma T, Yan T, Song Z, Liu C, Pan C, et al. ITGB4 Upregulation Is Associated with Progression of Lower Grade Glioma. Scientific Reports. 2024;14:421.

183. Shirakihara T, Kawasaki T, Fukagawa A, Semba K, Sakai R, Miyazono K, et al. Identification of Integrin A3 as a Molecular Marker of Cells Undergoing Epithelial-Mesenchymal Transition and of Cancer Cells with Aggressive Phenotypes. Cancer Science. 2013;104:1189-97.

184. Tan W, Chen G, Ci Q, Deng Z, Gu R, Yang D, et al. Elevated ITGA3 Expression Serves as a Novel Prognostic Biomarker and Regulates Tumour Progression in Cervical Cancer. Scientific Reports. 2024;14:27063.

185. Ghosh S, Koblinski J, Johnson J, Liu Y, Ericsson A, Davis JW, et al. Urinary-Type Plasminogen Activator Receptor/A3β1 Integrin Signaling, Altered Gene Expression, and Oral Tumor Progression. Molecular Cancer Research. 2010;8:145-58.

186. da-Silva JP, Lourenço S, Nico M, Silva FH, Martins MT, Costa-Neves A. Expression of Laminin-5 and Integrins in Actinic Cheilitis and Superficially Invasive Squamous Cell Carcinomas of the Lip. Pathology-Research and Practice. 2012;208:598-603.

187. Boelens MC, van den Berg A, Vogelzang I, Wesseling J, Postma DS, Timens W, et al. Differential Expression and Distribution of Epithelial Adhesion Molecules in Non-Small Cell Lung Cancer and Normal Bronchus. Journal of Clinical Pathology. 2007;60:608-14.

188. Da Silva RG, Tavora B, Robinson SD, Reynolds LE, Szekeres C, Lamar J, et al. Endothelial A3β1-Integrin Represses Pathological Angiogenesis and Sustains Endothelial-VEGF. The American Journal of Pathology. 2010;177:1534-48.

189. Shirakihara T, Kawasaki T, Fukagawa A, Semba K, Sakai R, Miyazono K, et al. Identification of Integrin A3 as a Molecular Marker of Cells Undergoing Epithelial–Mesenchymal Transition and of Cancer Cells with Aggressive Phenotypes. Cancer Science. 2013;104:1189-97.

190. Romanska HM, Potemski P, Krakowska M, Mieszkowska M, Chaudhri S, Kordek R, et al. Lack of CD151/Integrin A3β1 Complex Is Predictive of Poor Outcome in Node-Negative Lobular Breast Carcinoma: Opposing Roles of CD151 in Invasive Lobular and Ductal Breast Cancers. British Journal of Cancer. 2015;113:1350-7.

191. Ramovs V, te Molder L, Sonnenberg A. The Opposing Roles of Laminin-Binding Integrins in Cancer. Matrix Biology. 2017;57-58:213-43.

192. Baldwin LA, Hoff JT, Lefringhouse J, Zhang M, Jia C, Liu Z, et al. CD151-A3β1 Integrin Complexes Suppress Ovarian Tumor Growth by Repressing SLUG-Mediated EMT and Canonical Wnt Signaling. Oncotarget. 2014;5.

193. Srichai MB, Zent R. Integrin Structure and Function. In: Zent R, Pozzi A, editors. Cell-Extracellular Matrix Interactions in Cancer. New York, NY: Springer New York; 2010. p. 19-41.

194. Huang G, Zhou M, Lu D, Li J, Tang Q, Xiong C, et al. The Mechanism of ITGB4 in Tumour Migration and Invasion. Frontiers in Oncology. 2024;14.

195. Van Waes C, Kozarsky KF, Warren AB, Kidd L, Paugh D, Liebert M, et al. The A9 Antigen Associated with Aggressive Human Squamous Carcinoma Is Structurally and Functionally Similar to the Newly Defined Integrin A6β41. Cancer Research. 1991;51:2395-402.

196. Stewart RL, O'Connor KL. Clinical Significance of the Integrin A6β4 in Human Malignancies. Laboratory Investigation. 2015;95:976-86.

197. Kim TH, Kim HI, Soung YH, Shaw LA, Chung J. Integrin (A6β4) Signals through Src to Increase Expression of S100a4, a Metastasis-Promoting Factor: Implications for Cancer Cell Invasion. Molecular Cancer Research. 2009;7:1605-12.

198. Hou S, Wang J, Li W, Hao X, Hang Q. Roles of Integrins in Gastrointestinal Cancer Metastasis. Frontiers in Molecular Bioscience. 2021;8:708779.

199. Tang YL, Li GS, Li DM, Tang D, Huang JZ, Feng H, et al. The Clinical Significance of Integrin Subunit Alpha V in Cancers: From Small Cell Lung Carcinoma to Pan-Cancer. BMC Pulmonary Medicine. 2022;22:300.

200. Lin S, Shen Z, Yang Y, Qiu Y, Wang Y, Wang X. Expression Profiles of Radio-Resistant Genes in Colorectal Cancer Cells. Radiation Medicine and Protection. 2021;2:48-54.

201. Yang L, Zhang X, Hou Q, Huang M, Zhang H, Jiang Z, et al. Single-Cell RNA-Seq of Esophageal Squamous Cell Carcinoma Cell Line with Fractionated Irradiation Reveals Radioresistant Gene Expression Patterns. BMC Genomics. 2019;20:611.

202. Li H, Qiu Z, Li F, Wang C. The Relationship between MMP-2 and MMP-9 Expression Levels with Breast Cancer Incidence and Prognosis. Oncology Letters. 2017;14:5865-70.

203. Deng W, Peng W, Wang T, Chen J, Zhu S. Overexpression of MMPs Functions as a Prognostic Biomarker for Oral Cancer Patients: A Systematic Review and Meta-Analysis. Oral Health and Preventive Dentistry. 2019;17:505-14.

204. Miao C, Liang C, Zhu J, Xu A, Zhao K, Hua Y, et al. Prognostic Role of Matrix Metalloproteinases in Bladder Carcinoma: A Systematic Review and Meta-Analysis. Oncotarget. 2017;8:32309-21.

205. Jia H, Zhang Q, Liu F, Zhou D. Prognostic Value of MMP-2 for Patients with Ovarian Epithelial Carcinoma: A Systematic Review and Meta-Analysis. Archives of Gynecology and Obstetrics. 2017;295:689-96.

206. Jiang H, Li H. Prognostic Values of Tumoral MMP2 and MMP9 Overexpression in Breast Cancer: A Systematic Review and Meta-Analysis. BMC Cancer. 2021;21:149.

207. Saengboonmee C, Seubwai W, Pairojkul C, Wongkham S. High Glucose Enhances Progression of Cholangiocarcinoma Cells Via STAT3 Activation. Scientific Reports. 2016;6:18995.

208. Chetty C, Bhoopathi P, Rao JS, Lakka SS. Inhibition of Matrix Metalloproteinase-2 Enhances Radiosensitivity by Abrogating Radiation-Induced FoxM1-Mediated G2/M Arrest in A549 Lung Cancer Cells. International Journal of Cancer. 2009;124:2468-77.

209. Kunigal S, Lakka SS, Joseph P, Estes N, Rao JS. Matrix Metalloproteinase-9 Inhibition Down-Regulates Radiation-Induced Nuclear Factor-Kappa B Activity Leading to Apoptosis in Breast Tumours. Clinical Cancer Research. 2008;14:3617-26.

210. Jadhav U, Mohanam S. Response of Neuroblastoma Cells to Ionising Radiation: Modulation of in Vitro Invasiveness and Angiogenesis of Human Microvascular Endothelial Cells. International Journal of Oncology. 2006;29:1525-31.

211. Waller V, Pruschy M. Combined Radiochemotherapy: Metalloproteinases Revisited. Frontiers in Oncology. 2021;11:676583.

212. Määttä M, Virtanen I, Burgeson R, Autio-Harmainen H. Comparative Analysis of the Distribution of Laminin Chains in the Basement Membranes in Some Malignant Epithelial Tumours: The Alpha1 Chain of Laminin Shows a Selected Expression Pattern in Human Carcinomas. Journal of Histochemistry and Cytochemistry. 2001;49:711-26.

213. Lee H, Kim WJ, Kang HG, Jang JH, Choi IJ, Chun KH, et al. Upregulation of LAMB1 Via ERK/c-Jun Axis Promotes Gastric Cancer Growth and Motility. International Journal of Molecular Sciences. 2021;22.

214. Bai J, Zhao Y, Shi K, Fan Y, Ha Y, Chen Y, et al. HIF-1α-Mediated LAMC1 Overexpression Is an Unfavourable Predictor of Prognosis for Glioma Patients: Evidence from Pan-Cancer Analysis and Validation Experiments. Journal of Translational Medicine. 2024;22:391.

215. Fang L, Che Y, Zhang C, Huang J, Lei Y, Lu Z, et al. LAMC1 Upregulation Via TGFβ Induces Inflammatory Cancer-Associated Fibroblasts in Esophageal Squamous Cell Carcinoma Via NF-κB-CXCL1-STAT3. Molecular Oncology. 2021;15:3125-46.

216. Bai J, Zheng A, Ha Y, Xu X, Yu Y, Lu Y, et al. Comprehensive Analysis of LAMC1 Expression and Prognostic Value in Kidney Renal Papillary Cell Carcinoma and Clear Cell Carcinoma. Frontiers in Molecular Bioscience. 2022;9:988777.

217. Sun Y, Zhao C, Ye Y, Wang Z, He Y, Li Y, et al. High Expression of Fibronectin 1 Indicates Poor Prognosis in Gastric Cancer. Oncology Letter. 2020;19:93-102.

218. Zhang XX, Luo JH, Wu LQ. FN1 Overexpression Is Correlated with Unfavourable Prognosis and Immune Infiltrates in Breast Cancer. Frontiers in Genetics. 2022;13:913659.

219. Liang H, Yu M, Yang R, Zhang L, Zhang L, Zhu D, et al. A PTAL-miR-101-FN1 Axis Promotes EMT and Invasion-Metastasis in Serous Ovarian Cancer. Molecular Therapy - Oncolytics. 2020;16:53-62.

220. Liu X, Meng L, Li X, Li D, Liu Q, Chen Y, et al. Regulation of Fn1 Degradation by the P62/Sqstm1-Dependent Autophagy–Lysosome Pathway in HNSCC. International Journal of Oral Science. 2020;12:34.

221. Tang X, Tang Q, Yang X, Xiao ZA, Zhu G, Yang T, et al. FN1 Promotes Prognosis and Radioresistance in Head and Neck Squamous Cell Carcinoma: From Radioresistant

HNSCC Cell Line to Integrated Bioinformatics Methods. Frontiers in Genetics. 2022;13:1017762.

222. Meng Y, Hu X, Li S, Zeng X, Qiu L, Wei M, et al. miR-203 Inhibits Cell Proliferation and ERK Pathway in Prostate Cancer by Targeting IRS-1. BMC Cancer. 2020;20:1-14.

223. Luo J, Feng J, Wen Q, Qoyawayma C, Wang W, Chen L, et al. Elevated Expression of IRS-1 Associates with Phosphorylated Akt Expression and Predicts Poor Prognosis of Breast Invasive Ductal Carcinoma. Human Pathology. 2018;79:9-17.

224. Huang Y, Zhou L, Meng X, Yu B, Wang H, Yang Y, et al. IRS-1 Regulates Proliferation, Invasion and Metastasis of Pancreatic Cancer Cells through MAPK and PI3K Signalling Pathways. International Journal of Clinical and Experimental Pathology. 2018;11:5185.

225. Kaewlert W, Sakonsinsiri C, Lert-Itthiporn W, Ungarreevittaya P, Pairojkul C, Pinlaor S, et al. Overexpression of Insulin Receptor Substrate 1 (IRS1) Relates to Poor Prognosis and Promotes Proliferation, Stemness, Migration, and Oxidative Stress Resistance in Cholangiocarcinoma. International Journal of Molecular Sciences. 2023;24.

226. Yu F, Huang D, Kuang Y, Dong J, Han Q, Zhou J, et al. IRS1 Promotes Thyroid Cancer Metastasis through EMT and PI3K/Akt Pathways. Clinical Endocrinology. 2024;100:284-93.

227. Xiao Y, Zhu X, Li Q, Wang Z, Zuo Q, Liu X, et al. m6A-Mediated IRS1 Regulates the Development of Oral Squamous Cell Carcinoma through p53/Line-1 Signalling. Frontiers in Bioscience – Landmark. 2024;29.

228. Wei ML, Duan P, Wang ZM, Ding M, Tu P. High Glucose and High Insulin Conditions Promote MCF-7 Cell Proliferation and Invasion by Upregulating IRS1 and Activating the Ras/Raf/ERK Pathway. Molecular Medicine Reports. 2017;16:6690-6.